Modeling and Simulation of Oxidative Degradation of Ultra-High Molecular Weight Polyethylene (UHMWPE)

by

Vinay S. Medhekar

A thesis submitted to the Faculty of

WORCESTER POLYTECHNIC INSTITUTE

in partial fulfillment of the requirements for the

Degree of Master of Science

in

Chemical Engineering

by

Vinay S. Medhekar

August 2001

Prof. Robert W. Thomspon, Advisor

Prof. William G. McGimpsey, co-Advisor

Prof. Ravindra Datta, Department Head

Acknowledgements

I am greatly indebted to many people, directly and indirectly who helped me see through the successful completion of my thesis. I sincerely thank Prof. Robert W. Thompson for his invaluable advice and his patience throughout my learning process. I thank him not only for giving me important lessons in conducting research but upholding the research ethics that are so important for one's first step in research. There are few words to express the impact he had on my learning. I thank Prof. McGimpsey for his guidance as a co-advisor. I'm thankful to Dr. Aiguo Wang, Howmedica Inc., for providing our research work with financial support and guidance, and for sharing invaluable ideas and results.

I would like to thank Abhijit Phatak, Tony Thampan, Bradd Libby and other department graduate students who made my stay at WPI enjoyable and a learning experience. I would like to share this moment of accomplishment with my roommates Manish and Akshay who were with me through all the good and difficult times, and other friends who made my stay in Worcester a memorable one. Finally, I thank and seek blessings from my parents to whom I dedicate my first piece of research work.

Contents

List of tables:

List of figures:

Section 2.1.3

Section 3.1

Section 4.1

Section 4.2.

Section 4.3

Section 4.4

Chapter 1

Introduction

Ultra High Molecular Weight Polyethylene (UHMWPE) has been used successfully as a load bearing material for the past 30 years for total hip and knee joint replacements. It boasts a high rate of success. Data published by the American Academy of Orthopedic Surgeons [1] indicate that 138,000 hip prosthesis and 245,000 knee prosthesis were implanted in the United States in 1996. For 2030, these figures are projected to be 248,000 and 454,000, respectively. It essentially works as a cushioning material between tibial and femoral components, replacing cartilage. In the total hip system, UHMWPE is used as a liner inside the acetabular cup surrounding the ball of the femoral component. The molecular weight of the polymer is typically in the range of 2 to 6 million g/mole. The essential properties that make it a favorable bearing material are its high tensile stress, low coefficient of friction, and inertness to the chemicals found in body.

When the polymer is to be implanted into the body, it has to be sterilized first to the medical grade requirement. For UHMWPE the requirement is 99.9999% to ensure that all form of microbial contamination is eliminated [2]. There are several ways for sterilizing the material such as heating the material, exposing it to radiation such as Υ - irradiation, electron irradiation, or treating with chemicals. The heating technique requires reaching temperatures that are close to the melting point of the polymer [3],

which could lead to deformation of the polymer and general loss of mechanical properties. This method is usually not preferred. The treatment of polymer with ethylene oxide leads to the required level of sterilization but has proved to be hazardous to health of the people involved with the sterilization process. Ethylene oxide is a carcinogen, a reproductive hazard, a mutagen, and an irritant [2]. Gamma irradiation has been found to be the most effective in sterilization with low costs and negligible handling of the polymer. Gamma irradiation involves exposing the polymer to a large array of Co^{60} crystals, which forms the radiation source. The irradiation of polymers is usually carried in the presence of air, as it is economically suitable. However gamma radiation leads to formation of alkyl radicals by scission between carbon and hydrogen of the alkane molecule. Some of these alkyl radicals combine together increasing the length of the polymer chain. The molecular weight of the polymer increases leading to increase in wear resistance [4]. The crystallinity of the polymer increases due to cross-linking [5]. It also has the advantage that the polymer can be irradiated in the same packaging that they are kept in until implant.

On the disadvantage part, UHMWPE components (polymer component or in short PE) are irradiated with Co^{60} with 1.17 and 1.13 MeV photon energies that are 5 orders of magnitude larger than the average energy of the chemical bond [6,7]. When PE is irradiated, the long polyethylene chain undergoes C-H and C-C bond scission producing radicals. The former has been found to occur more readily [8]. Under continuous diffusion of oxygen in to the polymer, alkyl radicals engage in a series of chain reactions leading to the formation of various oxidative degradation products and generation of

more free radicals. The process of continuous oxidation results in the formation of smaller polyethylene chains and a decrease in the useful mechanical properties of the polymer such as mechanical strength, abrasion resistance etc. [9,10,11]. The polymer oxidation occurs not only during its normal functioning in the body when it is subjected to stress due to body movements but also during shelf storage prior to implantation, which could be up to 10 years. One interesting observation about the mechanical behavior of the polymer is that the most severe mechanical degradation has been found to occur at about 2 mm below the surface of the polymer [10,11]. Several studies [8,11,12,13] have reported the formation of subsurface white band, which is the most brittle part of the entire polymer section. This white band has been associated with severe mechanical failure. The products of oxidation may include ketones, aldehydes, acids, peroxides and esters, ketones being the chief ones that are found to the extent of 75 percent of all the degradation products formed [6,7,12,14]. Being formed in the largest amount, ketones naturally have been the key product of investigation. A striking result is that the formation of ketones during shelf aging begins with very low concentration at the surface, reaches a maximum around 1 – 3 mm and then drops down to a minimum value at about 5 mm and remains constant beyond it [6]. It repeats again at the other surface. It is generally accepted that the mechanical failure at the subsurface could be attributed to the maximum concentration of ketone formed by oxidative degradation of the polymer. There has been recent investigation about the white band in terms of concentration of additives in subsurface region. Additives are added to scavenge the residual catalyst components used in the manufacture of UHMWPE [15], and minimizing the effect of oxygen diffusing during shelf storage and use. There are circumstantial results by Willie

et. al. [13], who discovered high concentrations of calcium stearate, an additive, in the white band region compared to those near the center of the polymer orthopedic block. The presence of calcium stearate gave white color to the polymer at the subsurface. Why calcium stearate concentrated in the region at 2 mm from the surface though has not been answered.

One of the major problems associated with orthopedic polymer component is the production of debris. When in – vivo, the polymer undergoes mechanical degradation under the constant action of stress due to motion of the body parts, leading to the formation of fine polyethylene particles that has been associated with bone resorption and osteolysis [16,17]. It is estimated that the wear rates of 0.05 to 0.2 mm per year in a normal joint will generate about 25 to 100 mm^3 (25 to 100 mg) of polyethylene debris annually [18,19]. It is estimated that an elderly person will generate 20 to 40 billion UHMWPE particles in to the joint space every year [20]. The orthopedic implant can undergo mechanical failure as early as 2 years from the time of implant into the body leading to major replacement surgery. Also, the cost of surgery is high. For all the above reasons, it has become important to understand the process of oxidative degradation of the polymer. Many reports are available about the mechanical failure of the polymer, which includes several theories on mechanical wear [21,22].

We were interested in looking into the chemical nature of the system to see if we could predict the failure of the polymer from the chemistry point of view. As mentioned earlier, the maximum failure of the polymer occurs at the subsurface where the concentration of the ketone has been found to be the highest. There have been few studies

on the oxidation chemistry of UHMWPE and many of them repeat the models, modifying the steps to suit their purpose [12,23,24]. Our current purpose was to implement the general reactions involved in the oxidation of PE and then use this information to predict the ketone profiles with depth of the polymer as a function of aging time. It was also our goal to resolve various interpretations of the oxidative process found in the literature.

Chapter 2

Background

2.1 Previous Experimental Studies:

2.1.1 Structure and Chemical Properties:

Ultra High Molecular Weight Polyethylene (UHMWPE) is made up long chains of $–CH_2 –$ groups. The molecular weight of the polyethylene (PE) is between 2 to 6 million g/mol. UHMWPE is a semi-crystalline polymer made up of a two-phase viscoplastic solid at nanometer scale length. The crystalline domains are embedded within an amorphous matrix. The crystalline phase consists of folded rows of methylene groups packed in to lamellae, around 10 – 50 nm in thickness and on the order of 10 – 50 μm in length [15]. The inter-lamellar spacing is 50 nm based upon small – angle X-ray scattering measurements [25]. The amorphous phase surrounding the crystalline phase consists of randomly oriented polymer chains with crystalline lamellae interconnected by tie molecules. These tie molecules contribute to the mechanical resistance of the polymer. The crystallinity of UHMWPE is typically around 50 – 65%, more on the lower side [7].

UHMWPE has a good resistance to chemical attack from acids and alkali. The polymer is prone to the attack of oxygen. Oxygen can diffuse in to the amorphous region of the polymer causing localized strains, breaking the tie molecules. The boundaries are pulled apart thereby creating voids or micro-cracks [9]. UHMWPE can also absorb water and swell [14].

2.1.2 Sterilization

UHMWPE implants need to be sterilized before they are used in the body. The recommended sterilization level is 99.9999% [2]. As recently as 1995, the UHMWPE was typically sterilized with a nominal dose of 25 to 40 kGy of gamma radiation in the presence of air. But, recently there has been mounting evidence about large degradation of mechanical and chemical properties of the polymer when the polymer is irradiated in the presence of air. The diffusion of oxygen and its reaction with the alkyl radials formed due to irradiation result in continuous oxidative degradation. By 1998, many of the major orthopedic implant manufacturers were sterilizing using gamma irradiation under reduced oxygen atmosphere or using alternate sterilizing techniques such as ethylene oxide or gas plasma sterilization [15].

Ethylene oxide (EtO) provides effective sterilization for UHMWPE since there are no components that react or bind with the EtO gas. Studies [22,26,27] suggest that sterilization using EtO gas does not substantially influence the physical, chemical and mechanical properties of UHMWPE. In a study by White et al. [28], retrieved components sterilized with EtO have shown significantly less surface damage and delamination than gamma-irradiated samples of identical design. Though there are evident advantages to the EtO sterilization, it has been proven to be an industrial hazard for the people working in the sterilization process.

Low-temperature gas plasma is a relatively new technique to be applied for the sterilization of UHMWPE [27]. The technique involves exposing the UHMWPE surface

to the ionized gas at temperatures below 50 °C. Recent work [27,29] shows that gas plasma does not substantially affect the physical, mechanical and chemical properties of UHMWPE. It seems to be an attractive possibility for sterilization of UHMWPE.

2.1.3 Shelf aging

Irradiation of UHMWPE in air results in the formation of free alkyl radicals. Irradiation produces radicals randomly and uniformly throughout the polymer, irrespective of the crystal morphology [7]. The initial radicals formed are essentially alkyl radicals that react with oxygen to degrade to allyl and peroxy radicals. O'Neill et al. [30] evaluated the nature of these free radicals in shelf aging using Electron Spin Resonance (ESR) spectroscopy. They discovered that most of the alkyl radicals reacted within 70 days of irradiation leaving more stable peroxy radicals. Following reaction of alkyl radicals, there was little reduction in the number of spins, suggesting that either peroxy radicals are very stable or are regenerated continuously. They observed peroxy radicals stable up to 130 days of their experiments. Jahan et al., [31] observed that after irradiation peroxy radicals were present after 12 weeks of storage in air at room temperature. Essentially the alkyl radicals react quickly to form peroxy radicals, which are stable and react slowly to form oxidative degradation products. Zagorski and Rafalski [32] determined that the peroxy radicals usually manifest themselves in the form of hydroperoxides.

The reactivity of alkyl radicals is much higher in the amorphous region than in the crystalline region due to larger mobility [7]. Hence cross-links and the reaction between

alkyl radicals and oxygen preferentially occur in the amorphous regions or at the interface between amorphous and crystalline region. Seguchi and Tamura [33] concluded that the kinetics of alkyl radical decay is well explained by the diffusion theory assuming that the decay rate is controlled by the rate of radical migration in the crystallites towards the boundary. No reaction takes place in the crystalline region because of negligible diffusion of oxygen molecules. The radical migration was through a hydrogen abstraction mechanism, and was governed by a diffusion coefficient of 3.0×10^{-18} cm^2/sec at 20 °C. They also commented that the apparent stability of peroxy radicals could be because of their non-mobility, preventing the peroxy radicals to react.

The chief product of oxidation in UHMWPE are ketones, others being aldehydes, acids, peroxides, polyenyls and esters. Ketones are found to the extent of 75 percent of all the degradation products formed [6,7,12,14]. The concentration of ketone is low at the surface and increases up to 2 mm from the surface and then decreases leading to the formation of a subsurface peak [10,11,14]. Coote et al. [14] made studies on shelf-aged components for 2, 4, 6 and 8 years. They observed that the growth in ketone concentration was slow for the first four years but rapidly increased up to eight years. This suggests that the formation of ketone accelerates with the time of shelf aging. There are studies [9,34], which report on the role of hydroperoxide in the ageing mechanism with debate on its participation in the oxidation of the polymer. Coote et al. [14] made some important discoveries regarding the hydroperoxide profiles with the depth of polymer. In their experiments, the shelf ages for hydroperoxide profiles were from 2 to 8 years, the same components used for determination of ketone concentration. For shelf

aging, the hydroperoxide concentration dropped from the surface up to around 250 μm (0.025mm) below the surface and then remained constant with depth of polymer. The change in the profile from 2 to 8 years was imperceptibly small suggesting that the hydroperoxide remains unusually stable over years of shelf aging or reaches steady or equilibrium state. The profiles for hydroperoxide obtained by Coote et al. [14] are given in Figure 2.1.

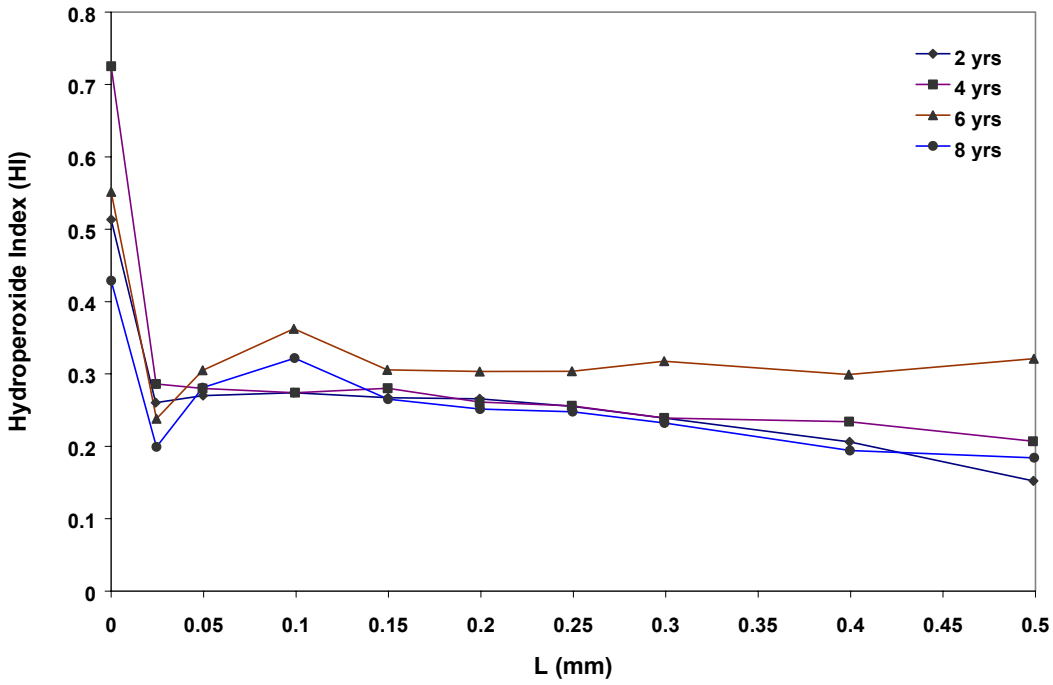

Figure 2.1: Concentration profile of hydroperoxide with depth of polymer for different years of shelf aging [14]

Costa et al. [35] made studies on the other species formed due to oxidation of the polymer. They observed distinct formation of esters and acids in EtO sterilized components, though low in concentration. For the gamma-sterilized components in air,

they detected ketone and ester groups. For one component, gamma-sterilized, they discovered the white band showing the presence of ketones and hydroperoxides. The authors did not find ketones at the surface, an observation similar to Coote et al. [14]. The oxidation level in gamma-irradiated components were at least one order of magnitude higher than those for EtO-sterilized polyethylene components. They commented that formation of ketones did not explain the oxidative degradation process in whole but must also add hydroperoxide formation.

The species are usually determined using Fourier Transform Infra Red (FTIR) spectroscopy. Thin slices of polymer about 50 – 100 μm are microtomed from the cross-section of articulate surface. For determination of species, they have to be first made IR active i.e. there should exist sufficient dipole moment on the functional group to absorb Infra red radiation. Ketones are IR active and absorb radiation at 1718 cm^{-1}. Ketones are determined in terms of Oxidation Index (O.I.), which is defined in terms of the height of the carbonyl peak to the height of the methylene peak.

$$O.I. = \frac{Carbonyl \quad Peak \quad Height \quad (1718 \quad cm^{-1})}{Methylene \quad Peak \quad Height \quad (1370 \quad cm^{-1})}$$

For species such as hydroperoxide and alcohols, which are not so active, they are treated with gaseous NO to form corresponding nitrites and nitrates, which are IR active. The hydroperoxides are characterized using hydroperoxide index, which is defined as the ratio of the height of the secondary hydroperoxides (secondary nitrate) peak to the height of the methylene peak.

$$H.I. = \frac{Secondary \quad Nitrate \quad Peak \quad Height \quad (1630 \quad cm^{-1})}{Methylene \quad Peak \quad Height \quad (1370 \quad cm^{-1})}$$

Coote et al. [14] did not observe the presence of nitrites meaning that alcohols were not present or if present they were below detectable range of IR. The acids are estimated as acid fluorides after reaction with SF_4. Ester identification is carried out with NH_3 or KOH [35].

2.1.4 Accelerated aging

The process of natural oxidative degradation takes years and it is not possible to wait that long for data to be available when testing new materials. Hence, the oxidation of polymer is frequently carried at elevated temperature and pressure of oxygen. Elevation in temperature and pressure leads to the increase in the relative rates of degradation reactions. Accelerated aging has been studied extensively with a combination of elevated temperatures and oxygen partial pressures [14,15,27,36]. In accelerated aging studies, the temperature has ranged from 60 to 127 °C, the oxygen pressure has been varied from pure oxygen to 102 atmospheres [15] and the aging duration is typically from 1 to 28 days. Sun et al. [37] provided with an accelerated aging protocol where specimens were thermally aged at 80 °C for up to 23 days with a slow initial heating rate of 0.6 °C/min. They compared the results with up to 10 years of shelf-aged components irradiated in air. They observed that maximum oxidation index for accelerated aging for above protocol compared well with seven to nine years of shelf aging. Though the peaks compared well,

their position were misplaced. The maximum oxidation index for shelf aged polymer were at the subsurface and those for accelerated aging were present at the surface. Coote et al. [14] also made this observation, albeit for different accelerated aging conditions.

McKellop et al. [38] made another interesting observation regarding accelerated aging. They compared the accelerated aging oxidation index profiles with four-year old retrieved component. They concluded that the results obtained for accelerated aging would be reasonably similar to the retrieved components.

2.2 Chemical reaction model

The literature [6,23,24,30,39,40,41] provides various chemical reactions considered to be occurring involving alkyl radicals formed after irradiation of PE and oxygen diffusing into the polymer. The most common among the ones discussed in the literature are presented below. (The bracketed terms denote the general notation that will be used throughout this paper since it is easy to handle them, with the asterisk (*) denoting radical species).

1) $R\text{-}CH_2\text{-}R_1\ (RH) \rightarrow R\text{-}CH^*\text{-}R_1\ (R^*) + H^*$

2) $R\text{-}CH^*\text{-}R_1 + O_2 \rightarrow R\text{-}CH(O\text{-}O^*)\text{-}R_1\ (RO_2^*)$

3) 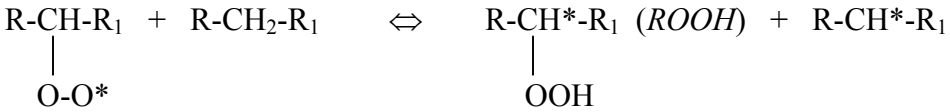

4) 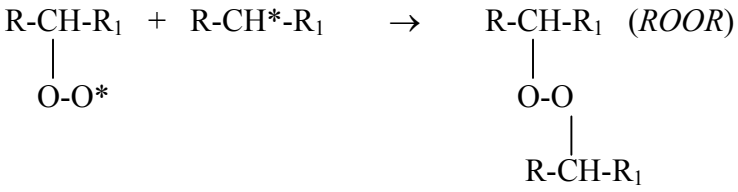

5) 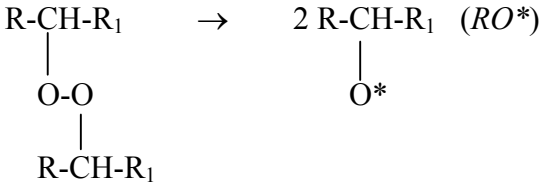

6) 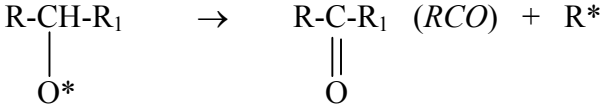

7) 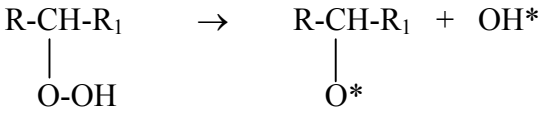

8) 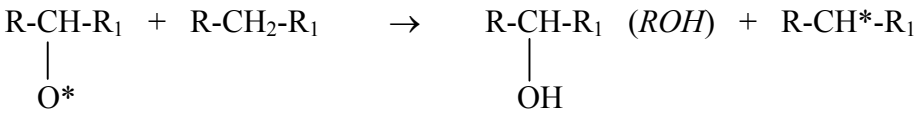

9) 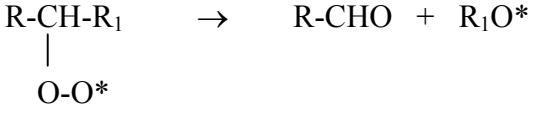

10) $R_1O^* \rightarrow R_2CHO + H^*$

11) $H^* + H^* \rightarrow H_2$

12) $2\ R\text{-}CH^*\text{-}R_1 \rightarrow$ 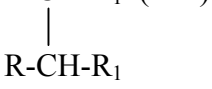 (*R-R*)

13) $OH^* + R\text{-}CH_2\text{-}R_1 \rightarrow R\text{-}CH^*\text{-}R_1 + H_2O$

14) $R\text{-}CHO + O_2 + 2\ R\text{-}CH_2\text{-}R_1 \rightarrow$ 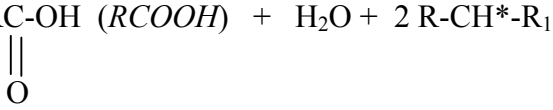

15) $RCOOH +$  $\rightarrow$ 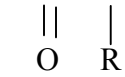 (*RCOOR*) $+ H_2O$

16)  $\rightarrow$ acids, esters etc.

17)  $\rightarrow$  $+ H_2O$ (*cage reaction*)

The reactions can be written in more compact form as follows:

01) $RH \rightarrow R^* + H^*$

02) $R^* + O_2 \rightarrow RO_2^*$

03) $RO_2^* + RH \rightarrow ROOH + R^*$

04) $RO_2^* + R^* \rightarrow ROOR$

05) $ROOR \rightarrow 2RO^*$

06) $RO^* \rightarrow RCO + R_1^*$

07) $ROOH \rightarrow RO^* + OH^*$

08) $RO^* + RH \rightarrow ROH + R^*$

09) $RO_2^* \rightarrow RCHO + R_1O^*$

10) $R_1O^* \rightarrow R_2CHO + H^*$

11) $H^* + H^* \rightarrow H_2$

12) $R^* + R^* \rightarrow R\text{-}R$ (cross linking reaction)

13) $RH + OH^* \rightarrow R^* + H_2O$

14) $RCHO + O_2 + 2RH \rightarrow RCOOH + H_2O + 2R^*$

15) $RCOOH + ROH \rightarrow RCOOR + H_2O$

16) $ROOH \rightarrow$ acids, esters, etc.

17) $ROOH \rightarrow RCO + H_2O$

where R_1 is a radical specie and R_2 is alkane chain with a functional group formed due to scission of long alkane molecules with terminal carbon radical.

In reaction (16) hydroperoxides degrade to products such as acids, aldehydes, and esters [6,42,43]. Since there is no information available on the exact nature of these reactions, or the quantification of the concentration of acids, esters etc., we would only consider that ROOH decomposes to give oxidative degradation products. The formation of ketones from hydroperoxides (by the cage reaction (17)) was contested in the literature not to occur in the polymer at the conditions of shelf aging and for accelerated aging [24]; we will assume that the hydroperoxide decomposition (if it occurs) will not yield ketones.

Reactions (14) and (15) are not elementary reactions but involved many steps. But for completeness and to be brief we have added the reactions in the final form. Further the species involved in these reactions are ones that are involved only in those reactions and do not affect other elementary steps. We will consider models that involve the formation of ketones as all our models were fitted to the experimental ketone concentration. Further, there is no experimental data available for species such as aldehydes, alcohols, esters, and acids, in quantitative form to involve them in any form of model. Coote et al. [14] worked on the determination of alcohols by derivatization with NO but did not observe them. Hence it was our hypothesis that either alcohols were not formed or were formed in negligible amount. Tabb [44] obtained similar results in his studies. Thus, we neglected reactions (7) and (8). Reaction (1) takes place during irradiation and the alkyl radicals are present during the aging period. During post irradiation, reaction (1) does not occur and hence it does not figure in the oxidation process. The hydrogen termination reaction occurs very rapidly and hydrogen readily diffuses out of the polymer. For our study, we considered that reaction (11) had already

taken place and hydrogen did not remain in the polymer to have any effect on post irradiation process. Reactions (9) and (10) do not have any experimental validation to include them in mathematical formulation and also they are least likely reactions to occur [12]. Hence the models that are considered are based on the following reactions:

1') $R^* + O_2 \rightarrow RO_2^*$

2') $RO_2^* + RH \rightarrow ROOH + R^*$

3') $RO_2^* + R^* \rightarrow ROOR$

4') $ROOR \rightarrow 2RO^*$

5') $RO^* \rightarrow RCO + R_1^*$

6') $R^* + R^* \rightarrow R_2$ (*cross-linking reaction*)

7') $ROOH \rightarrow$ acids, esters, etc.

We assumed that the decomposition of ROOR and the corresponding reaction of RO* was very fast [41]. Hence, reactions (3'), (4'), and (5') were combined to form an overall reaction as follows:

$RO^* + R^* \rightarrow 2RCO + 2R^*$

And the set of reactions of interest becomes:

1") $R^* + O_2 \rightarrow RO_2^*$

2") $RO_2^* + RH \rightarrow ROOH + R^*$

3") $RO_2^* + R^* \rightarrow 2RCO + 2R^*$

4") $ROOH \rightarrow$ acids, esters, etc.

5") $R^* + R^* \rightarrow R_2$ (*cross-linking reaction*)

When the polymer was irradiated, it was assumed that the free radicals were equally distributed in the amorphous and crystalline region. The proportion of each region was assumed to be 50% each [7,9,45]. The radicals in the crystalline region are locked and not easily accessible to the oxygen due to very low diffusion coefficient in crystalline domains [7,9]. Hence, the majority of the radicals that undergo reaction were from the amorphous region. Out of these, many radicals cross-linked to form branched chains (reaction 5"). Some of them reacted with oxygen to undergo a series of reactions leading to the degradation of the polymer. The usual percentage of R* that undergoes oxidative degradation was quoted to be around 10% in the literature [7,30,46].

2.3 Earlier Simulation and Modeling:

The starting point for our simulations was the paper by Daly and Yin [12] who developed a model to explain the subsurface oxidation behavior. They proposed the following model that was developed by the combination of various elementary steps, which resulted in:

$R^* + O_2 \rightarrow RO_2^* \quad (k_1)$

$R^* + RO_2^* \rightarrow RCO + 2R^* \quad (k_2)$

Table 2.1: List of physical parameters of the polymers used by Daly and Yin for simulation of their model. The rate constants were obtained by best fit.

Length of the polymer	1.42	Cm
D_{O2} diffusion coefficient	1.14×10^{-9}	Dm^2/s
O_2 conc. at the surface	7.23×10^{-5}	mol/L
Initial R* conc.	6.98×10^{-3}	mol/L
Age of the component	10.9	Years
Rate constant k_1	0.13×10^{-2}	L/mol. s
Rate constant k_2	0.95×10^{-5}	L/mol. s

The system parameters that they determined are given in Table 2.1. Their model was able to fit the experimental data values with reasonably good precision, but there were limitations and flaws with the derivation of the model that make it unacceptable. One, the model does not have any provision for hydroperoxides. In fact to develop the model, the authors assumed that the hydroperoxides decomposed immediately as soon as they were formed which runs contrary to the observed behavior [14]. Further, the model could not explain the almost constant concentration of hydroperoxide profile with time. Two, the derivation of the second reaction step was obtained by addition of alkyl radicals (R*) to both sides of an elementary equation making it seem that one ketone molecule is

formed by the reaction of alkyl radical and peroxy radicals, that is, initially their derivation reached the equation:

$$RO_2^* \rightarrow RCO + R^*$$

Adding R* on both sides, they derived

$$R^* + RO_2^* \rightarrow RCO + 2R^*$$

Reaction between R* and RO_2* is given in literature [41], but gives two molecules of ketones per molecule of peroxy radical reacted:

$$R^* + RO_2^* \rightarrow 2RCO + 2R^*$$

The addition of an alkyl radical on both sides of the reaction step would be right arithmetically but not from the kinetics point of view since the formation of ketones now included the concentration of alkyl radicals in the rate equation. Next, from the derivation of the model, the concentration of alcohols formed should be half of that of the ketone concentrations, but Coote et al. [14] did not find any alcohols in the system. Finally, 100% of the initial alkyl radical concentration was assumed to react, which is not true since several studies suggest that most of the alkyl radicals cross-link immediately after irradiation [7,23,30,46].

2.4 Simulations and Modeling

We made use of the above system parameters and attempted to develop a more viable model that could explain the ketone as well as the hydroperoxide profile sufficiently well. Our further attempt had been to apply these models to various processing conditions such as aging under the presence of reduced oxygen, in vacuum or inert environment and in-vivo aging, accelerated aging, effect of higher and lower irradiation dose on the ketone concentration. We present some of the models that we have evaluated to explain the polymer degradation. Our attempt is to fit the experimental data taken from Daly and Yin's paper [12] with the simulated ketone formation employing various models. To do this we optimized the rate constants employing various optimization techniques discussed in Chapter 3.

Chapter 3

Optimization techniques

3.1 Introduction

The parameters that best fit the experimental curve were determined by minimizing the difference between the experimental and the simulated data. The parameters that characterized the system were involved in non – linear partial differential equations. As an example to show how the techniques were applied, the experimental data used were the ketone concentration from Daly and Yin's paper. If Y*i*(X*i*) represents the experimental ketone concentration values and S*i*(X*i*) are the simulated ones obtained by solving the partial differential equations, the function to be minimized was

$$F = \sum_i (S_i(X_i) - Y_i(X_i))^2$$

The parameters were selected by the optimization algorithm in such a manner that the function kept decreasing. The search of the best parameters was terminated when the function F fell below an acceptable value. There were numerous techniques available to solve the problem. We show two techniques we employed in determination of the best rate constants.

3.2 Direct Search Method for optimization [Edgar and Himmelblau (47)]

The technique was very simple. To explain the technique of optimization, we pick the simple example of Daly and Yin's model [12]. This model was considered because it employed two reaction rate equations and thus two rate constants. This made it convenient to explain the techniques employed for the optimization of our models. The reaction system in Daly and Yin's model [12] was given as follows:

$R^* + O_2 \rightarrow RO_2^* \quad (k_1)$

$RO_2^* + R^* \rightarrow RCO + 2R^* \quad (k_2)$

Writing the mass balance in partial differential equation form we have

$$\frac{\partial[O_2]}{\partial t} = D\frac{\partial^2[O_2]}{\partial x^2} - k_1[O_2][R^*]$$
$$\frac{\partial[R^*]}{\partial t} = -k_1[R^*][O_2] + k_2[RO_2^*][R^*]$$
$$\frac{\partial[RO_2^*]}{\partial t} = k_1[R^*][O_2] - k_2[R^*][RO_2^*]$$
$$\frac{\partial[RCO]}{\partial t} = k_2[R^*][RO_2^*]$$

In the above set of partial differential equations, there are two parameters viz. k_1 and k_2, which once determined, should give us the solution to the set of equations. These are the parameters to be determined in such a manner that the function F falls below an acceptable value.

We started with a guess value of the rate constant parameters. The direct search technique followed a simple step procedure.

1) It increased one of the parameters, say k_1, by a pre – set incremental value given by Δk_1. The simulated ketone concentration values were evaluated at this new rate constant and then we evaluated the function F. We stored this value as F_1 corresponding to F ($k_1 + \Delta k_1$, k_2).
2) Similarly the technique then decreased the value of the first rate constant by the same incremental value Δk_1. The function was evaluated at this new rate constant and stored in a value F_2 corresponding to F ($k_1 - \Delta k_1$, k_2).
3) Next, the technique selected the function that has smaller of the two values (F_1 or F_2). It retained the rate constants that gave the minimum function as the new set of refined rate constants. For example, if $F_2 < F_1$, then the new rate constants are $k_1 = k_1 - \Delta k_1$ and $k_2 = k_2$.
4) It checked whether the function $F = F_2$ had dropped below the termination criteria. If it did, then the technique stopped and the rate constants were returned as the best rate constants. If not then the technique proceeded to step 5.
5) Similarly as in step 1 and 2, the technique evaluated $F_3 = F (k_1, k_2 + \Delta k_2)$ and $F_4 = F (k_1, k_2 - \Delta k_2)$, where Δk_2 was an incremental value in F_2.
6) Given the next two function values, the technique then compared the value and selected one that was minimum and refreshed the rate constants. It then checked whether the function had dropped below the termination criteria. If it did, then the

technique stopped and the rate constants were reported as the best rate constants. If not then the procedure was repeated from step 1.

The technique can be well represented by a figure for a two-dimensional function such as the model above. The Figure 3.1 shows the contours of a decreasing function on a two-dimensional plane with decreasing values toward the center of the plane. The search was successful when the optimization technique took the function to the bottom of the "well".

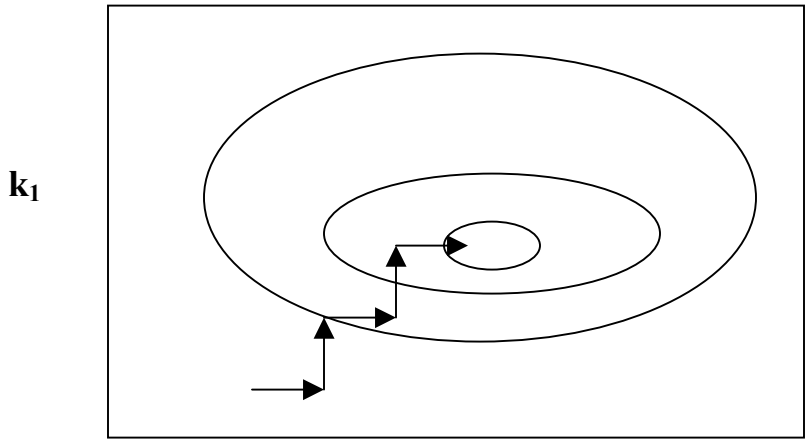

Figure 3.1. Function approaches minimum with steps taken parallel to the axis of the plane.

The Direct Search technique begins as shown with an initial guess and then proceeds by picking the rate constants that minimize the function F. The technique is very well suited for optimization of two parameters.

3.2.1. Sequential Programming:

The nature of the solution technique was sequential in nature, which meant, we needed to solve for each increment and decrement. This sequential problem was written in Fortran 77 to apply the technique to minimize the function for Daly and Yin's model. The time required for the minimization program to run sequentially on an IBM RS/6000 SP 7044-270 workstation, 375 MHz and 64-bit single processor was 1153.8 sec or 19.23 minutes. This time went up with the number of parameters to be optimized. To implement the above optimization program, we sequentially changed the value of each rate constant (parameter) to determine the function value, the program kept a record of all the function values determined and then compared to evaluate the minimum. The evaluation of the function value for each rate constant was the time consuming part of the iteration. To decide on the next best pair of rate constants, the algorithm had to evaluate four function values corresponding to increment and decrement in each rate constant and then compared the four to decide on the best.

3.2.2 Parallel Computation [48]

Evaluation of the each function value corresponding to each increment and decrement of the rate constants (parameters) is an independent process with respect to each other. This means, $F(k_1, k_2)$, $F_1(k_1 + \Delta k_1, k_2)$, $F_2(k_1 - \Delta k_1, k_2)$, $F_3(k_1, k_2 + \Delta k_2)$ and

F_4 (k_1, k_2 - Δk_2) can be evaluated independently by different processors without affecting each other and then brought together to compare. In sequential programming each function is determined independently, one after another and at the end compared for the minimum function. But if we employ five parallel processors to compute each function individually, the time required to compute one function can now be effectively used for computing five function values simultaneously. Hence, it was thought worthwhile to invest time in writing a parallel algorithm to evaluate all the five function values at the same time employing 5 parallel processors, and then using the fifth processor to compare the best value. This way the time required to evaluate the function value for one set of rate constants was now utilized for evaluating five function values simultaneously, thereby effectively reducing the time of computation.

The parallel computation was carried out on IBM RS/6000 SP, a UNIX operated machine with 16 nodes, 2 processors on each node, totaling to 32 processors. The IBM SP uses MPI (Message Passing Interface) as message passing library, a consortium-produced standard used by all of the parallel and distributed processing machine vendors. When operated on SP, the program was divided into smaller tasks to be carried out, and assigned to different processors. A master processor or the root processor that controlled the I/O from different processors was assigned. Each processor computed the task given to it and returned the answer to the root. The root then decided further actions to be taken based on the algorithm (copy in appendix A.3). The I/O between processors took place through MPI. There were two modes of running the program:

1) **Interactively**: This method was used when the program was to be used interactively i.e. there would be I/O of data during the running of the program. This had a disadvantage; the processors were accessed when they are available. For example if processor 1 was busy due to other programs running on it, then the CPU time required to compute a task would be higher which in turn would affect the operation of other processors. Depending on the way the parallel program is written, the other processors would have to wait idly until processor 1 completed the task. Hence, this method was not used, as it would essentially not give the correct time of computation.

2) **Batch process**: This method was used when there was no I/O to be carried out when the program was running. The SP would allot a definite task period for all the processors thus giving the correct time of computation. This method was used to run the program.

In the present case, we had the root processor (processor 0) accept all the constants, boundary conditions, etc., and broadcasted them to four other processors. The processors were always numbered and depending on which number processor was running, corresponding action was taken. Hence, if we had to optimize a two parameter function such as one the for Daly and Yin's model [12], $F(x_1, x_2)$, then we carried out the following optimization procedure:

Evaluate

$F_1 = F(k_1 + \Delta k_1, k_2)$

$F_2 = F(k_1 - \Delta k_1, k_2)$

$F_3 = F(k_1, k_2 + \Delta k_2)$

$F_4 = F(k_1, k_2 - \Delta k_2)$

The four function values that were the difference functions were computed by each processor simultaneously. After each function was evaluated, the values were sent to the root processor that compared the values of all the functions and kept the one that was minimum. The root processor employed MPI_REDUCE and MPI_MINLOC to find the minimum function. It checked for the termination criteria and if not met then the corresponding rate constants were broadcasted to the four processors and the process continued until the function F fell below termination criteria.

The parallel program was written in MPI, compiled and run on the super computer. The optimization was carried for Daly and Yin's model [12]. The rate constants obtained by Daly and Yin's model [12] were:

$k_1 = 0.13E\text{-}02$

$k_2 = 0.95E\text{-}05$

Employing the direct search method for optimization, we obtained the following results:

1) The best value for k's in sequential programming:

$k_1 = 0.1312E\text{-}02$

$k_2 = 0.9208E\text{-}05$

2) The best value for k's in parallel programming:

k_1 = 0.1318E-02

k_2 = 0.9740E-05

The direct search method gave a good estimate of the rate constants and was quite accurate on the order of magnitude. It would have been possible to go for better estimate by decreasing the criteria for termination, but that would have unnecessarily consumed a lot of computation time and it would never had pin pointed the exact values since the method would only oscillate at the bottom of the "hill". Manually zeroing on the best rate constants and comparing by eye often achieved finer results.

The results for optimization on SP 6000 are given below:

Time for sequential program (A): *1153.8 sec*

Time for parallel program (using 5 processors; B): *253.62 sec*

Ideal speedup (C; number of processors) = *5*

Realized speedup (D = A/B) = *4.55*

Efficiency = (C/D)*100 = *91%*

One would observe that the computation time was reduced by 4.55 times with parallel computation. The efficiency would never be 100% because no program can be made completely parallel. There are always sequential parts to be carried out such as I/O, and in our case selecting the minimum function from the set of five functions determined.

The number of processors to be employed increased with the number of parameters to be optimized in the order of $2n + 1$ where n were the number of parameters.

The efficiency suggested that the effort of parallelizing the program was worth the time saved in computation. This had further implications as we went for optimization of more than two parameters.

3.3 Levenberg – Marquardt (LM) method for optimization of non – linear systems

The technique of Direct search method though was appropriate for two parameter system, for higher parameter systems, the method would converge very slowly and usually did not converge on the values that would give a good fit. To overcome the problem we had to turn to techniques that would not only converge fast but also on the global minimum. For non – linear systems, the most popular technique used is Levenberg – Marquardt method for optimization.

The L-M method falls in the broad class of Gradient method. It is an indirect method of optimization i.e. here the search for the minimum value was not carried out by determining several function values and then finding the minimum but considering that the function would have zero gradient at the point of extremum.

If F ($\mathbf{x}$) is a function of n different independent variables denoted by vector $\mathbf{x}$, then at the extremum we have

∇ F ($\mathbf{x}$) = 0 where ∇ F ($\mathbf{x}$) is a partial derivative of F with respect to each variable.

The negative gradient ($-\nabla$ F ($\mathbf{x}$)) gives the direction of steepest descent in an optimization process. Thus during optimization, the next best values are determined by moving in the direction of steepest descent that would take you to the minima.

Search direction = s = $-\nabla$ F ($\mathbf{x}$)

$$\mathbf{x}^{k+1} = \mathbf{x}^{k} + \lambda^{k} s^{k}$$

where λ is the step size to be taken in the direction of descent and k is the k^{th} iteration during the search for the minima.

Chapter 4

Models

4.1 Model 1: Reversible formation of ROOH

4.1.1 Shelf aging

One of the observations made by Coote et al. [14] about the constant hydroperoxide profile and high temperature aging indicated that the reaction of formation of hydroperoxide could be reversible. The reaction scheme considered is given as follows:

1) $R^* + O_2 \rightarrow RO_2^*$ (k_1)

2) $RO_2^* + RH \leftrightarrow ROOH + R^*$ (k_2/k_3)

3) $RO_2^* + R^* \rightarrow 2RCO + 2R^*$ (k_4)

Writing the partial differential equations to represent the system we have:

$$\frac{\partial[O_2]}{\partial t} = D\,\frac{\partial^2[O_2]}{\partial x^2} - k_1[O_2][R^*]$$

$$\frac{\partial[R^*]}{\partial t} = -k_1[R^*][O_2] + k_2[RH][RO_2^*] - k_3[ROOH][R^*] + k_4[RO_2^*][R^*]$$

$$\frac{\partial[RO_2^*]}{\partial t} = k_1[R^*][O_2] - k_2[RO_2^*][RH] + k_3[ROOH][R^*] - k_4[R^*][RO_2^*]$$

$$\frac{\partial[RCO]}{\partial t} = 2k_4[R^*][RO_2^*]$$

$$\frac{\partial[ROOH]}{\partial t} = k_2[RO_2^*][RH] - k_3[ROOH][R^*]$$

The above set of partial differential equations was solved using a forward difference explicit method. There are four parameters (rate constants) that had to be

optimized by fitting the experimental curve with the simulated data values. The optimization involved minimizing the difference between the experimental and the simulated values. Levenberg-Marquardt method of non-linear optimization was employed to get the desired rate constants. There are few assumptions and simplifications made in the simulation of all the following models:

1) The diffusion constant value given by Daly and Yin [12] (1.14×10^{-9} dm^2/sec) did not fit their experimental data with our models. This is partly because the initial alkyl radical concentration considered for our models was 10% (to be explained in point 6) of the initial alkyl radical concentration considered by Daly and Yin [12]. For lower concentration of alkyl radicals, the diffusion of oxygen has to be low so that right amount of oxygen is available to form the ketone subsurface peak. So we used the diffusion constant as one of the parameters to be optimized. The diffusion constant value obtained by Daly and Yin [12] was experimentally measured and diffusion constant values reported in our work were all fitted values. In all the models discussed in this chapter, the diffusion constant values were approximately half that reported by Daly and Yin (1.14×10^{-9} dm^2/sec) [12] and around one third reported in the literature (1.57×10^{-9} dm^2/sec) [49]. Our fitted values were 0.58×10^{-9} and 0.64×10^{-9} dm^2 /sec.

2) The rest of the constants such as the polymer block dimensions, the permeability of oxygen used were the same as determined by Daly and Yin [12].

3) At the start of the shelf aging process, oxygen equal to the solubility of it in PE at 25 °C was considered to be present in the component. The solubility of oxygen in the polymer decreases slightly [49] with increase in temperature. For our simulation of accelerated aging at 80 °C, we neglected the change in the solubility of oxygen in the polymer. This will not have any perceptible effect on the results.

4) The PE was assumed to be composed of 50% crystalline and 50% amorphous region. The alkyl radical distribution was assumed to be uniform throughout the polymer (through the crystalline and amorphous region), as found in an earlier study [14].

5) The crystalline region is not accessible to the oxygen due to very low diffusivity [7], and hence we assumed that the alkyl radicals trapped in the crystalline region did not undergo oxidative degradation.

6) Due to the low mobility of the polymer chains in the crystalline region [7,9] these alkyl radicals last for a long time without undergoing major reactions except cross-linking to some extent. In the amorphous regions, alkyl radicals cross-link to a very large extent leaving around 20% of the initial alkyl radical concentration in the amorphous region (10% of the overall initial alkyl radical concentration) to react with oxygen to form various products [7,30,46,50]. For all our models, the initial alkyl radical concentration value, $R_i = 7.60 \times 10^{-4}$ mol/L gave a very good fit for ketone species. The value for initial alkyl radical concentration determined by Daly and Yin [12] for their model was 6.98×10^{-3} gmol/L. As mentioned as one of Daly and Yin's drawbacks, they

did not consider the cross-linking reactions and hence used this value for fitting their model. Our value of initial alkyl radical concentration for the best fit (remaining after cross-linking reaction in the amorphous region) was ~11% of the initial alkyl radical concentration given by Daly and Yin [12] which agreed very closely to the percentage reported in literature.

7) In the accelerated aging, we assumed all the trapped radicals to be released due to heat effects since the mobility of the polymer chain in the crystalline region increases with temperature. Further negligible amount of initial alkyl radical concentration in the crystalline region would have cross-linked since accelerated aging was carried within days of irradiation.

The best rate constants derived for the model I are given in table 4.1.

Table 4.1: Parameters optimized for best fit between Daly and Yin's experimental data [12] and model 1.

Parameters	Values	Units
K_1	5.50×10^{-3}	L/mol. s
K_2	1.00×10^{-9}	L/mol. s
K_3	7.95×10^{-3}	L/mol. s
K_4	3.75×10^{-4}	L/mol. s
R* (initial alkyl radical conc.)	7.60×10^{-4}	gmol/L
D_{O2} (diffusivity of oxygen in PE)	5.80×10^{-10}	dm^2 / sec

The plot for ketone fit for 10.9 years of shelf aging is given in Figure 4.1.1. The experimental values were taken from Daly and Yin [12].

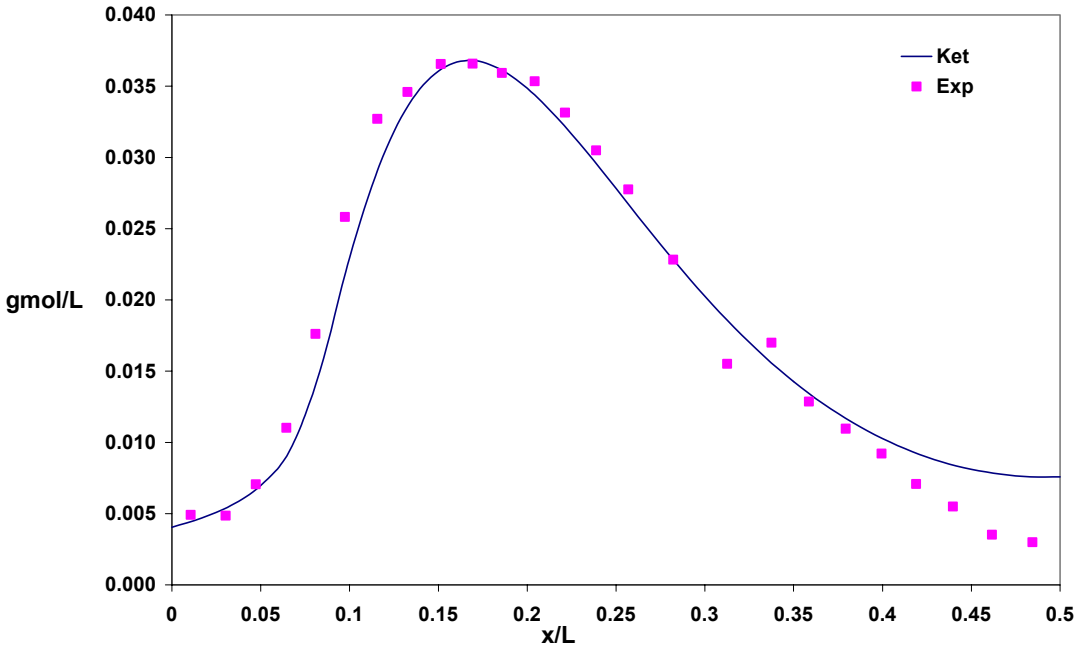

Figure 4.1.1: Ketone conc. for 10.9 years of shelf aging with depth of PE. Experimental data obtained from Daly and Yin's model [8].

.

The model was quite successful in obtaining a good fit to the experimental data. The increase in the concentration of ketones with years of shelf aging was well represented by the model and given in Figure 4.1.2.

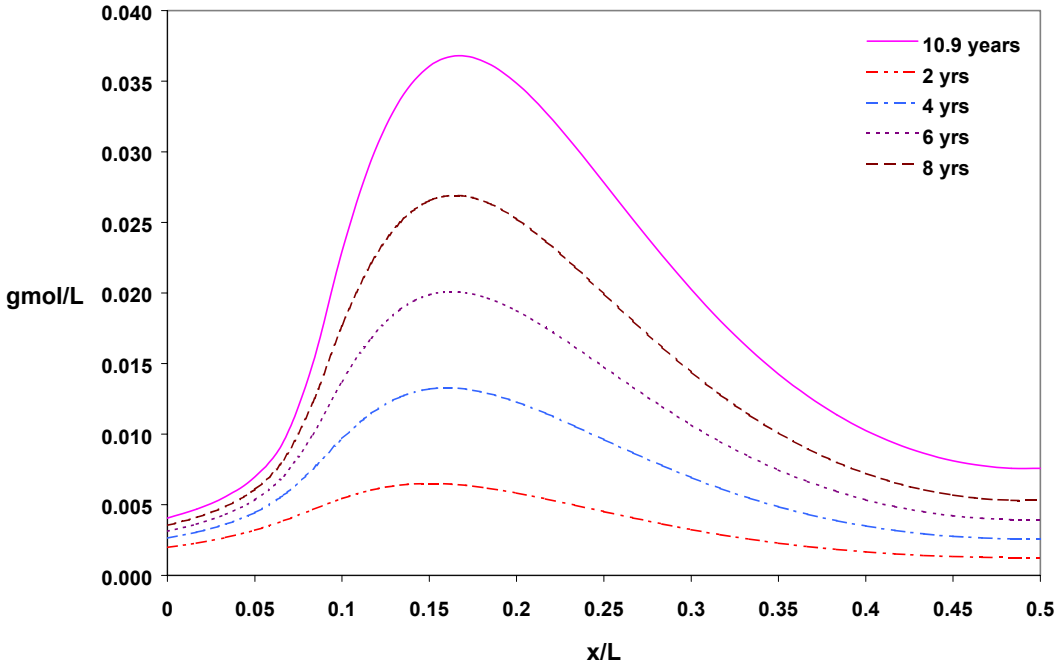

Figure 4.1.2: Variation of ketone concentration with number of years of shelf aging. The concentration increases with shelf age of the PE.

The model can be used to predict the nature of profiles for other species. We plot the hydroperoxide concentration profile with shelf age of the polymer and the results are given in Figure 4.1.3.

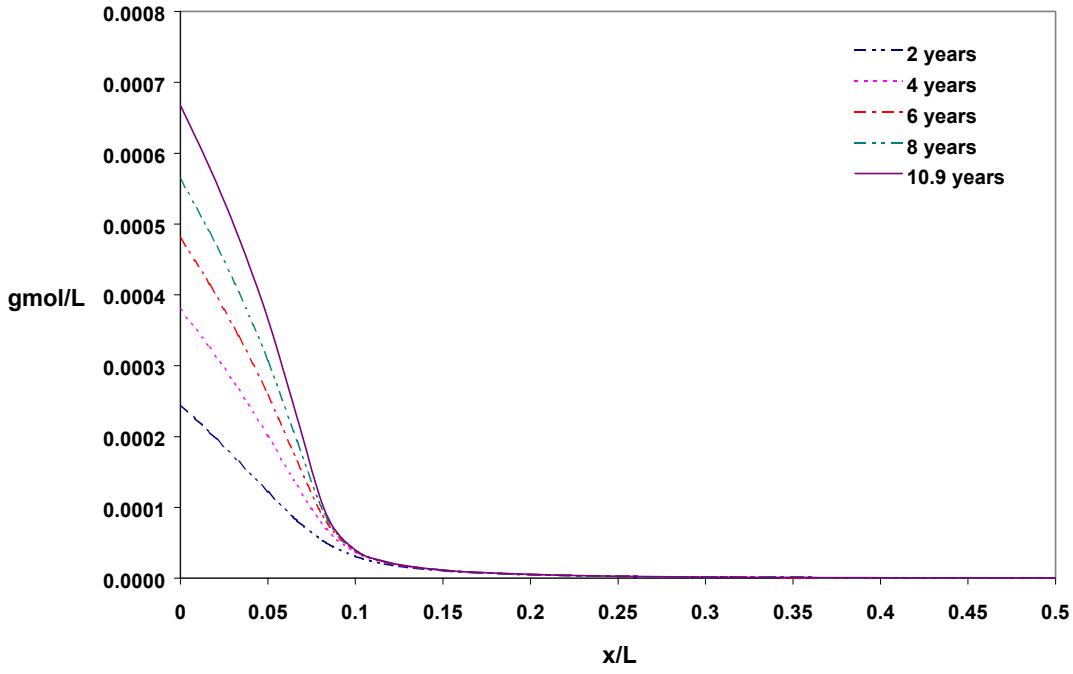

Figure 4.1.3: Hydroperoxide concentration variation with shelf age of PE component. The plot is concentration of hydroperoxide with depth of the polymer

The concentration of hydroperoxide kept increasing with time, especially near the surface. The model fit the experimental values of the ketone but did not gave satisfactory curves for the hydroperoxide profiles with the nature of hydroperoxide curves not similar to what Coote et al. observed [14]. Further the concentration of hydroperoxide did not remain constant with time that was against what Coote et al. observed [14]. The increase in the peak concentration of ketone was linear with time. Studies [12,14,36] have suggested that the increase in peak concentrations were not linear but accelerated with time.

The model was applied to the ketone concentration data for shelf age of 5.8 years from Daly and Yin [12]. The fit to the 5.8 years of shelf aging is shown in Figure 4.1.4.

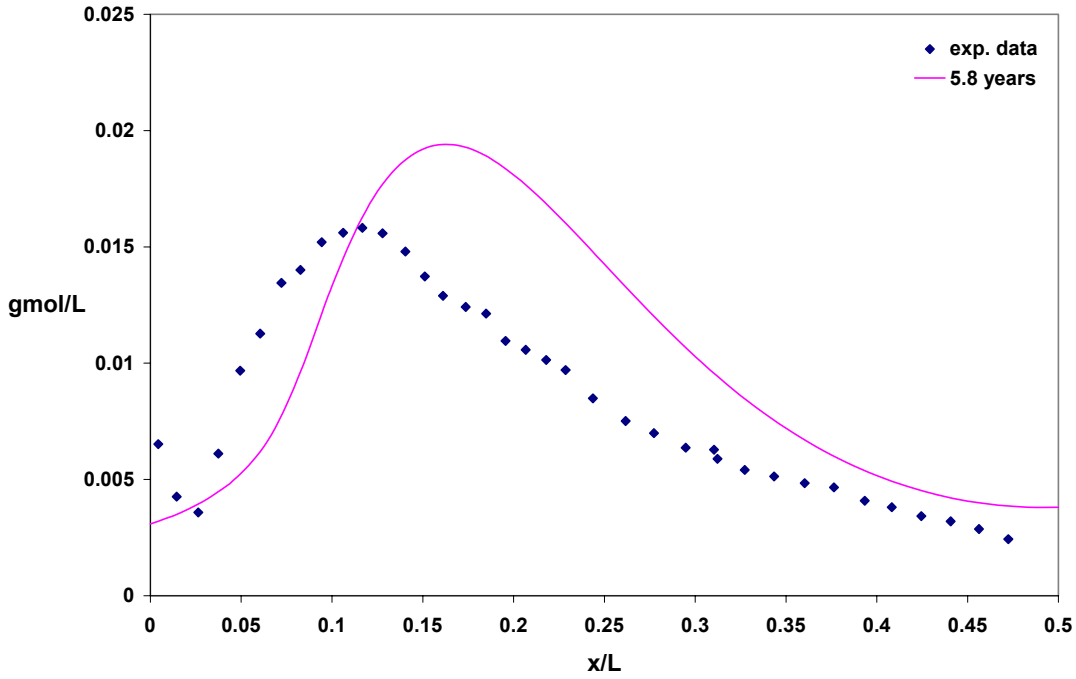

Figure 4.1.4: Ketone concentration profile for 5.8 years of shelf aging obtained by applying model I. Experimental data obtained from Daly and Yin [12].

The ketone profile for 5.8 years did not give a very good fit but captured the nature of the curve. The model predicted larger concentration values for 5.8 years of shelf aging because the model did not provide the accelerated production of ketone with time. The shelf-aged polymer would have lower concentration for lesser years whose formation would accelerate with aging of the polymer.

4.1.2 Accelerated aging

For accelerated aging, we assumed that all the alkyl radicals that were trapped in the crystalline region were released leading to the sudden increase in the concentration of alkyl radicals compared to the O_2 concentration. Further, the aging was usually carried

out for 1 – 13 weeks [14]. Raising the initial concentration of R* to add in the locked 50% of the alkyl radicals from the crystalline region, we plotted the ketone and hydroperoxide profiles for different aging periods of 1, 3, 5, 7, 9, and 13 weeks. Due to increase in the temperature, the rate constants and diffusion constant would increase. Pauly [49], reported an equation for determining the diffusion constant in High Density PE at higher temperature as

$D = Do \times \exp(-E_D/RT)$ where

E_D = 36.8 kJ/mol, D is the diffusivity of oxygen at temperature T (K).

R = 8.3144×10^{-23} kJ/mol. K.

Do is obtained by plugging the value of D determined by optimization at 25 °C (298.15K). Using this value of Do, the diffusivity at 80 °C was determined. It turned out that the diffusivity value increased 10 times at 80 °C.

The value of the rate constants were increased approximately by 10 times the one determined for shelf aging. The aging time considered were same for which Coote et al. determined experimental values i.e. 1, 3, 5, 7, 9, and 13 weeks. The time of aging are arbitrary since the rate constants selected were arbitrary. To get the feel of the variation of hydroperoxide curve, we also plot profiles for 0.01, 0.1, and 0.5 weeks. The values of the parameters are given in Table 4.2

Table 4.2: The parameters for accelerated aging for model I.

Parameters	Values	Units
K_1	5.50×10^{-2}	L/mol. S
K_2	1.00×10^{-8}	L/mol. S
K_3	7.95×10^{-2}	L/mol. S
K_4	3.75×10^{-3}	L/mol. S
R* (initial alkyl radical conc.)	4.25×10^{-3}	gmol/L
D_{O2} (diffusivity of oxygen in PE)	5.80×10^{-9}	dm^2 / sec

The plot for the ketone concentration with depth of PE component is given in Figure 4.1.5 and for hydroperoxide concentration is given in Figure 4.1.6.

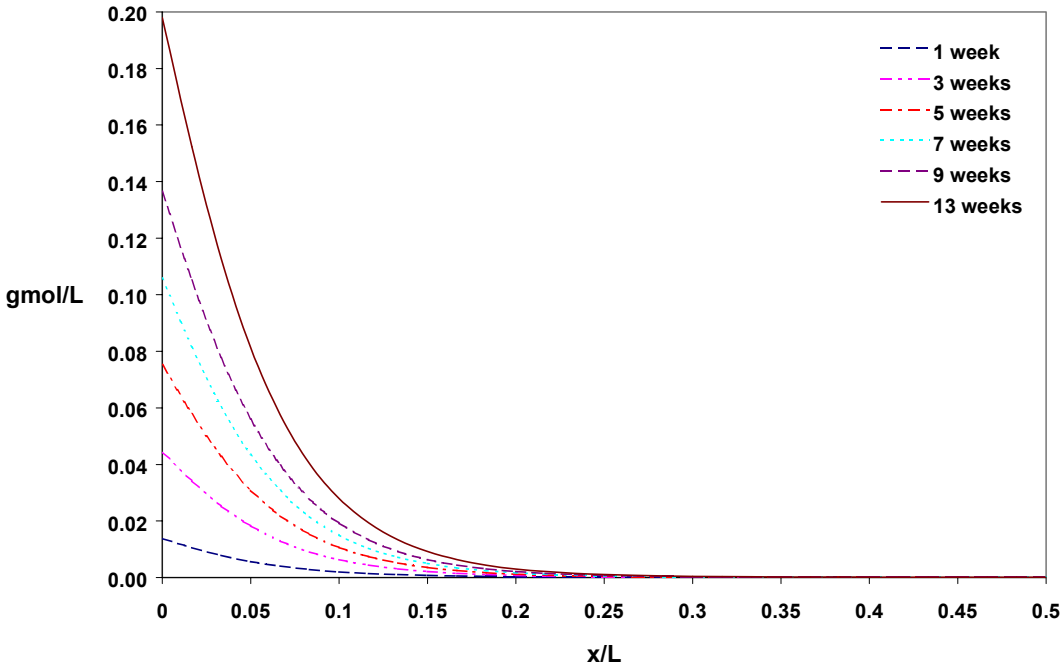

Figure 4.1.5: Variation of Ketone concentration with depth of PE component for accelerated aging. The aging period varies from 1 to 13 weeks. The plot is obtained with model I

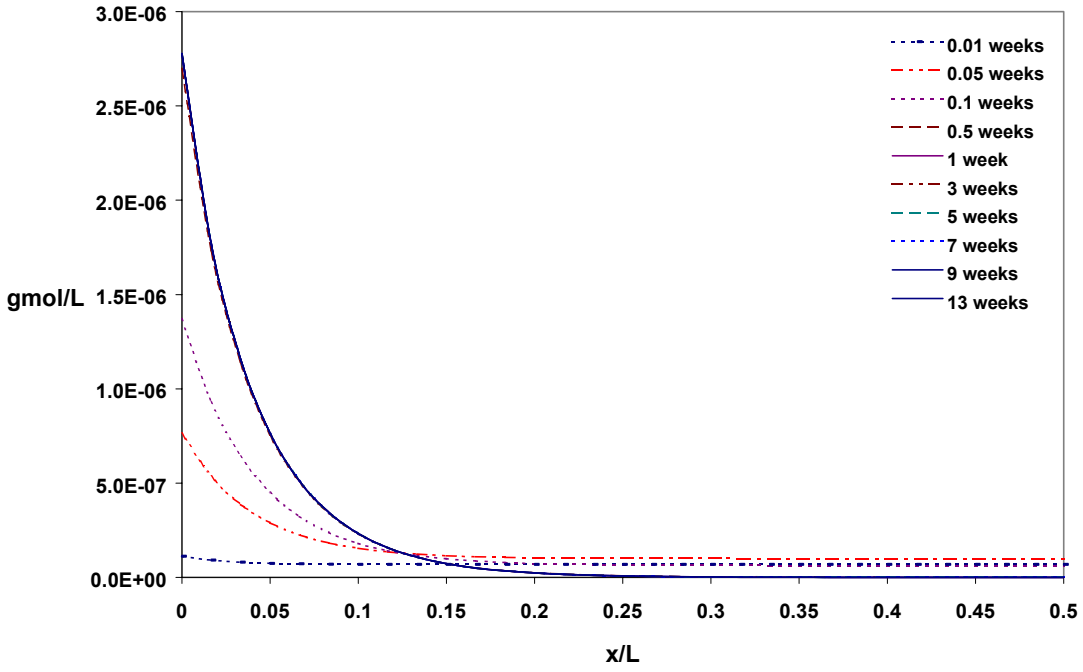

Figure 4.1.6: Variation of hydroperoxide concentration with depth of PE component for accelerated aging of UHMWPE. The plot is made for accelerated aging period varying from 0.01 to 13 weeks. The plot is obtained by model I.

From the accelerated aging profiles, the concentration of ketone kept increasing with time in sync with Coote's et al. [14] observation. The formation of ROOH reached a steady state with a single profile for all periods of accelerated aging of one and more weeks. For time less than 1 week, the hydroperoxide profile increased to the constant value it achieves at 1 week. For time period of 0.01 weeks, which is close to start time, the hydroperoxide showed almost constant concentration profile. The steady profile with time after one week was observed because of the quick formation and simultaneous decomposition of hydroperoxides, maintaining equilibrium. The ketone concentration formed after 13 weeks was higher than those for the shelf aged polymer for 10.9 years in terms of absolute values. This observation was similar to experimental studies made by

Coote et al. [14]. The model did not exhibit the increase and then decrease in the concentration of hydroperoxide.

4.1.3 Shelf aging at reduced oxygen concentration

Many studies have been performed in reduced O_2 atmosphere leading to lower extent of oxidation than those aged in air [46,51]. The studies reported that the oxidation was less severe when the PE was kept in atmosphere containing low oxygen concentration than at higher oxygen concentration. In absence of oxygen (vacuum or inert atmosphere), the shelf aging shows very low oxidation of the polymer. We applied the above model for the case where the shelf aging of the polymer was done in reduced oxygen concentration to determine profiles to be expected. The in-vivo concentration of oxygen is approximately one eighth that of atmospheric oxygen concentration [15] which corresponds to ~ 2%. The oxygen concentration considered were 20% (atmospheric pressure), 10%, 8%, 6%, 3%, 2% (similar to the in-vivo oxygen concentration), and 0% (vacuum or inert atmosphere). Henry's Law relates the solubility of oxygen to the partial pressure of oxygen in the atmosphere:

$$[O_2]_s = S\,[P_{O2}]$$

S (0.00881 mL(stp)/mL atm) is the solubility [12], P_{O2} is the partial pressure of oxygen in atmospheres and $[O_2]_s$ is the corresponding concentration of oxygen in air. Since all the measurements are carried at same temperature, the solubility, which is a function of temperature, remains constant. Hence a half decrease in partial pressure would correspondingly decrease the concentration in half. For partial pressure of 0.2 atm.

(20% oxygen composition), the concentration determined was 7.23 x 10^{-5} gmol/L. For 10% of oxygen, the concentration will be half, 3.62 x 10^{-5} gmol/L, and so on. These values were used as the boundary condition at the external surface.

In the case of the vacuum, we assumed that there was initial oxygen dissolved in the polymer equal to the solubility of oxygen in the polymer at 20% oxygen in air (which usually happens during processing of the polymer under normal atmospheric conditions). The shelf age was 10.9 years. The observations are given in Figure 4.1.7. The ketone peak was predicted to shift towards the polymer surface with reduced oxygen concentration. The ketone peak hit the exposed surface end of the polymer, which occurred at around 6% of the oxygen concentration and then the ketone concentration decreased at the surface. We further observed that there was a minimum concentration of oxygen required to form subsurface ketone peak. The concentration of ketone in vacuum was very low as compared to other profiles and supported the observation about reduced oxidation in the absence of oxygen. Further, assuming that the concentration of oxygen plays major role in in-vivo oxidation, one can get an idea about the intensity of oxidation to be expected in in-vivo performance of the polyethylene at about 2% O_2 (though the role played by mechanical stress on the polymer in in-vivo cannot be neglected and has to be combined with degradation due to oxidation reaction to get complete picture). The model very well demonstrates the importance of the oxygen in the atmosphere near the surface of the polymer.

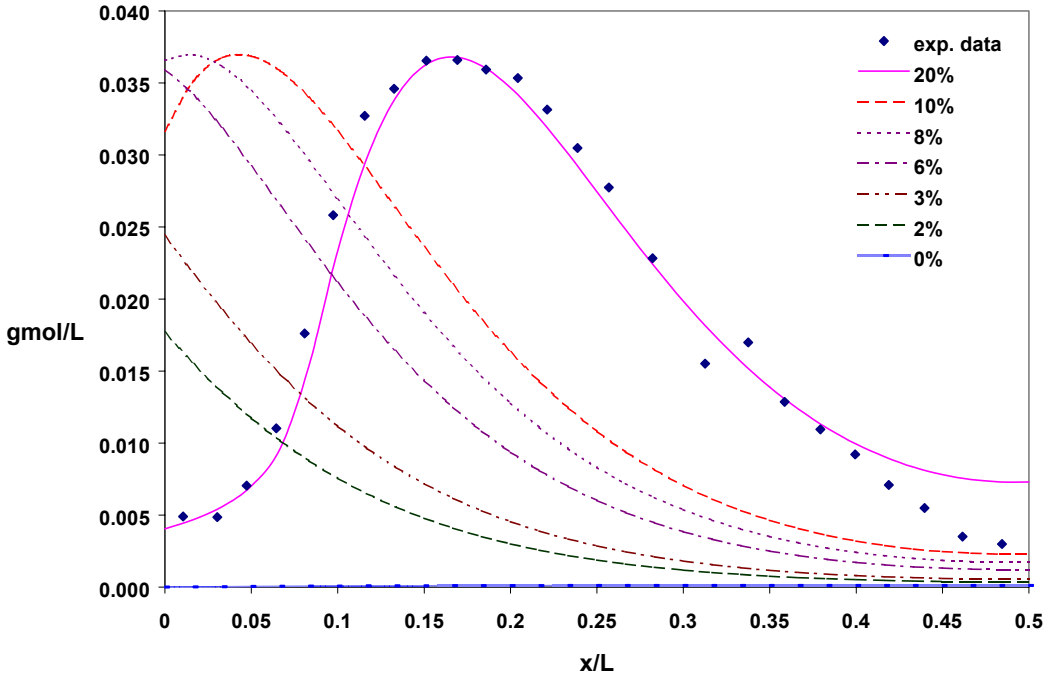

Figure 4.1.7: Ketone concentration profiles with depth of the polymer for decreasing oxygen concentration in contact with polyethylene. The shelf-aging period is 10.9 years. The experimental data is from Daly and Yin [12]. The oxygen curves shift to left with decreasing O_2 concentration.

4.1.4 Shelf aging at different initial alkyl radical concentration

The concentration of alkyl radical formed is directly proportional to the irradiation intensity and dose rate [9]. The increase in the radical concentration is approximately linear with the radiation dose. To understand the effect of the higher radiation dose, we increased the concentration of alkyl radicals in the following order: $1.0R_i$, $1.2R_i$, $1.5R_i$, $2.0R_i$, $3.0R_i$, and $3.5R_i$ where R_i was the initial concentration that we

started with for the above model (7.60 x 10^{-4} gmol/L). The ketone profiles obtained for 10.9 years of atmospheric shelf aging period are given in Figure 4.1.8.

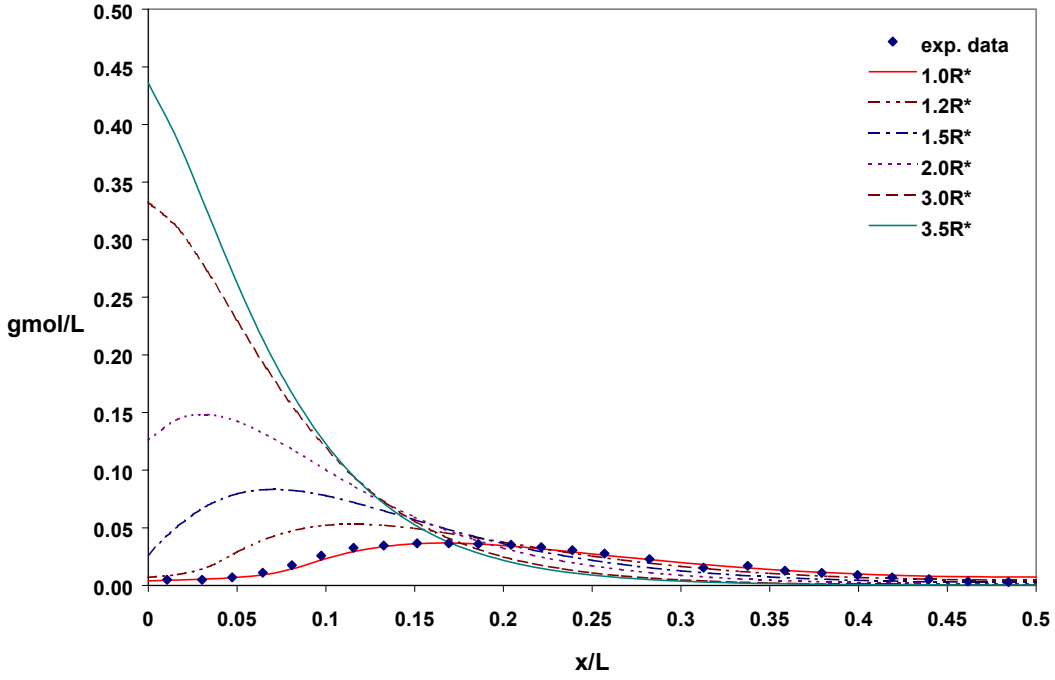

Figure 4.1.8: Variation of ketone concentration with radiation dose for shelf age period of 10.9 years. The ketone concentration increases significantly with irradiation dose with the maximum shifting towards the surface.

We observed in Figure 4.1.8 that for shelf aging period of 10.9 years, the increase in irradiation dose led to increase in the concentration of ketone significantly, causing enhanced oxidative degradation. As the initial alkyl radical concentration was increased, the situation became more similar to accelerated aging process where the concentration of alkyl radicals was high. The ketone curve was predicted to shift to the left with a gradual increase in the peak value. The peak was lost after a much higher initial alkyl radical concentration and the ketone concentration dropped from the surface to the center of the

polymer. The results obtained here support earlier studies about the higher degradation of PE with higher irradiation dose [9]. Much research work has been done to reduce the presence of these alkyl radicals so that oxidative degradation could be reduced by a considerable extent. To get an idea to the nature of the profiles of ketone species expected for shelf aging period of 10.9 years for low initial alkyl radical concentration, we ran the simulation for initial alkyl radical concentration of $1.0R_i$, $0.9R_i$, $0.8R_i$, $0.6R_i$, $0.3R_i$, and $0.1R_i$. The plots of ketone concentration with initial alkyl radical concentration are given in Figure 4.1.9. The aging period was 10.9 years and the experimental data was from Daly and Yin [12]

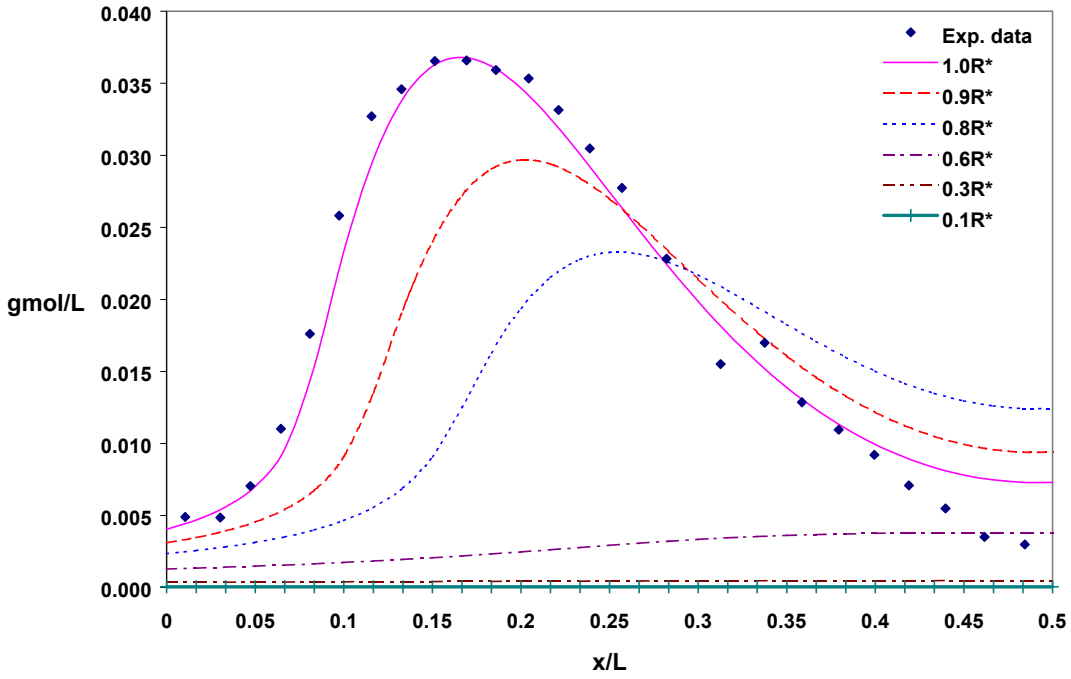

Figure 4.1.9: The variation of ketone concentration with reduced radiation dose for PE shelf aged for 10.9 years. The ketone concentration formation decreases with maximum shifting towards right.

From Figure 4.1.9, we observed that the ketone concentration decreased rapidly with decrease in the initial alkyl radical concentration. The decrease was non-linear. This can be explained with the help of the reaction that involves the formation of ketones. We consider the two reactions that led to the formation of ketones:

$R^* + O_2 \rightarrow RO_2^* \quad (k_1)$

$RO_2^* + R^* \rightarrow 2\,RCO + 2\,R^* \quad (k_2)$

The formation of ketone can be written in partial differential equation as follows:

$$\frac{\partial[RCO]}{\partial t} = k_2[RO_2^*][R^*]$$

When the initial concentration of alkyl radicals decreases, it also reduces the overall concentration of peroxy radicals that would be formed. Thus, in the partial differential equation, the decrease in the right hand term was non-linear since both the alkyl radical and the peroxy radical concentration had simultaneously decreased. Hence, the decrease in the concentration of ketone was non-linear which is a consequence of mass balance.

The ketone peak shifted to the right and then it flattened out at lower concentrations. The model acknowledged the fact that the lower concentration of initial alkyl radicals would lead to lesser amount of degradation.

4.2 Model II: Irreversible formation of hydroperoxide

4.2.1 Shelf aging

The literature provides evidence for the reaction involving degradation of hydroperoxide to products such as acids, aldehydes and esters [35]. Also, there has not been any support to the reversible nature of the hydroperoxide formation reaction, suggesting that formation of hydroperoxides was irreversible. A continuous formation and degradation of hydroperoxide could lead to almost constant concentration over a period of time when both the reaction of formation and consumption of hydroperoxide equate. This might explain the reaction system and especially the constant concentration of hydroperoxide observed by Coote et al. [14].

The reaction scheme considered was as follows:

$R^* + O_2$	$\rightarrow$	RO_2^*	(k_1)
$RO_2^* + RH$	$\rightarrow$	$ROOH + R^*$	(k_2)
$RO_2^* + R^*$	$\rightarrow$	$2RCO + 2R^*$	(k_3)
$ROOH$	$\rightarrow$	acids, esters, etc.	(k_4)

The partial differential equations that models above reactions are as follows:

$$\frac{\partial[O_2]}{\partial t} = D\,\frac{\partial^2[O_2]}{\partial x^2} - k_1[O_2][R^*]$$

$$\frac{\partial[R^*]}{\partial t} = -k_1[R^*][O_2] + k_2[RH][RO_2^*] - k_3[ROOH][R^*] + k_4[RO_2^*][R^*]$$

$$\frac{\partial[RO_2^*]}{\partial t} = k_1[R^*][O_2] - k_2[RO_2^*][RH] + k_3[ROOH][R^*] - k_4[R^*][RO_2^*]$$

$$\frac{\partial[RCO]}{\partial t} = 2k_4[R^*][RO_2^*]$$

$$\frac{\partial[ROOH]}{\partial t} = k_2[RO_2^*][RH] - k_3[ROOH][R^*] - k_5[ROOH]$$

The model for irreversible formation of hydroperoxide was fitted to Daly and Yin's data for 10.9 years of shelf aging [12]. The fit to the data is given in Figure 4.2.1.

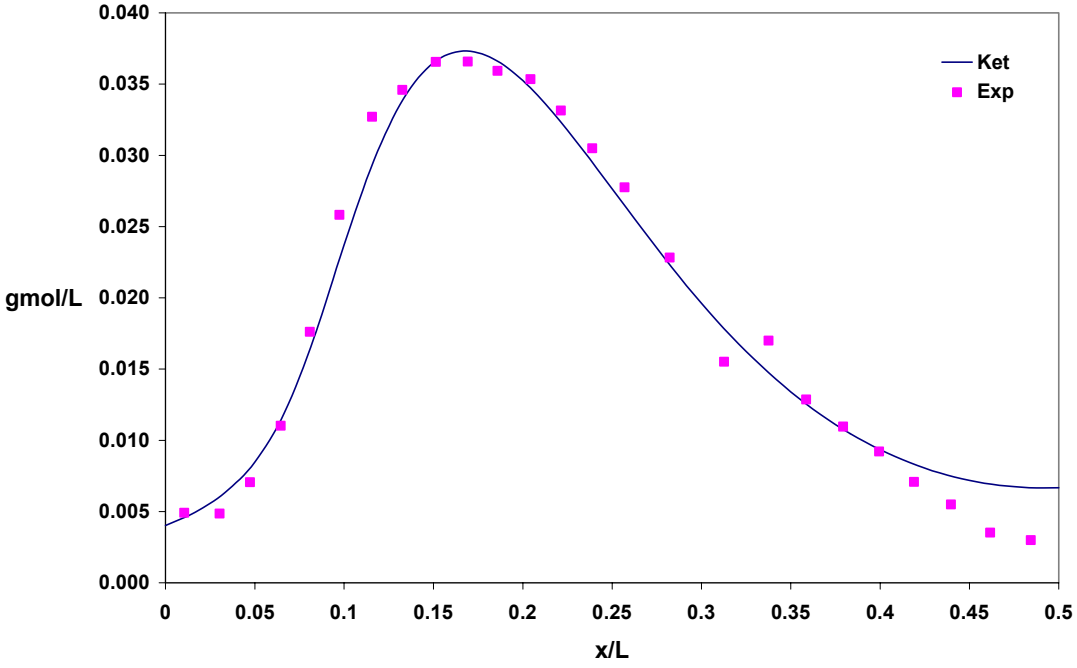

Figure 4.2.1: Ketone concentration fit to the experimental data of Daly and Yin [12] with model II. The shelf age period is for 10.9 years.

The rate constants and parameters that give the best fit for ketone employing model II are given in Table 4.3.

Table 4.3: Parameters obtained for best-fit using model II for Daly and Yin's experimental values [12].

Parameters	Values	Units
K_1	6.00×10^{-3}	L/mol. s
K_2	5.00×10^{-11}	L/mol. s
K_3	3.80×10^{-4}	L/mol. s
K_4	5.00×10^{-7}	1/ s
R_i (initial alkyl radical conc.)	7.60×10^{-4}	gmol/L
D_{O2} (diffusivity of oxygen in PE)	5.80×10^{-10}	dm^2 / sec

The ketone species profiles obtained by model II for different shelf aging period (2, 4, 6, 8, and 10.9 years) are given in Figure 4.2.2. The corresponding profiles for hydroperoxide for different shelf aging period are given in Figure 4.2.3.

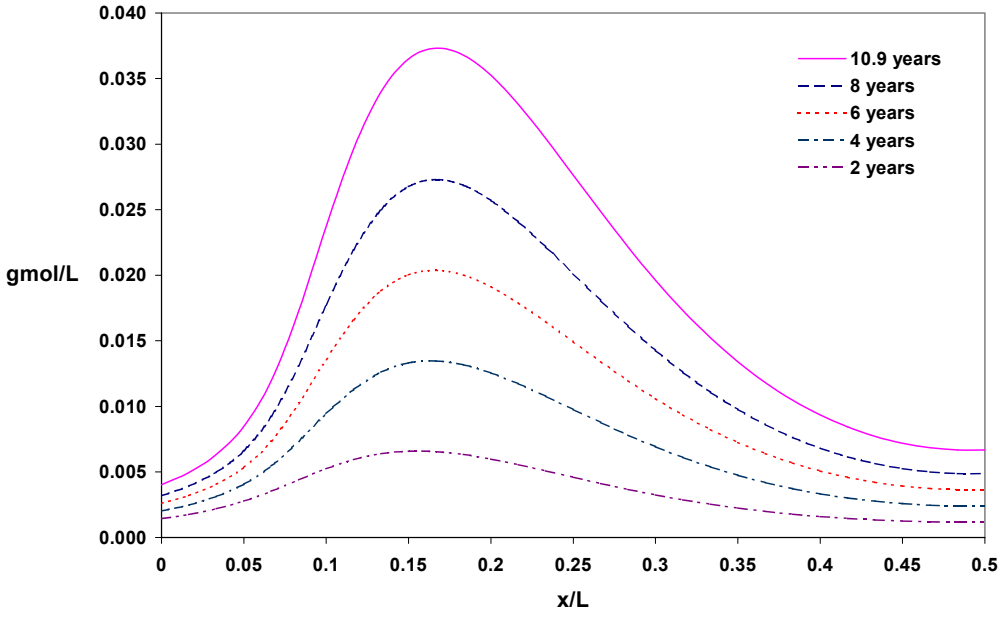

Figure 4.2.2: Ketone concentration profile for different years for shelf aging obtained by employing model II.

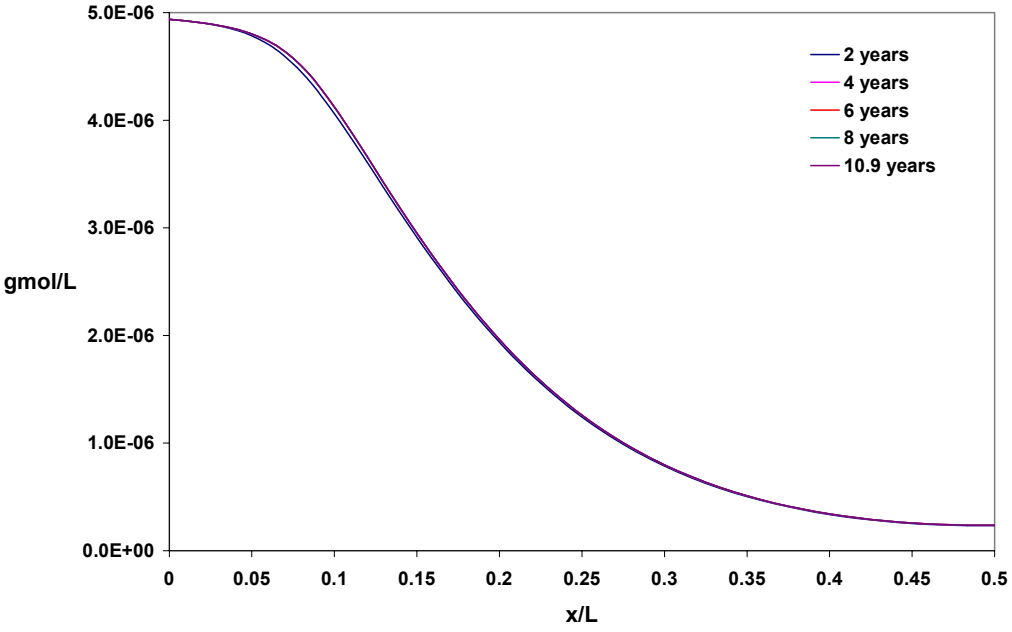

Figure 4.2.3: Hydroperoxide profile obtained for different years of shelf aging employing model II

The model predicted a good fit for the ketone concentration profile with depth of the polymer for Daly and Yin's experimental data (10.9 years of shelf aging). The ketone concentration increased uniformly with shelf age. It did not show accelerated growth in ketone's concentration for shelf aging, which had its effect on the fit for 5.8 years of shelf aging.

The model was applied to the experimental data obtained for 5.8 years of shelf aging by Daly and Yin [12]. The data fit is given in Figure 4.2.4.

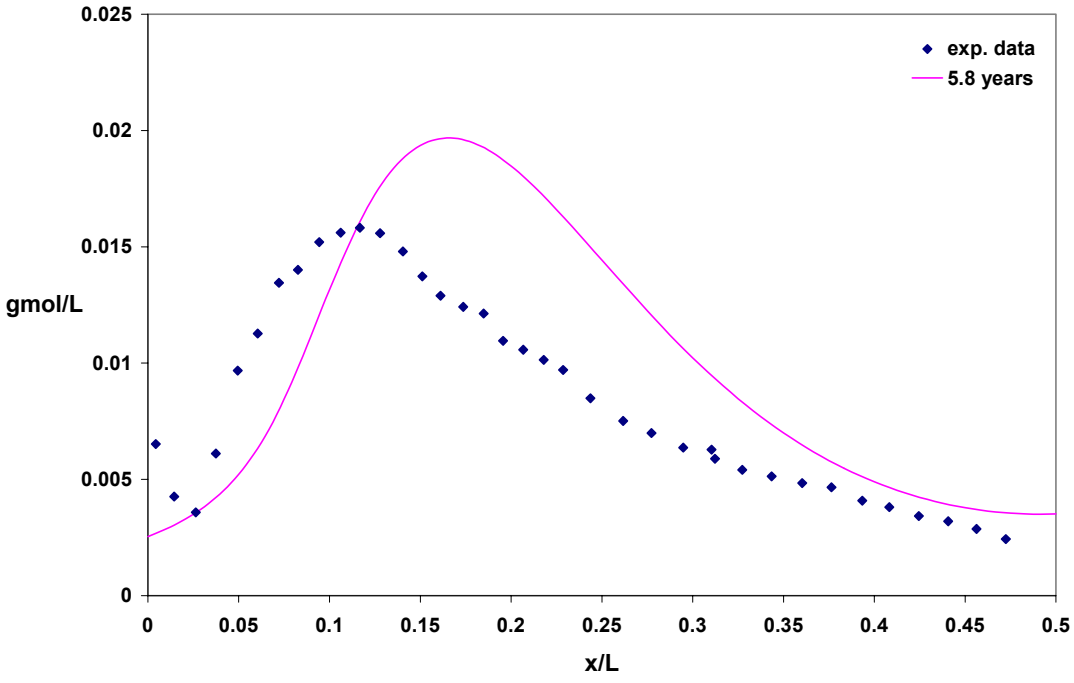

Figure 4.2.4: Ketone concentration profile obtained by Model II for 5.8 years of shelf aging. The experimental data obtained from Daly and Yin [12].

The fit was marginally better than the previous model as the peak was slightly closer to the experimental data peak. The difference in the two plots was due to steady rise in the concentrations of ketones determined by the model, but in reality the ketone shows non-linear (accelerated) growth. The experimental data lies below the predicted curve.

One good prediction by the model for hydroperoxide profiles was that they reached a constant concentration value with shelf age of the polymer. This was similar to what Coote et al. [14] observed. The model gave a good representation as compared to earlier model. The hydroperoxide curve gradually decreased up to 10% of the half-length of the PE component and then fell sharply to level out in the last 10% of the length. In Coote et al.'s profiles for hydroperoxide, the concentration dropped up to 50% of the surface value at around 0.025 mm and then remained constant in the bulk of the component. The hydroperoxide profile obtained by model II drops by an order of magnitude. The model does not adequately confirm to the nature of the Coote et al.'s [14] experimental data for hydroperoxide. The ketone profiles were sensitive to the rate constant for the formation of hydroperoxides (k_2) and were greatly influenced by it. If k_2 was increased, the ketone concentration shifted to left and then decreased. This follows from the fact that peroxy radicals are consumed in the formation of both hydroperoxides and ketones. An increase in the formation of hydroperoxide would deplete the peroxy radicals required for the formation of ketone, thereby affecting the ketone fit to the Daly and Yin's experimental values [12]. For a decrease in k_2, the ketone concentration shifts to the right slightly. The k_2 for correct fit of ketone concentration for 10.9 years of shelf

aging was very low and any decrease beyond two orders of magnitude did not affect the ketone concentration profile.

The rate constant for the decomposition of hydroperoxide (k_4) only affected the final concentration values of hydroperoxide but did not change the shape of the profile. For example consider the 10.9 years of shelf aging (Figure 4.2.5). The hydroperoxide curve obtained was inverse sigmoidal in shape. The absolute value of the hydroperoxide concentration changed with the change in the rate constant k_4 (decomposition of hydroperoxide) but did not affect the sigmoidal shape of the profile. The drop in the hydroperoxide concentration obtained by model II, from the surface value to the bulk was always an order of magnitude. The nature of the hydroperoxide concentration was represented on a relative basis. Only the shape of the hydroperoxide curve was true but not the concentration, the concentration values were dependent on the rate constant for decomposition reaction of hydroperoxide. To fix the hydroperoxide concentration, it would be necessary to fit the model II to hydroperoxide experimental data. Nevertheless it is possible to accomplish it and does not render the effectiveness of the model.

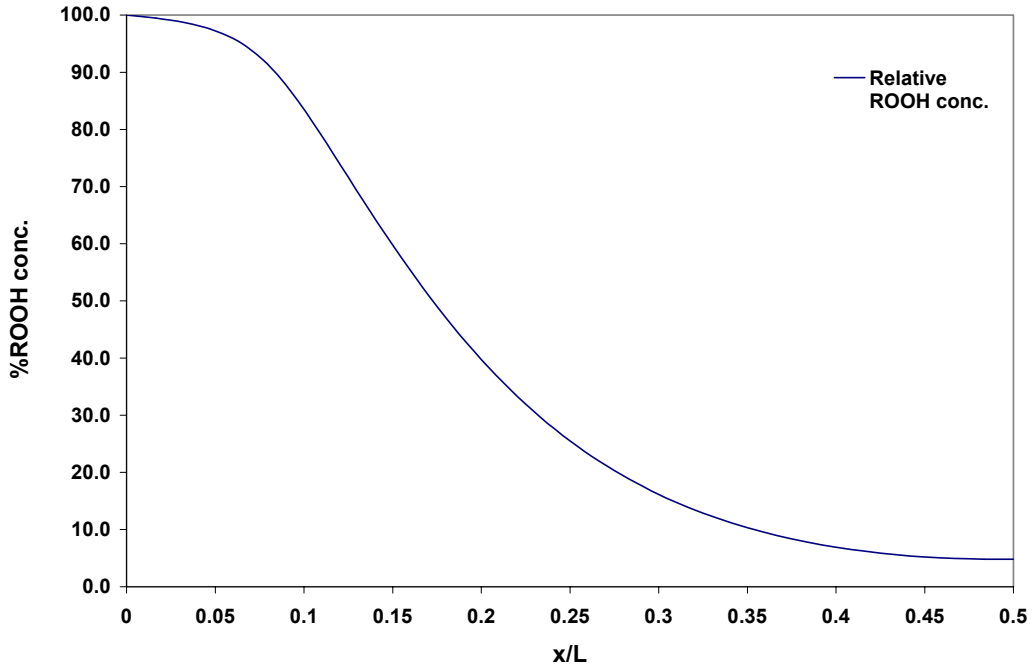

Figure 4.2.5: Hydroperoxide profile for 10.9 years of shelf aging on a relative basis. The nature of the profile is true to the model and not the absolute values in terms of concentration of hydroperoxide, which varies with rate constant for decomposition of hydroperoxide.

The hydroperoxide profiles reached steady value with shelf age of the PE, similar to the experimental work of Coote et al. [14] but did not confirm to the shape of the curve they obtained. The decomposition of hydroperoxide produces products such as esters, aldehydes, acids, etc. The model suggests that these products would only increase with shelf age of the polymer. Costa et al. [42] made similar observations.

4.2.2 Accelerated aging

For accelerated aging, the rate constants were again increased by 10 times the ones for shelf aging and the time of aging was 1, 3, 5, 7, 9, and 13 weeks. For hydroperoxide, to understand the development of its profiles, the time profile for 0.01, 0.05, 0.1, and 0.5 weeks were included. The diffusion constant, by calculations similar to earlier model, was ten times the original fitted value. The initial alkyl radicals now include the ones from the crystalline region released due to the effect of heat. The parameters are given in Table 4.4.

Table 4.4: Parameter for accelerated aging for model II.

Parameters	Values	Units
K_1	6.00×10^{-2}	L/mol. s
K_2	5.00×10^{-10}	L/mol. s
K_3	3.80×10^{-3}	L/mol. s
K_4	5.00×10^{-6}	L/mol. s
R_i (initial alkyl radical conc.)	4.25×10^{-3}	gmol/L
D_{O2} (diffusivity of oxygen in PE)	5.80×10^{-9}	dm^2 / sec

The ketone profiles for accelerated aging are given in Figure 4.2.6 and those for hydroperoxide are given in Figure 4.2.7.

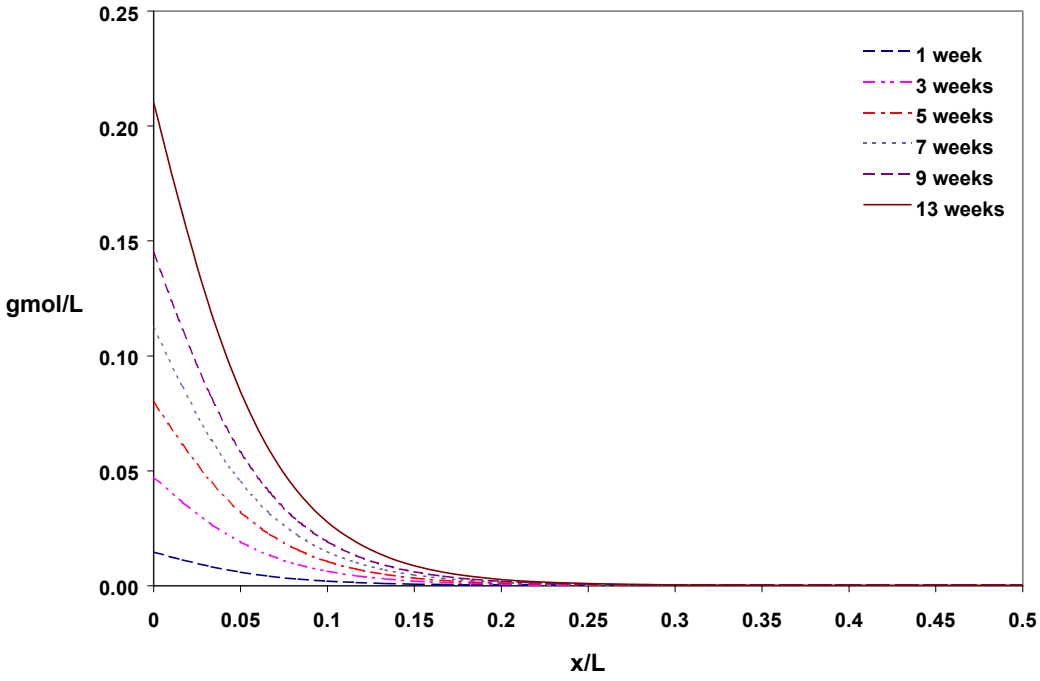

Figure 4.2.6: Ketone concentration for different accelerated aging period obtained employing model II. The ketone concentration increases monotonically.

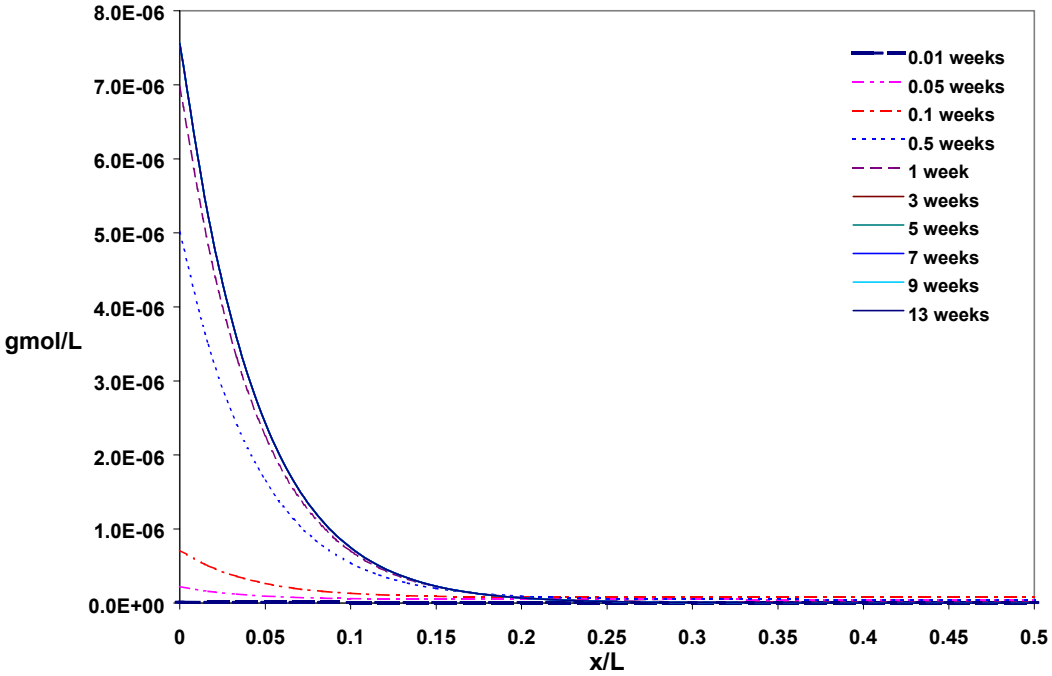

Figure 4.2.7: The hydroperoxide profiles for different accelerated aging period obtained using model II.

The concentration of ketone and hydroperoxide increased with time. The ketone concentration near the surface of the polymer for 13 weeks of accelerated aging, was on an average 5 – 6 times higher than the peak ketone concentration for 10.9 years of shelf aging, an observation resembling close to what Coote et al. observed [14]. The accelerated aging produced more ketones near the surface in terms of absolute concentration. The hydroperoxide curve reached a steady value again suggesting that the hydroperoxide reactions reach a steady state. The hydroperoxide concentration increases from 0.01 weeks up to 0.5 weeks. Then the rate of increase reduces with stabilization of the hydroperoxide profile after 1 week. The experimental hydroperoxide concentration obtained by Coote et al. increased up to 5 weeks and then decreased for accelerated aging [14]. With the formation and decomposition of hydroperoxide during accelerated aging, we expected to capture this behavior. The model did not predict this kind of behavior. Since hydroperoxide was related to the formation of alkyl radicals (reaction (1) & (2)), the hydroperoxide concentration can drop with an initial increase if the alkyl radicals are continuously depleted. This is similar to the chain reaction

$$A \rightarrow B \rightarrow C$$

If the concentration of A were constant at the beginning with no addition of A, B, or C during the reaction, then the concentration of B (which is an intermediate species) would first increase leading to more formation of C. And when the second reaction accelerates due to high concentration of B, the concentration of B would fall.

But from reactions (2) and (3), we have continuous formation of alkyl radicals leading to their sustenance. Hence, it would be unlikely that model II would predict an

increase and then decrease in the concentration of hydroperoxide though it formed an intermediate species. Though the model did not capture the essence of this behavior, the rate of formation of hydroperoxide first increased from 0.01 weeks up to 0.5 weeks and then decreased from 0.5 weeks to 1 week. After that a steady state was reached. The time period in weeks is arbitrary because of the selection of arbitrary rate constants (10 times those at shelf age). Hence the time period of accelerated aging are for representation purpose only.

4.2.3 Shelf aging at reduced oxygen concentration

It was again interesting to observe the effect of reduced oxygen concentration on the ketone profiles with the depth of polymer. The oxygen concentration considered were 20% (atmospheric content), 10%, 8%, 6%, 3%, 2% (in-vivo oxidation atmosphere), and 0% (vacuum or inert atmosphere). The profiles were obtained for 10.9 years of shelf aging and are given in Figure 4.2.8.

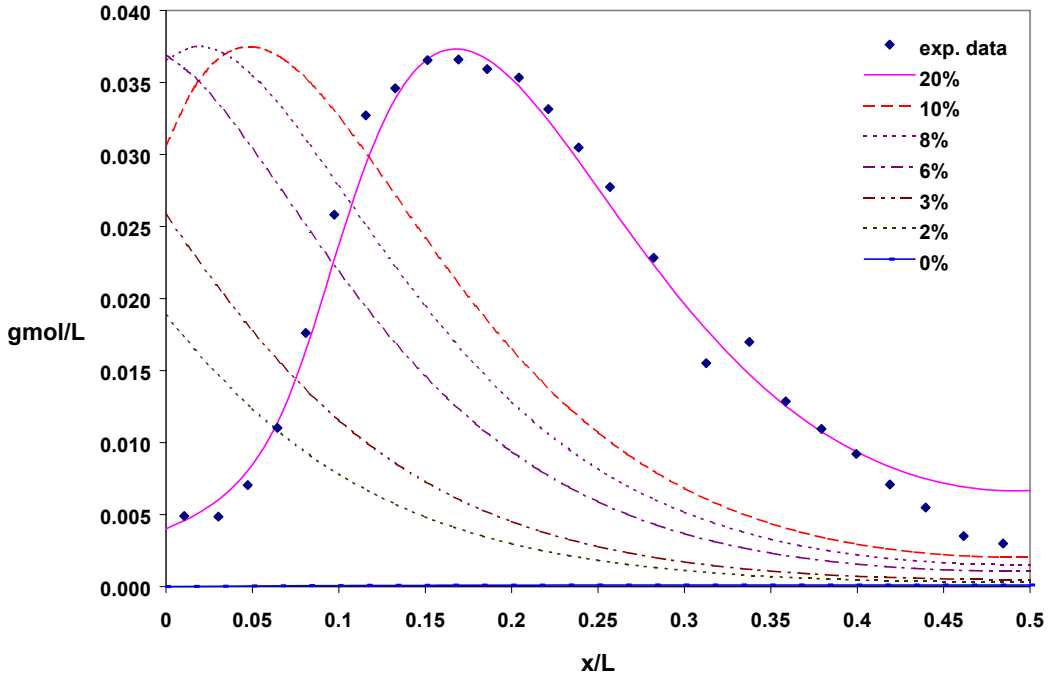

Figure 4.2.8: Ketone concentration profile for reduced oxygen concentration obtained by employing model II. The experimental data is from Daly and Yin [12] for shelf age of 10.9 years.

The peak of the ketone curve shifted to left with decreasing O_2 concentration. For 6% O_2 concentration, the maximum ketone concentration (subsurface peak) occurred at the surface and then the concentration decreased at the surface. The 0% O_2 concentration (inert atmosphere) gave negligible concentration of ketone that supported the facts of occurrence of very low oxidation in the polymer in the absence of oxygen atmosphere [14,52]. This oxidation represents the baseline oxidation due to only the pre – dissolved amount of O_2. All other oxidation results were due to oxygen diffusion. Similar results were obtained for different shelf aging time. For in-vivo oxidation, the maximum concentration of ketone occurred at the surface suggesting that maximum oxidative

degradation would take place at the surface if the polymer orthopedic components were implanted immediately after irradiation. This is rarely the case and there is usually a large period of shelf storage before the PE component is implanted. Hence, in studies reported for failure due to subsurface oxidation of retrieved components [11], the period of aging was from 0 to greater than 8 years.

4.2.4 Shelf aging at different initial alkyl radical concentration

The model was run for the different initial alkyl radical concentration for the shelf age of 10.9 years that correspond to higher initial dose of gamma radiation. The investigation carried out led to profiles very much similar to the former model. The profiles are presented in Figure 4.2.9.

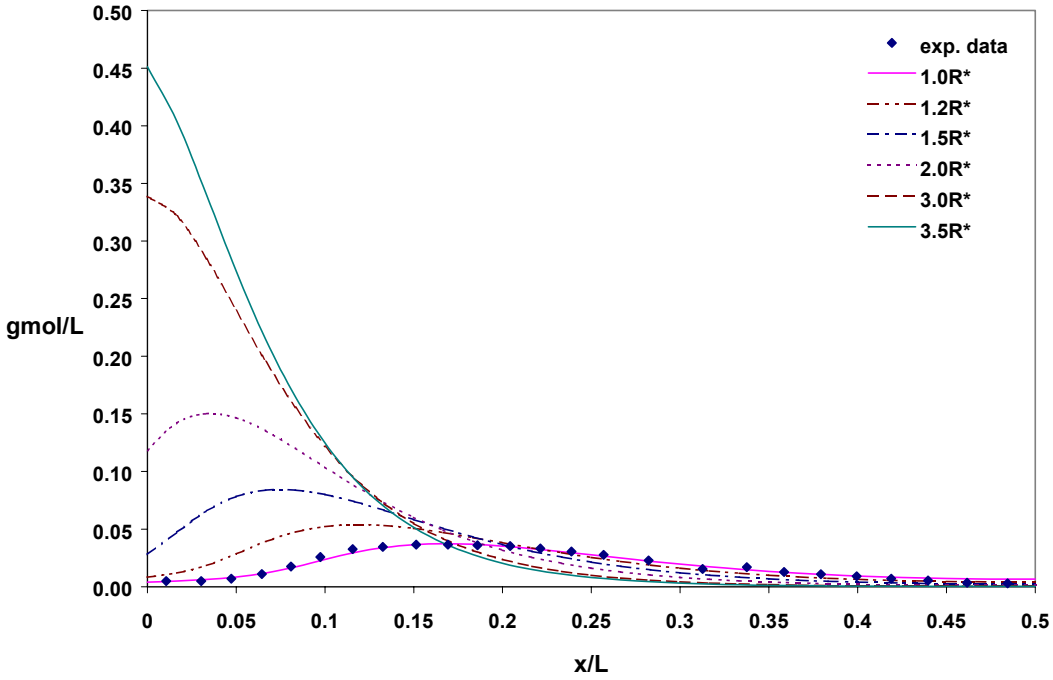

Figure 4.2.9: The ketone concentration variation with higher initial alkyl radical concentration corresponding to higher gamma radiation dose obtained by employing model II. The period of shelf aging is 10.9 years with experimental data from Daly and Yin [12].

From Figure 4.2.9, we observed that the ketone concentration kept increasing and shifted to the left. Hence, irradiation of the polymer at higher dose is not recommended. As studies suggest [23,30,46] extinguishing the free radicals by heat treatment would explain the higher stability of the polymer. As the initial alkyl radical concentration increased, we observed that the profile approached those for accelerated aging (where the trapped alkyl radicals were released for oxidation from the crystalline region). The initial radical concentrations were reduced to see what the model predicted. The concentration values considered were the same considered in the previous model viz. $0.9R_i$, $0.8R_i$, $0.6R_i$, $0.3R_i$, $0.1R_i$ where R_i is the initial alkyl radical determined for shelf aging of the

polymer. The profiles were for 10.9 years of shelf aging and the experimental data were taken from Daly and Yin [12]. The results are given in Figure 4.2.10.

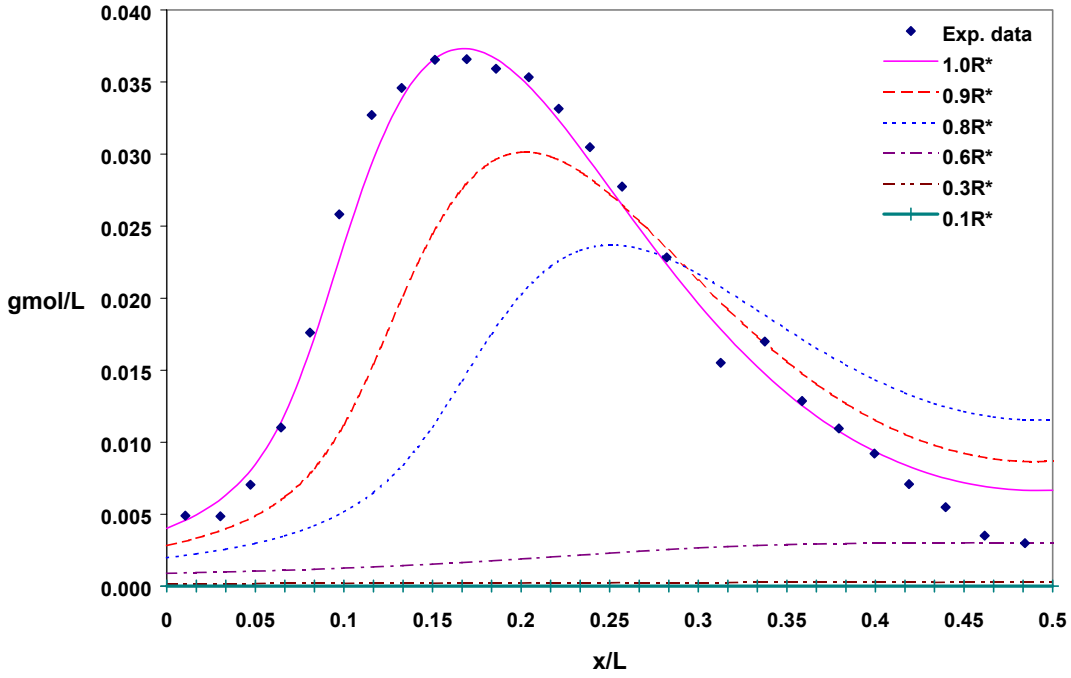

Figure 4.2.10: Ketone concentration profile for low initial alkyl radical concentration corresponding to lower gamma radiation dose or quick extinguishing of the radicals. Experimental data was taken from Daly and Yin [12] for 10.9 years of shelf aging.

The ketone concentration decreased with decrease in the initial alkyl radical concentration. This suggests that low concentration of alkyl radical is preferred to reduce oxidative degradation process. The decrease in the ketone concentration predicted by this model was non-linear. The decrease was sharp between 0.8R* and 0.6R*. The profile for 0.3R* and 0.1 R* are touches the baseline of the plot. The explanation for this non-linear behavior is similar to the one given for model I.

4.3 Model 3: Model based on reaction considered by Petruj and Marchal.

4.3.1 Shelf aging

In the literature, there are various reactions that lead to the formation of ketones. In the case involving radicals, there was one interesting reaction that has been used by Petruj and Marchal [24], to model the formation of ketones and hydroperoxides. The formation reaction involved participation of hydroperoxides but did not lead to their consumption.

The reaction can be shown to occur as follows:

$$RO_2^* + ROOH \rightarrow ROOH + RCO + OH^*$$

$$OH^* + RH \rightarrow R^* + H_2O$$

The reaction can be represented schematically as follows [16]:

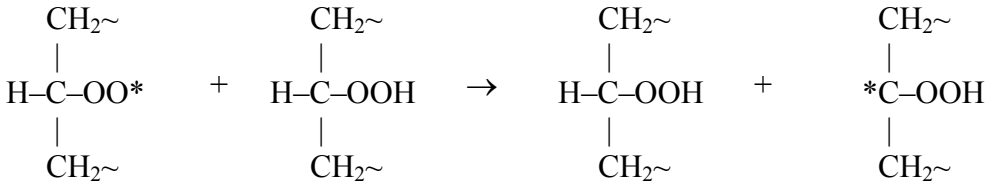

The above form of reaction was noted to occur quite frequently in organic chemistry texts and was our next attempt to understand the chemistry of the degradation process. Degradation of hydroperoxide results in acids, esters etc. as contended in literature [4,49,50]

The following set of reactions were considered:

$R^* + O_2 \rightarrow RO_2^*$ (k1)

$RO_2^* + RH \rightarrow ROOH + R^*$ (k2)

$RO_2^* + ROOH + RH \rightarrow RCO + ROOH + R^* + H_2O$ (k3)

$R^* + R^* \rightarrow R_2$ (k4)

$ROOH \rightarrow$ acids, esters, etc. (k5)

$R^* + RO_2^* \rightarrow 2RCO + 2R^*$ (k6)

Writing the partial differential equations for the above set of reactions:

$$\frac{\partial[O_2]}{\partial t} = D\,\frac{\partial^2[O_2]}{\partial x^2} - k_1[O_2][R^*]$$

$$\frac{\partial[R^*]}{\partial t} = -k_1[R^*][O_2] + k_2[RH][RO_2^*] + k_3[RO_2^*][ROOH][RH]$$
$$- k_4[R^*]^2 + k_6[R^*][RO_2]$$

$$\frac{\partial[RO_2^*]}{\partial t} = k_1[R^*][O_2] - k_2[RO_2^*][RH] - k_3[RO_2][ROOH][RH] - k_6[R^*][RO_2^*]$$

$$\frac{\partial[RCO]}{\partial t} = k_3[RO_2][ROOH][RH] + 2k_6[R^*][RO_2^*]$$

$$\frac{\partial[ROOH]}{\partial t} = k_2[RO_2^*][RH] - k_5[ROOH]$$

The above sets of reactions were optimized for rate constants and diffusion coefficient using Levenberg – Marquardt method for Daly and Yin's [12] experimental ketone concentration data values for shelf age of 10.9 years. The initial alkyl radical

concentration was assumed to be the same considered for previous models. The parameters for best fit obtained are given in Table 4.5.

Table 4.5: The parameters that best fit the experimental data by Daly and Yin [12] with model III.

Parameters	Values	Units
K_1	5.631×10^{-3}	L/mol. s
K_2	1.000×10^{-15}	L/mol. s
K_3	1.203×10^{-3}	L/mol. s
K_4	0.000×10^{-0}	L/mol. s
K_5	0.000×10^{-0}	1/ s
K_6	3.783×10^{-4}	L/mol. s
R* (initial alkyl radical conc.)	7.600×10^{-4}	gmol/L
D_{O2} (diffusivity of oxygen in PE)	5.800×10^{-10}	dm^2 / sec

The optimization for the parameters of model II predicted that the mutual termination of free radicals and the decomposition of hydroperoxides were not likely to occur since $k_4 = k_5 = 0$. It was interesting to note that ROOH decomposition reaction was considered by the optimization program not to occur.

The plots of ketone for 10.9 years of shelf aging in atmospheric oxygen is given in Figure 4.3.1 and for corresponding hydroperoxide curve is given in Figure 4.3.2. The experimental data was taken from Daly and Yin [12].

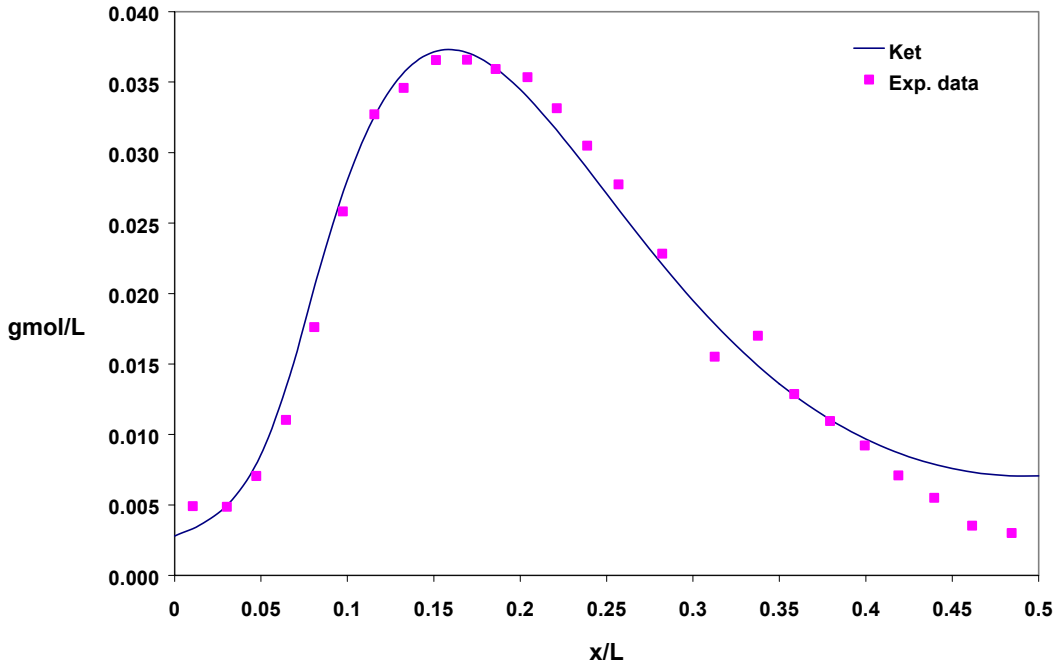

Figure 4.3.1: Ketone concentration plot with the depth of the polymer for shelf aging period of 10.9 years.

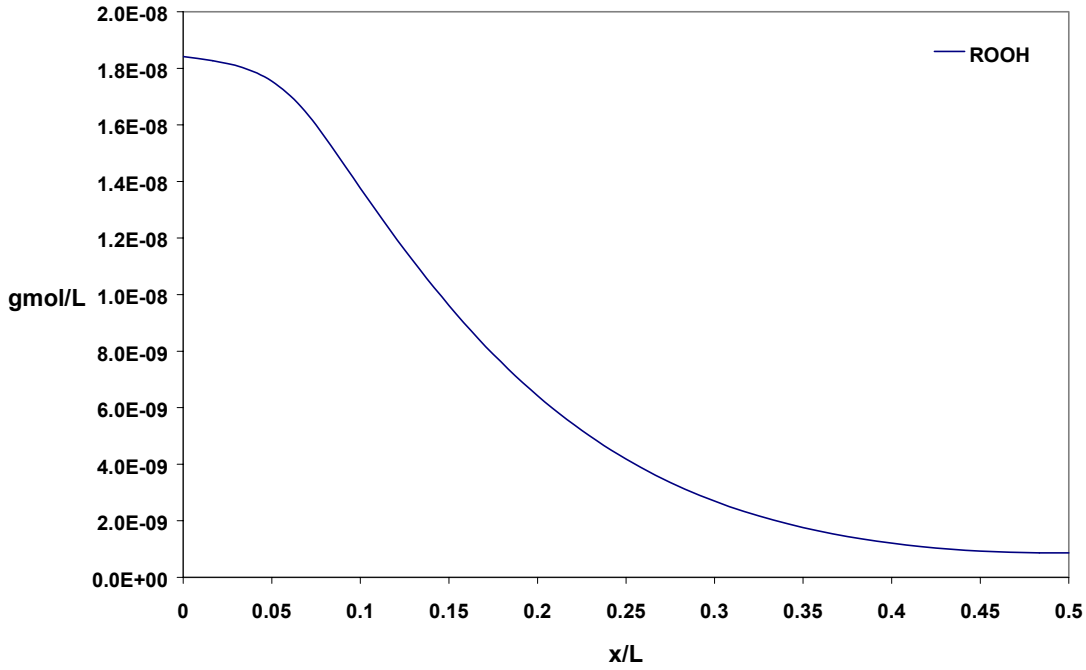

Figure 4.3.2: Hydroperoxide plot with the depth of PE component for shelf aging period of 10.9 years.

The model fitted the ketone curve quite accurately to the experimental data. The hydroperoxide curves decreased continuously with almost constant value near the surface. The rate constant for the formation reaction of hydroperoxide was determined to be very low (~10^{-15}). Hence, the concentration values for hydroperoxide were very low (Figure 4.3.2). The hydroperoxide concentration did affect the final concentration of ketones as given by equation (3). So, the values of the hydroperoxide concentration obtained from optimization of the parameter were not without consequences. We noted that the rate constant for the decomposition of hydroperoxides, k_5, was negligibly small indicating that for the model to fit the experimental ketone curve, the hydroperoxide decomposition reaction should not affect the ketone concentration. This provided an

explanation for increasing concentration of hydroperoxides with time as shown in Figure 4.3.4. If we were to manually increase the rate constant for hydroperoxide decomposition reaction so that hydroperoxide reaches a steady concentration represented as in model II, the ketones did not fit the experimental curve very well.

The ketone plots for different years of shelf aging obtained by employing model III is given in Figure 4.3.3 and corresponding hydroperoxide plots are given in Figure 4.3.4.

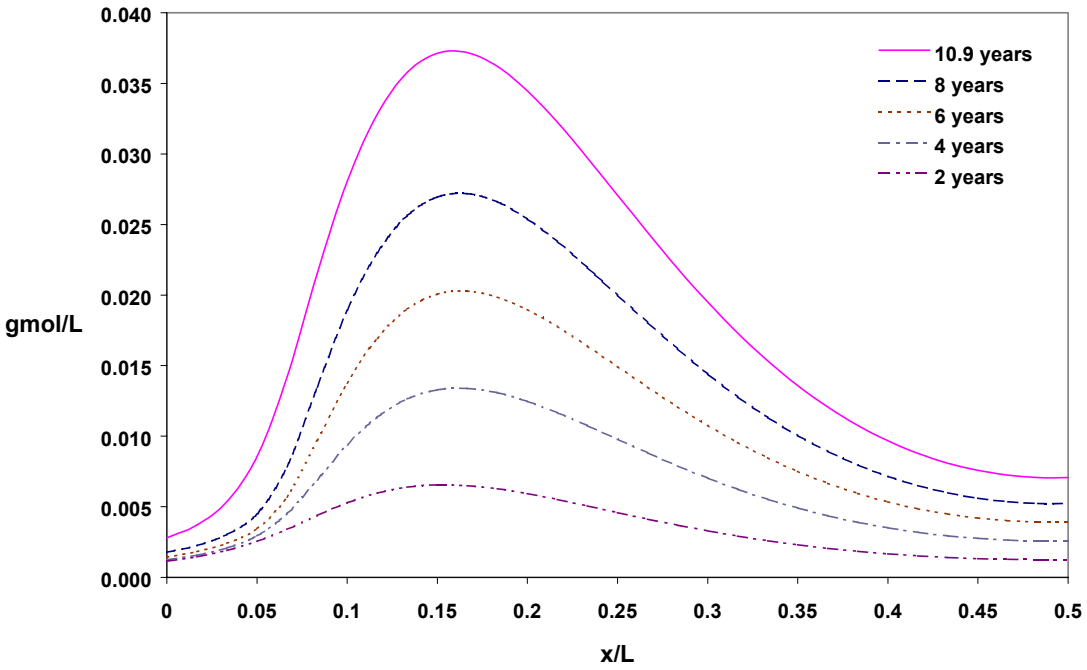

Figure 4.3.3: Ketone concentration plot for 2,4,6,8, and 10.9 years of shelf aging. Plots obtained using model III

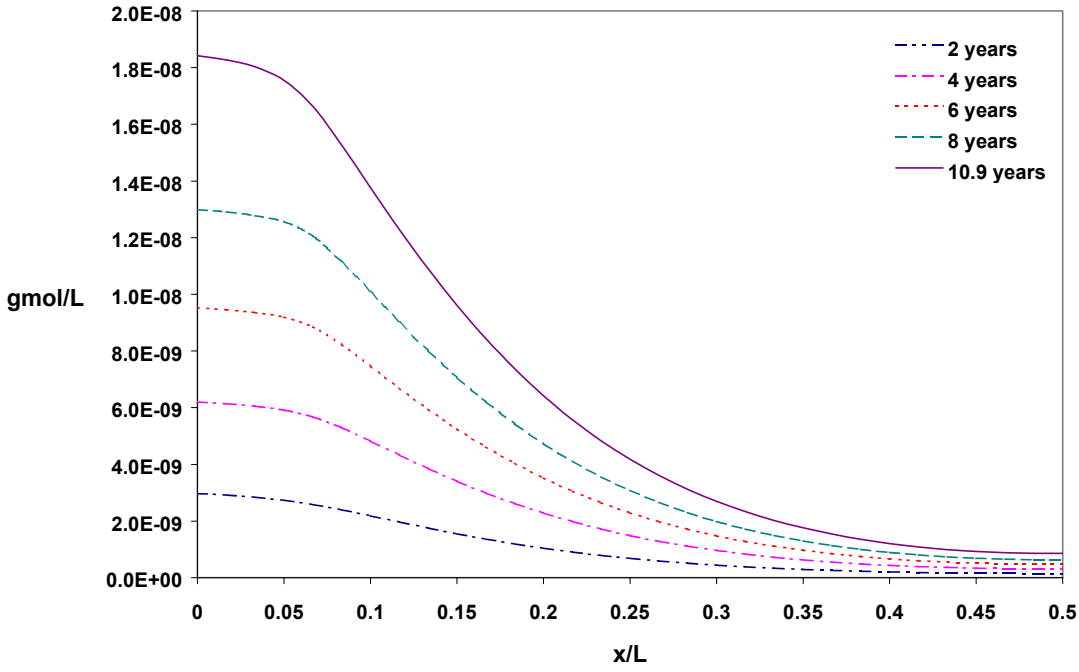

Figure 4.3.4: Hydroperoxide concentration plots for 2, 4, 6, 8, and 10.9 years of shelf aging. Plots obtained using model III.

Finally we applied the model to 5.8 years of shelf aging data by Daly and Yin [12]. The results are given in Figure 4.3.5.

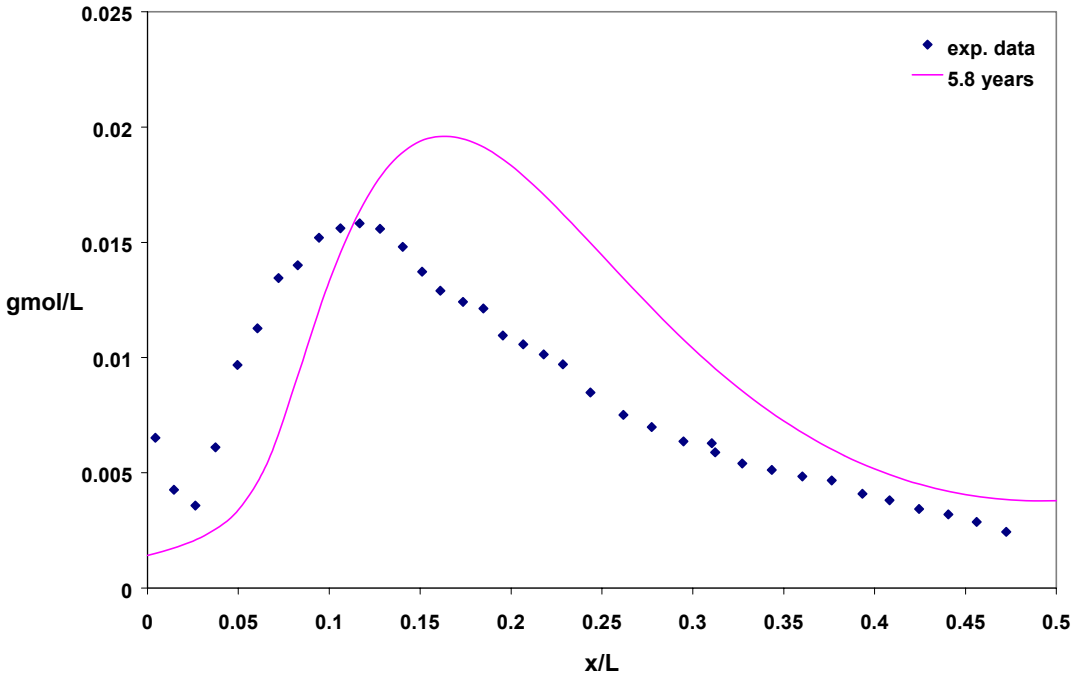

Figure 4.3.5: Ketone concentration profile with depth of the PE component for shelf age of 5.8 years. The experimental data was taken from Daly and Yin

The fit compared quite well to the experimental data provided by Daly and Yin [12] though the curve is more to the right. The hydroperoxide profiles predicted by the model displayed very low concentration values compared to other models. The fit to the 10.9 years shelf age experimental data is not much improved by the reaction,

$RO_2^* + ROOH + RH \rightarrow RCO + ROOH + R^* + H_2O$;

but its absence did not provide a good fit.

4.3.2 Accelerated aging

The model was applied to accelerated aging period of 1, 3, 5, 7, 9 and 13 weeks. Since the hydroperoxide profiles kept increasing with accelerated aging period, similar behavior can be expected at time periods lower than 1 week. Hence no attempts were made to plot hydroperoxide profiles for period lesser than 1 week. The highest concentrations for ketone were obtained near the surface and were roughly 5 – 7 times higher than those for maximum shelf aging process. No subsurface peaks were formed as observed by Coote et al. [14]. For simulations of accelerated aging, the rate constants were increased by 10 times for representation purpose. The diffusivity constant was calculated to be 10 times the one for shelf aging. It had been assumed that heating the PE for accelerated aging led to the release of the uncombined radicals from the crystalline region, as had been discussed for earlier models. The parameters used for the accelerated aging are given in Table 4.6.

Table 4.6: Parameters for model III used in accelerated aging for 1, 3, 5, 7, 9, and 13 weeks.

Parameters	Values	Units
K_1	5.631×10^{-2}	L/mol. s
K_2	1.000×10^{-14}	L/mol. s
K_3	1.203×10^{-2}	L/mol. s
K_4	0.000×10^{-0}	L/mol. s
K_5	0.000×10^{-0}	L/mol. s

K_6	3.783×10^{-3}	L/mol. s
R* (initial alkyl radical conc.)	4.250×10^{-3}	gmol/L
D_{O2} (diffusivity of oxygen in PE)	5.800×10^{-9}	dm^2 / sec

The ketone profiles obtained are given in Figure 4.3.6 and the corresponding hydroperoxide profiles are given in Figure 4.3.7.

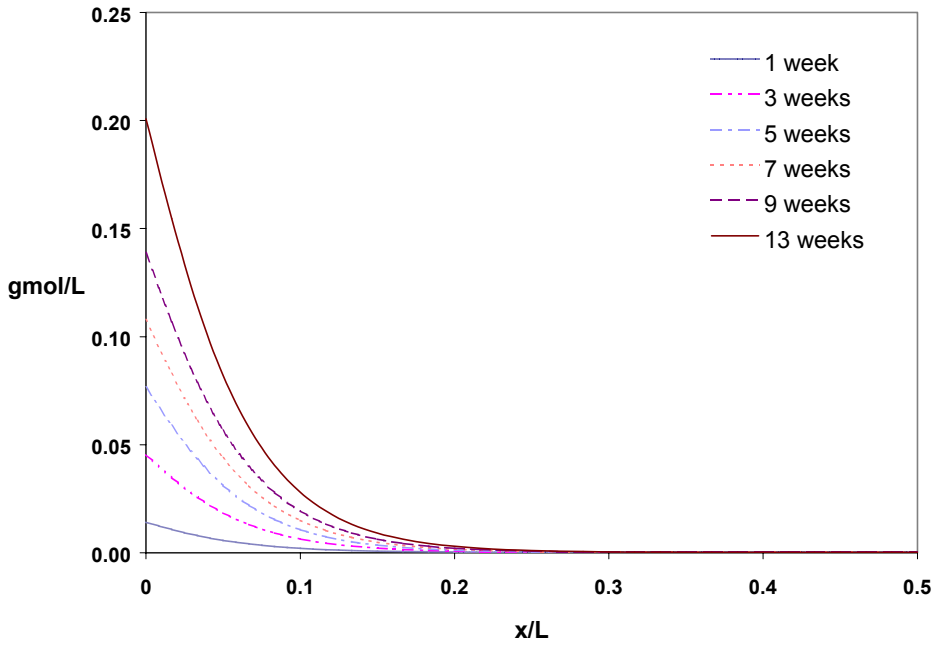

Figure 4.3.6: Ketone concentration profiles for different accelerated aging period obtained using model III.

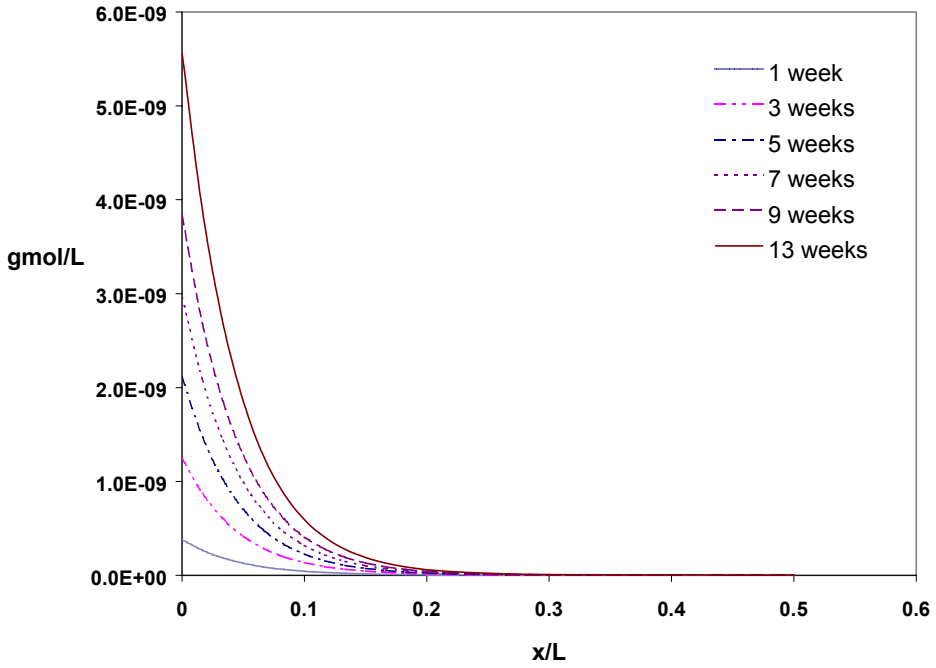

Figure 4.3.7: Hydroperoxide concentration profile for increasing accelerated aging period obtained using model III.

The hydroperoxide concentration kept increasing with time as a result of $k_5 = 0$. The model was not able to simulate the behavior obtained by Coote et al., viz. increase in the hydroperoxide concentration up to 5 – 7 weeks followed by decrease in it [14]. This was largely due to the fact that the hydroperoxide decomposition reaction was determined (by optimization for ketones) not to occur. The only reaction that would affect the hydroperoxide was its formation reaction. Hence, we observed continuous increase in the hydroperoxide concentration for shelf and accelerated aging contrary to what we observed in previous models. This model did not provide much qualitative information

than other models. The model required reaction (6) to be indispensable for the characteristic maximum in the ketone curve:

$$R^* + RO_2^* \rightarrow 2RCO + 2R^* \qquad (k_6)$$

To test the effect of the second reaction characterizing this model, namely,

$$RO_2^* + ROOH + RH \rightarrow RCO + ROOH + R^* + H_2O \qquad (k_3)$$

we set the rate constant $k_3 = 0.0$, and obtained ketone curve given in Figure 4.3.8.

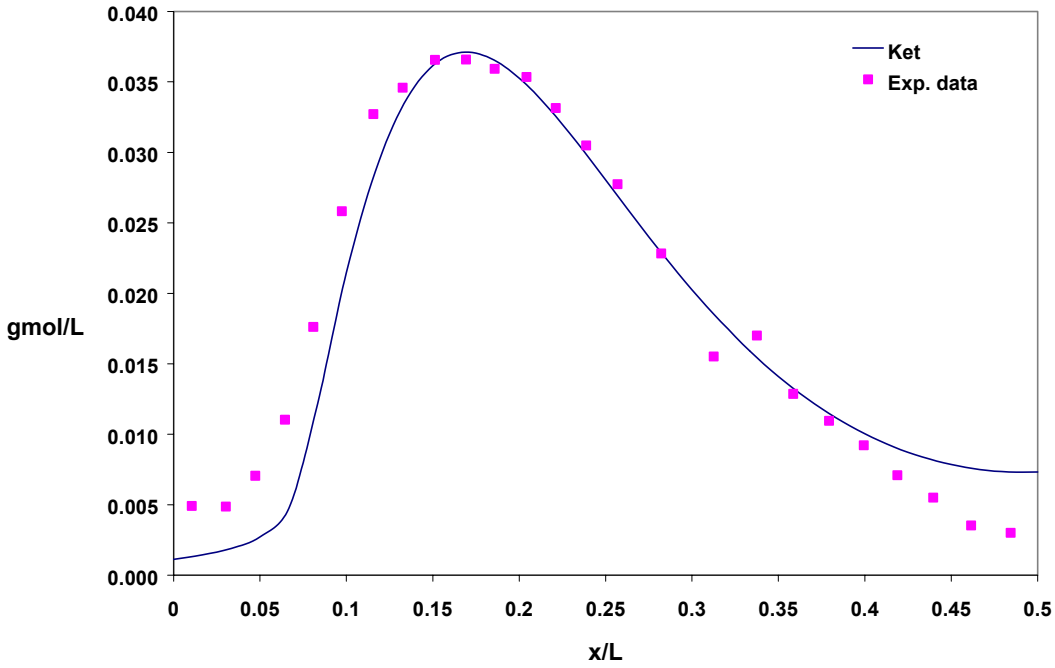

Figure 4.3.8: Ketone plot obtained using model III in absence of the third reaction in the model. The plot is made for 10.9 years of shelf aging with experimental data from Daly and Yin [12].

The curve obtained in Figure 4.3.8 was a decent representation of the experimental data. One could say that the third reaction only refined the fit. Since the third reaction did not involve consumption or formation of ROOH, the ROOH profile for 10.9 years of shelf aging was not much affected. The ROOH profile in the absence of third reaction in model III is given in Figure 4.3.9, which was nearly same as in Figure 4.3.2. The small difference in the two figures for hydroperoxide was due to slight consumption of peroxy (RO_2*) in reaction (3).

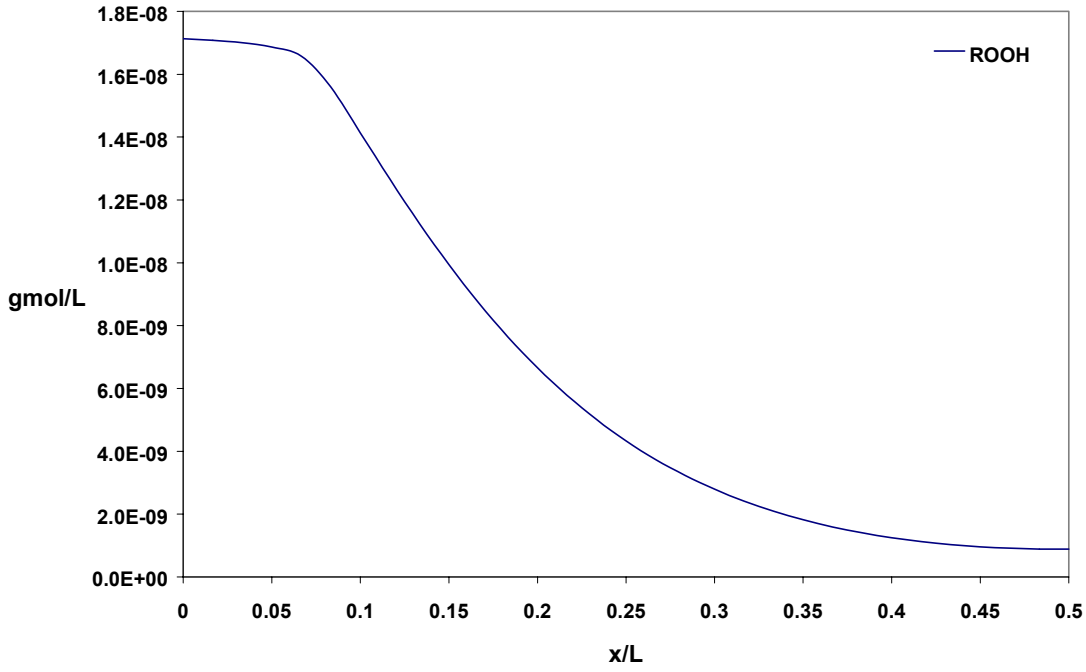

Figure 4.3.9: Hydroperoxide profile for 10.9 years of shelf aging in absence of third reaction in the model III.

Now, we included only the third reaction as the reaction of formation of ketones to determine its role in the ketone subsurface peak. The rate constant for the reaction (6) was made equal to zero (k_6 = 0.0) for which, we obtained very low concentration of ketones and the fit between the experimental and the simulated data was poor. The result is shown in Figure 4.3.10. Experimental data were taken from Daly and Yin [12].

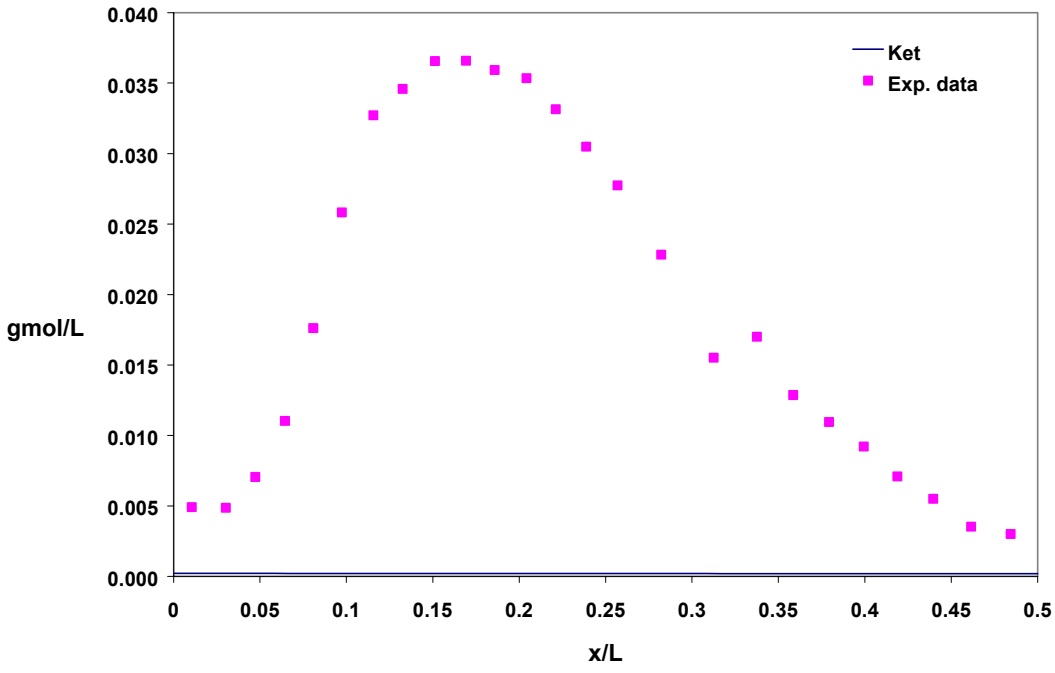

Figure 4.3.10: Ketone concentration profile in absence of the sixth reaction in model III for shelf aging period of 10.9 years.

The corresponding hydroperoxide profile was also plotted, with the reaction (6) assumed not to occur, to observe the effect of the third reaction on the formation of hydroperoxide. The hydroperoxide profile is plotted in Figure 4.3.11. The ROOH profile decreased almost linearly with the depth of the polymer, the nature of the profile being

closer to what Coote et al. [14] observed, but since the corresponding ketone curve fit was poor (Figure 4.3.10), it did not hold much credit.

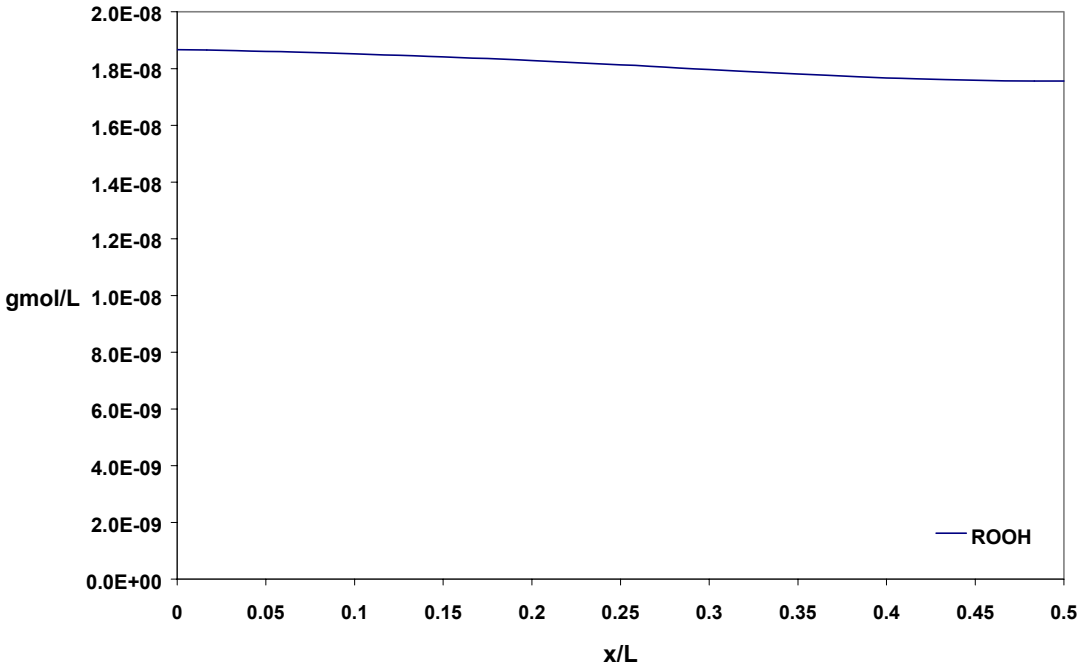

Figure 4.3.11: Hydroperoxide profile for 10.9 years of shelf aging. The plot was made by disregarding the sixth reaction of model III to determine the effect of third reaction on the formation of both ketone and hydroperoxide

The optimization program was run removing the reaction (6) from the set of reactions for model III, and we obtained ketone and hydroperoxide concentration curves quite similar to the ones shown in Figure 4.3.10 and Figure 4.3.11, suggesting that the third reaction was not capable alone to give a ketone subsurface peak. The results thus proved that the reaction between alkyl radicals and peroxy radicals was important for the formation of a ketone subsurface peak.

4.3.3 Shelf aging at reduced oxygen concentration

The variation of ketone profile with oxygen concentration at the surface of the polymer was considered with this model using the rate parameter in Table 4.5. The oxygen composition of air considered were 20% (atmospheric conditions), 10%, 8%, 6%, 3%, 2% (in-vivo oxidation concentration), and 0% (vacuum or inert atmosphere). The model predicts similar behavior what the previous models did and results are displayed in Figure 4.3.12.

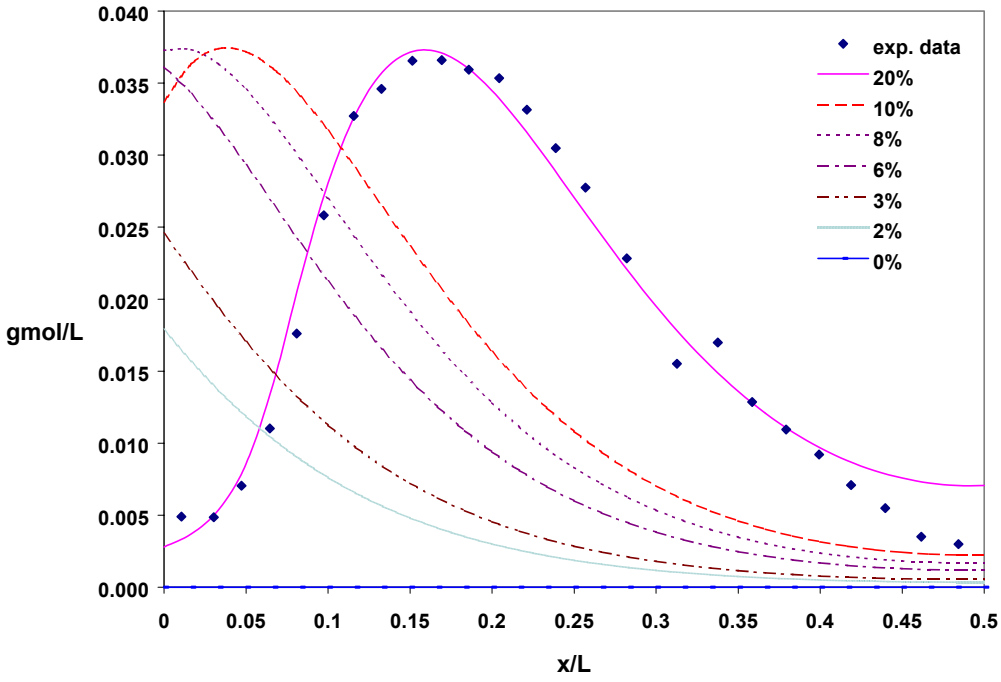

Figure 4.3.12: Variation of ketone concentration with reduced oxygen concentration.

The model predicted shift of ketone curve to the left with decrease in the oxygen concentration. The concentration of ketone at the PE surface reached maximum at oxygen composition of 8% and then decreased at the surface.

4.3.4 Shelf aging at different initial alkyl radical concentration

The variation of ketone concentration with irradiation dose was considered for the present model. Since the formation of alkyl radicals varied linearly with the irradiation dose, we considered multiples of alkyl radical concentration present initially after irradiation. Thus in light of this argument, we considered the following radical concentrations: $1.0R_i$, $1.2R_i$, $1.5R_i$, $2.0R_i$, $2.5R_i$, $3.0R_i$, and $3.5R_i$ where R_i was the initial concentration of alkyl radical ($7.6x10^{-4}$ gmol/L). The ketone concentration profiles are given in Figure 4.3.13. All plots were made for shelf age of 10.9 years. Experimental data were taken from Daly and Yin [12].

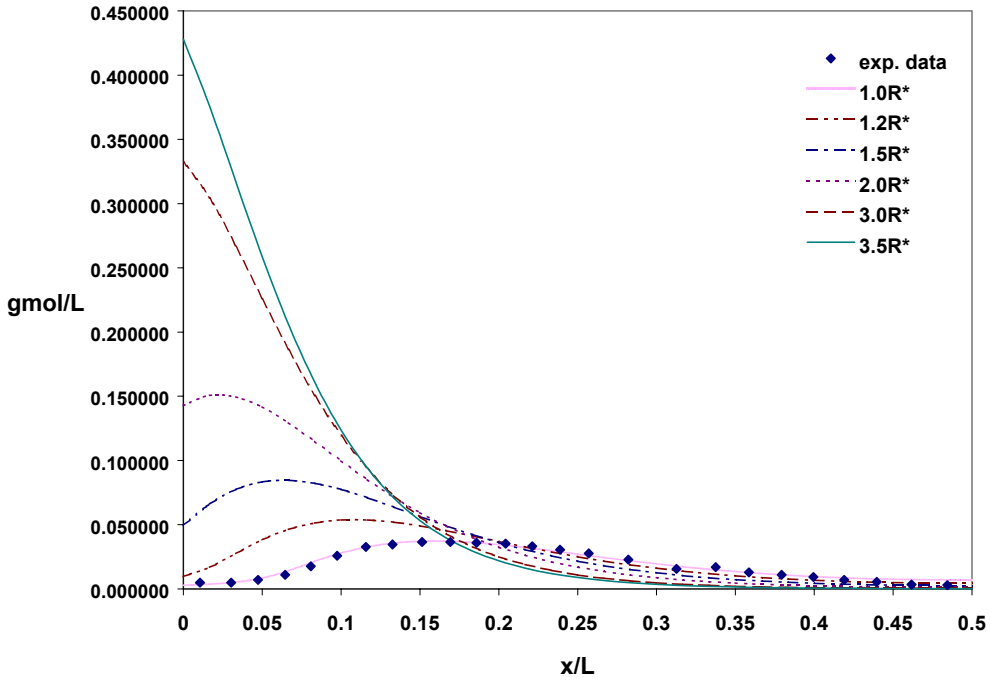

Figure 4.3.13: Variation of ketone concentration with initial alkyl radical concentration (higher initial radiation dose). All curves are for shelf aging period of 10.9 years.

The model predicted higher concentrations of ketone with increase in irradiation dose. The ketone profile shifted towards the surface of the polymer ultimately eliminating subsurface peak. The ketone profile then continuously decreased with depth of the polymer. Increased irradiation is harmful for the polymer since it leads to higher oxidative degradation as has been observed from Figure 4.3.13.

The model was used to plot predicted ketone profiles for reduced initial alkyl radical concentrations. The plots were made for the initial concentrations of alkyl radical

of $0.9R_i$, $0.8R_i$, $0.6R_i$, $0.3R_i$, and $0.1R_i$ where R_i is the initial alkyl radical concentration considered for fitting of the ketone experimental data from Daly and Yin [12], (7.60×10^{-4} gmol/L). The ketone concentration plots obtained are given in Figure 4.3.14.

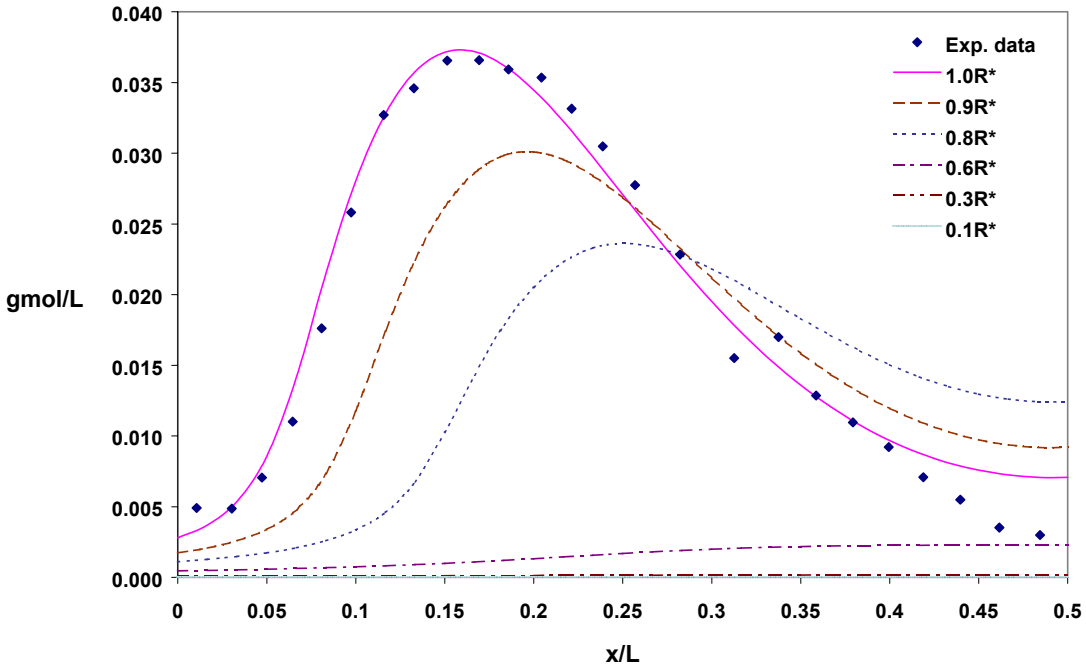

Figure 4.3.14: Variation of ketone concentration with lower initial alkyl radical concentration (lower initial radiation dose). The shelf age is 10.9 years.

The model predicted lower initial alkyl radical concentrations reduced the formation of ketone. The ketone concentration decreased rapidly with the initial alkyl radical concentration. The decrease was due to combined effect of lower alkyl and correspondingly peroxy radical concentrations. Since both the species were involved in the formation of ketone (reaction (6)), decrease in both the species caused greater decrease in the ketone concentration.

4.4 Model 4: Irreversible formation of ROOH with the formation of second-generation alkyl radicals

4.4.1 Shelf aging

The models I, II, and III have not been able to give almost constant profile for hydroperoxide with the depth of polymer. In an attempt to get the profile for hydroperoxide similar to what Coote et al. observed in his experimental studies [14] for hydroperoxide, we were investigating different reaction schemes available in the literature.

The current model is based on the study done by Matsuo and Dole [23]. The authors have suggested that the earlier study done by Bach [53] considered the first two steps of the irreversible formation of ROOH in model II not to be a chain reaction. Based on the argument given by Matsuo and Dole [23], we write down the model given below:

$$R^* + O_2 \rightarrow RO_2^* \qquad (k_1)$$

$$RO_2^* + RH \rightarrow ROOH + R'^* \qquad (k_2)$$

$$R'^* + O_2 \rightarrow R'O_2^* \qquad (k_3)$$

$$R'^* + R'O_2^* \rightarrow 2R'CO + 2R'^* \qquad (k_4)$$

$$ROOH \rightarrow \text{acids, esters, etc.} \qquad (k_5)$$

$$R'O_2^* + ROOH + RH \rightarrow ROOH + RCO + R'^* + H_2O \qquad (k_6)$$

Where R'* is second-generation alkyl radicals as explained in following sections.

The model also includes the reaction given by Petruj and Marchal (reaction (6)) [24]. In reaction (6), the ketone formation involved the hydroperoxide but did not affect the concentration of hydroperoxides since they were formed in the same reaction.

The initial radicals generated by irradiation have very large energy left over from the irradiation process. This energy is sufficient to overcome the energy barrier of the reaction (2) to give hydroperoxide and another alkyl radical (R'*). However Bach [53] showed that these alkyl radicals that were formed in reaction (2) do not possess sufficient energy to overcome the energy barrier for the formation of ROOH. The only path it can follow is through the formation of oxidation products. Thus, the initial alkyl radicals generated during the irradiation would all be consumed for the formation of hydroperoxides producing a second generation of alkyl radicals (R'*), that could no longer form hydroperoxides but could react to form ketones (due to lower energy). The formation of hydroperoxides would stop once all initial batches of alkyl radicals were consumed (presumably quickly). Since we assumed that the initial alkyl radical concentrations were uniformly distributed in PE, the resulting profile for the hydroperoxide would also be uniform throughout the polymer. If we assumed that hydroperoxide did not decompose, but remained stable throughout, then the profiles could be expected to be uniform over any period of time. This could sufficiently explain the almost constant concentration of hydroperoxide. When the initial alkyl radicals are extinguished in the formation of hydroperoxide, no more alkyl radicals would remain with sufficient energy to form them. Hence, the hydroperoxide formation would stop after a period of time. But, the ketone concentration would keep on increasing by the

reactions of the second-generation alkyl radicals formed in the second step. Also this process separates out the formation of ketone and hydroperoxide i.e. not the same alkyl radicals (different energy) participate in the formation of hydroperoxide and ketone.

To develop partial differential equations we make certain assumptions. It is quite possible that R* can participate in reaction (4) by combining with $R'O_2$* and RO_2*, and RO_2* can participate in reaction (4) by combining with R* and R'*. RO_2* can also participate in reaction (6). Accordingly, the reactions added to the model were:

$$R'O_2^* + R'^* \rightarrow 2\,RCO + 2\,R'^* \qquad (k_4)$$

$$R'O_2^* + R^* \rightarrow 2\,RCO + 2\,R'^* \qquad (k_4)$$

$$RO_2^* + R'^* \rightarrow 2RCO + 2\,R'^* \qquad (k_4)$$

$$RO_2^* + R^* \rightarrow 2RCO + 2\,R'^* \qquad (k_4)$$

$$R'O_2^* + ROOH + RH \rightarrow RCO + R'^* + ROOH + H_2O \qquad (k_6)$$

$$RO_2^* + ROOH + RH \rightarrow RCO + R'^* + ROOH + H_2O \qquad (k_6)$$

All these reactions along with the reactions given on page 86 were considered for simulation. But due to large number of reactions formed by all above combinations, it was difficult for the optimization program to provide reasonably accurate values of the rate constants. Hence the six reactions given on page 86 were considered for optimization on the basis of simplicity and by the assumption that they form representative reactions and are most likely to occur. Then for the various combinations of reactions such as

reaction between R'* and RO_2*, the rate constant determined for the reaction (4) was used. It was further assumed that the alkyl radicals formed by reaction 2, 4, and 6 were all second-generation alkyl radicals since they do not have left over energy from the irradiation process. The termination reaction between two R* to give R-R is very fast and occurs again in the amorphous region only.

The partial differential equations defining the mass balance for set of reactions on page 86 are given as follows:

$$\frac{\partial[O_2]}{\partial t} = D\frac{\partial^2[O_2]}{\partial x^2} - k_1[O_2][R^*] - k_3[R'^*][O_2]$$

$$\frac{\partial[R^*]}{\partial t} = -k_1[R^*][O_2]$$

$$\frac{\partial[R'^*]}{\partial t} = k_2[RH][RO_2^*] - k_3[R'^*][O_2] + k_4[R'O_2^*][R'^*] + k_6[R'O_2^*][ROOH][RH]$$

$$\frac{\partial[RO_2^*]}{\partial t} = k_1[R^*][O_2] - k_2[RO_2^*][RH]$$

$$\frac{\partial[R'O_2^*]}{\partial t} = k_3[R'^*][O_2] - k_4[R'O_2^*][R'^*] - k_6[R'O_2^*][ROOH][RH]$$

$$\frac{\partial[RCO]}{\partial t} = 2k_4[R'^*][R'O_2^*] + k_6[R'O_2^*][ROOH][RH]$$

$$\frac{\partial[ROOH]}{\partial t} = k_2[RO_2^*][RH] - k_5[ROOH]$$

Optimizing above set of reactions for best fit of parameters, we obtain rate constants as given in Table 4.7.

Table 4.7: Parameters obtained for best-fit using model IV.

Parameters	Values	Units
K_1	5.00×10^{-2}	L/mol. s
K_2	3.60×10^{-4}	L/mol. s
K_3	5.70×10^{-3}	L/mol. s
K_4	3.90×10^{-4}	L/mol. s
K_5	1.00×10^{-14}	1/ s
K_6	3.00×10^{-8}	L^2/mol^2. s
R* (initial alkyl radical conc.)	7.60×10^{-4}	gmol/L
D_{O2} (diffusivity of oxygen in PE)	6.40×10^{-10}	dm^2 / sec

The value of the diffusion constant for the best fit obtained by optimization was 0.64×10^{-9} gmol/L as against 0.58×10^{-9} gmol/L for the previous three models. All profiles obtained were for 10.9 years of shelf aging fitted to the experimental data from Daly and Yin [12]. The ketone fit obtained by application of model IV is given in Figure 4.4.1.

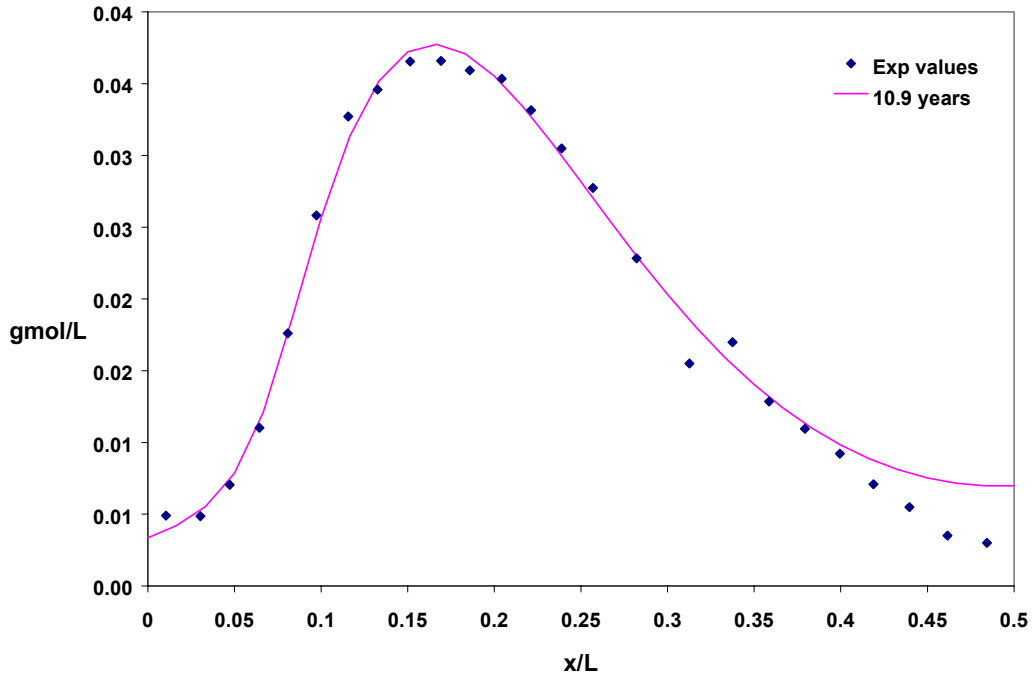

Figure 4.4.1: Ketone concentration profile with depth of polymer obtained using model IV. The curve is fitted to experimental data from Daly and Yin [12]. The shelf age period is 10.9 years.

The simulated ketone curve fit the experimental data very well. The model was applied for shelf age period of 2, 4, 6, 8, and 10.9 years with the experimental data taken from Daly and Yin [12]. The results are given in Figure 4.4.2. The increase in the concentration of ketone profile with shelf age was again determined to be linear as against accelerated growth for experimental data by Daly and Yin [12] and Coote et al. [14]. The corresponding hydroperoxide profiles are plotted in Figure 4.4.3.

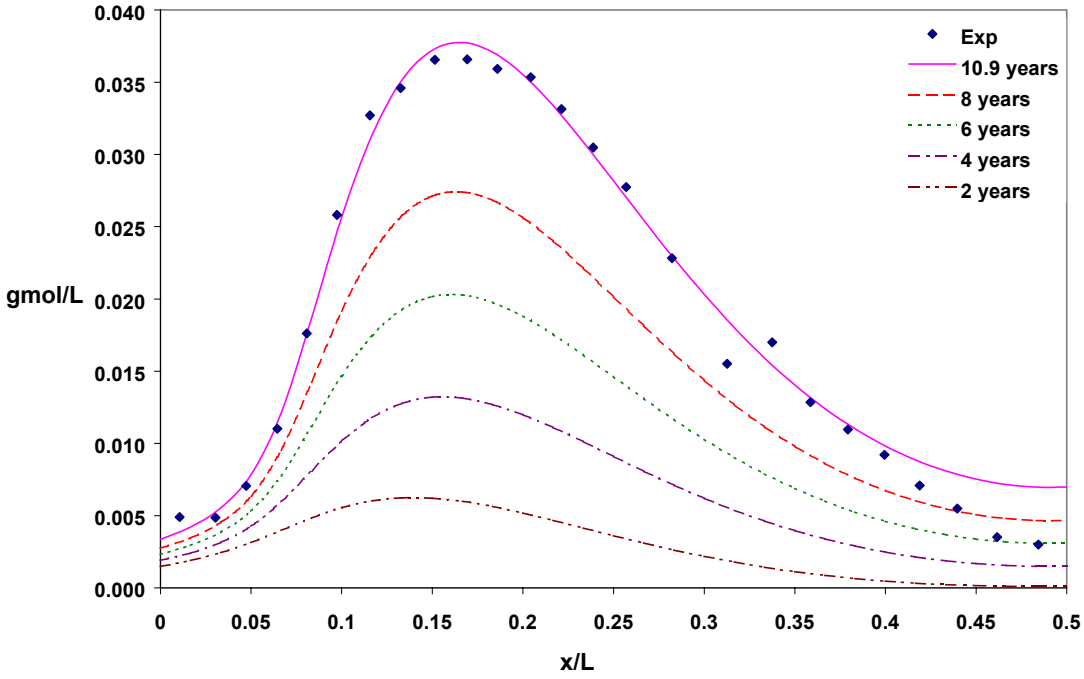

Figure 4.4.2: Ketone concentration profile for different shelf aging period of PE.

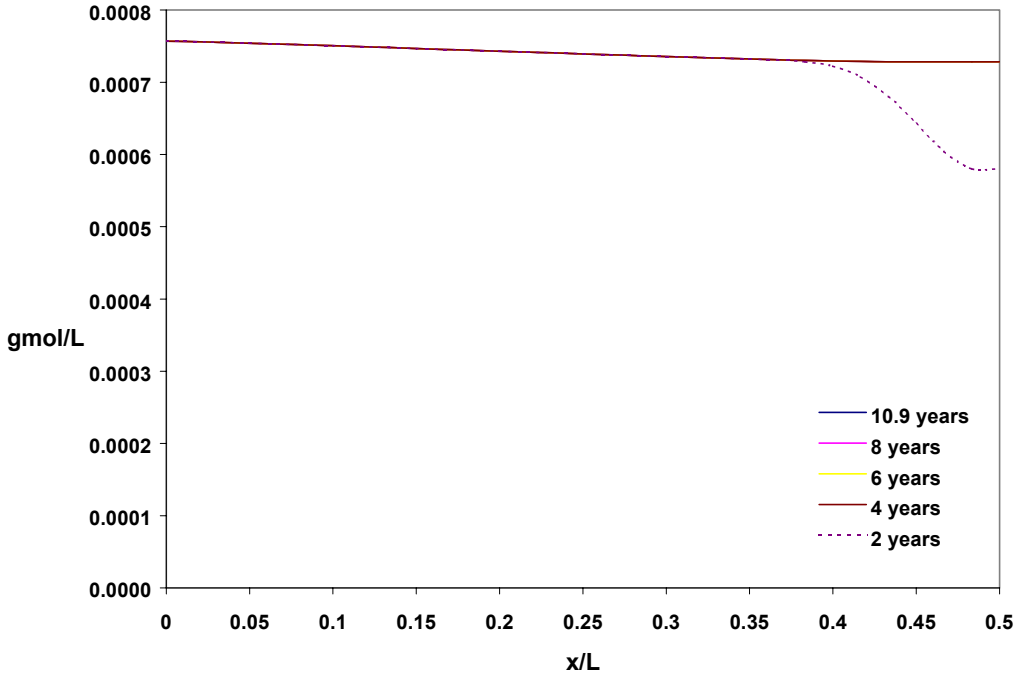

Figure 4.4.3: Hydroperoxide profiles obtained using model IV for different shelf aging period of PE component.

The hydroperoxide curve reached almost constant value throughout the depth of PE. A slight decrease in the profiles were because of involvement of RO_2* in the formation of ketones by reactions (4) and (6). In the initial part of the curve, the profile did not drop up to 0.025 mm by half the concentration value at the surface, but reached almost steady level as was observed by Coote et al. [14]. This could be because the distribution of initial alkyl radicals may not have been uniform (though we assumed uniform concentration) as it is highly dependent on the method of irradiation, type of polymer, distribution of crystalline and amorphous regions. Except for the skin layer of the polymer component, the model provides the best representation of hydroperoxide with shelf age. Further, the model also corroborates the observation that the profiles do not change with shelf age.

The ketone curves increased linearly with time and shifted towards right. The hydroperoxide curves were linear with almost constant value with the depth of the polymer. For the 2 years of shelf aging, hydroperoxide plot did not reach constant value at the center of the polymer. This implies that for the determined parameters of model IV, for all the initial alkyl radicals to react the time required was greater than 2 years. This may not necessarily be true since the parameters have been fitted to the 10.9 years of shelf aging. And hydroperoxides would have been formed long before 2 years are up. We surely must accept that there is some missing link in the reaction steps that have not been reported in the literature, and that we have not considered the reactions leading to other species such as acids, esters etc. since there was no experimental data available. More experimental data would be needed to add in reactions to make the picture complete.

The model has been very successful in predicting the shelf and the accelerated aging among all the models considered so far. To make the analysis complete, plots of R'* and R'O_2* for shelf age of 2, 4, 6, 8, and 10.9 years are required. The plots for R'* are given in Figure 4.4.4 and for R'O_2* are given in Figure 4.4.5.

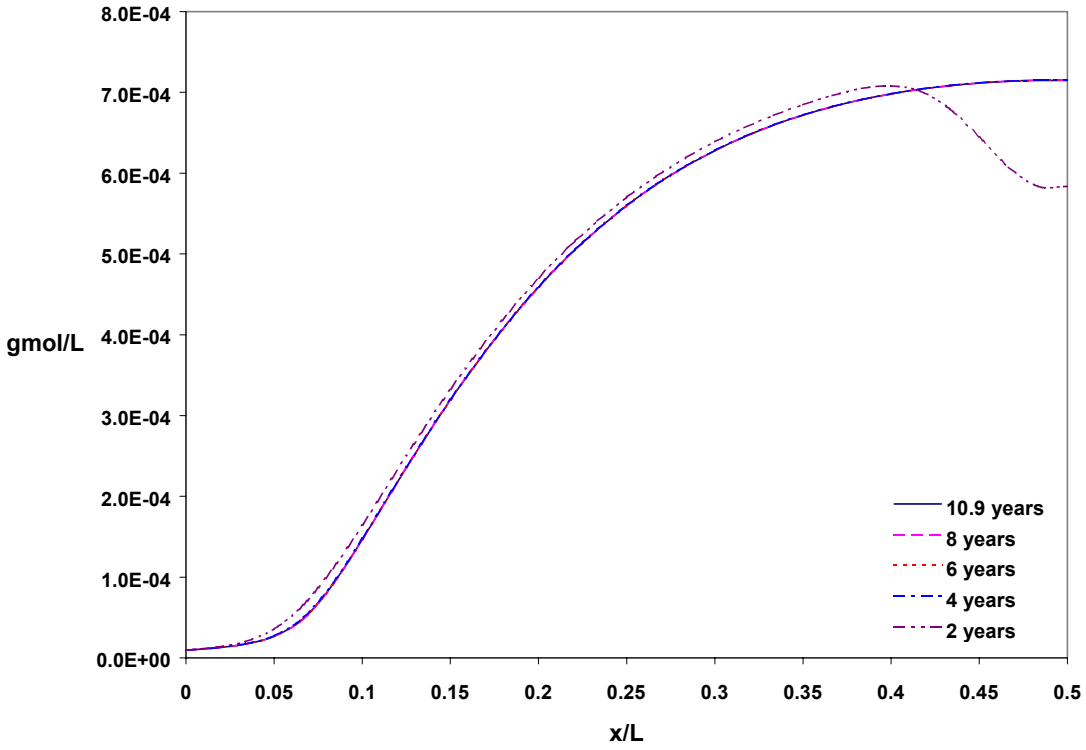

Figure 4.4.4: Variation of second-generation alkyl radical (R'*) concentration with shelf-age of the polymer. Plots are made for 2, 4, 6, 8, and 10.9 years.

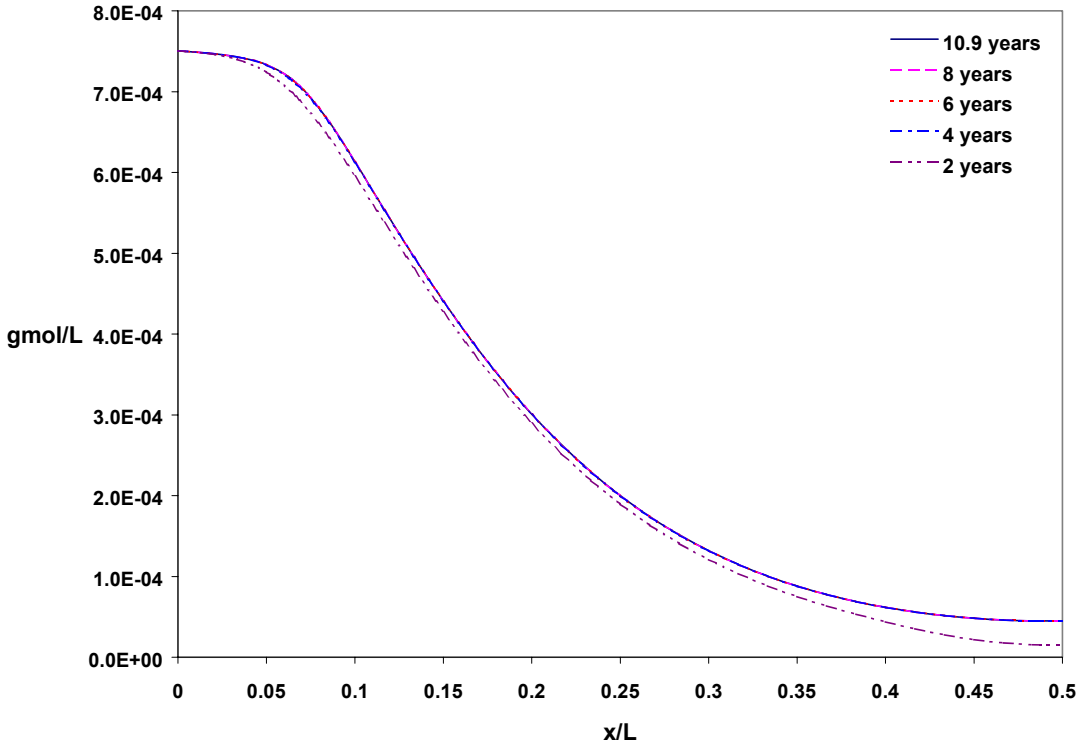

Figure 4.4.5: Variation of peroxy radicals produced from second-generation alkyl radicals ($R'O_2^*$) with shelf-age of the polymer. The plots are made for 2, 4, 6, 8, and 10.9 years.

From Figure 4.4.4, the alkyl radical concentration increased from the surface to the center of the polymer component. For two years of shelf aging, the concentration near the center of the polymer component did not reach the steady value, similar to the hydroperoxide concentration in Figure 4.4.3. The concentration reached a steady value from four years of shelf aging onwards. For the peroxy radicals, $R'O_2^*$, the concentration reached a steady value after two years.

The total concentration of alkyl radicals (R'* and R*) and peroxy radicals (RO_2* and $R'O_2$*) were plotted for shelf age of 2, 4, 6, 8, and 10.9 years in Figure 4.4.6 and Figure 4.4.7 for information purpose.

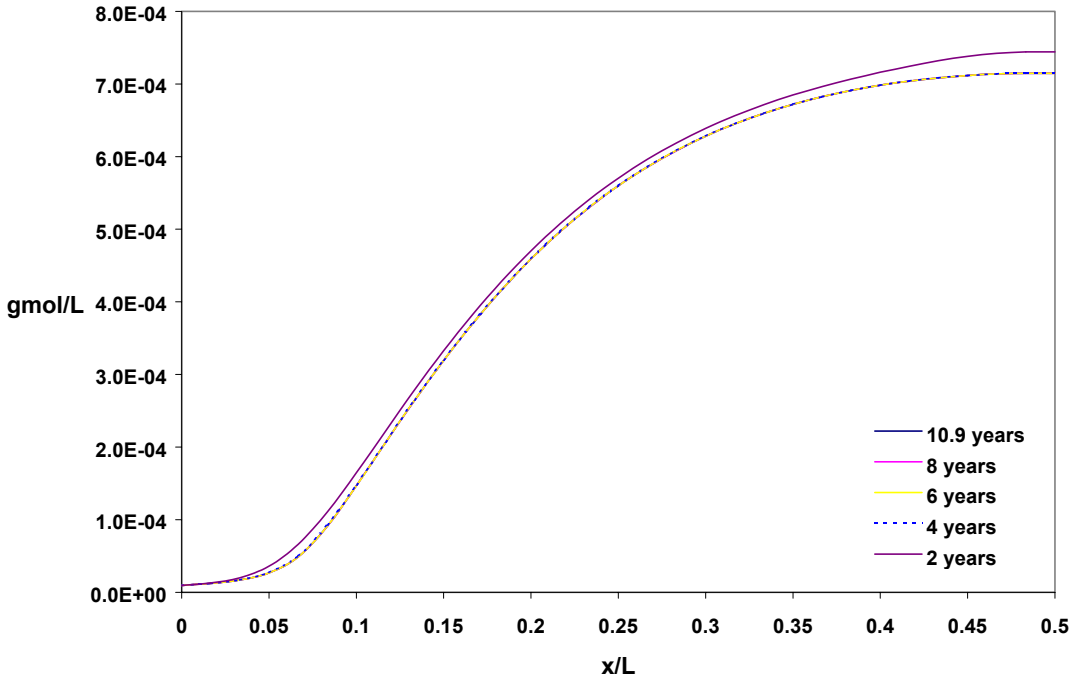

Figure 4.4.6: Variation of total alkyl radical (R* and R'*) concentration with shelf age of 2, 4, 6, 8, and 10.9 years.

In Figure 4.4.6, the concentration of total alkyl radical concentration decreased up to 2 years due to decrease of the first generation alkyl radicals (R*) and formation of second-generation alkyl radicals (R'*). At the center of the polymer component, there was no dip in the concentration profile as observed for second-generation alkyl radicals in Figure 4.4.4 because the first-generation alkyl radicals were not all consumed and added to the total concentration.

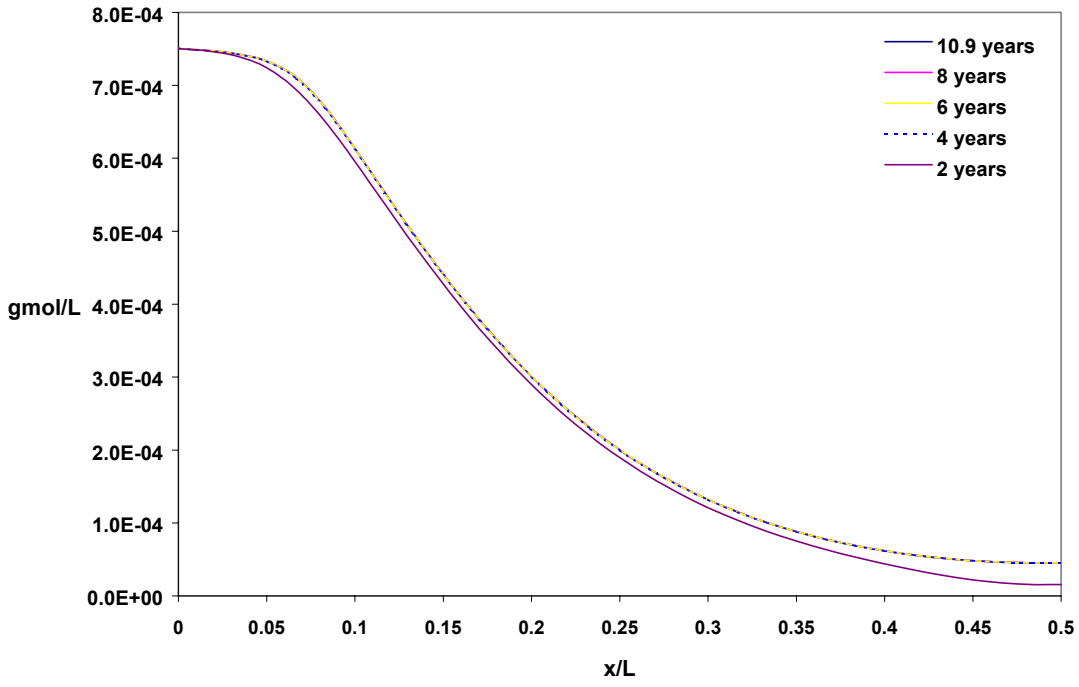

Figure 4.4.7: Variation of total peroxy radical concentration with shelf age of 2, 4, 6, 8, and 10.9 years.

For the peroxy radicals, the concentration increased beyond two years and stabilized at four years of shelf aging.

Finally the model was fitted to the 5.8 years shelf age data provided by Daly et al. [12]. The plot is shown in Figure 4.4.8.

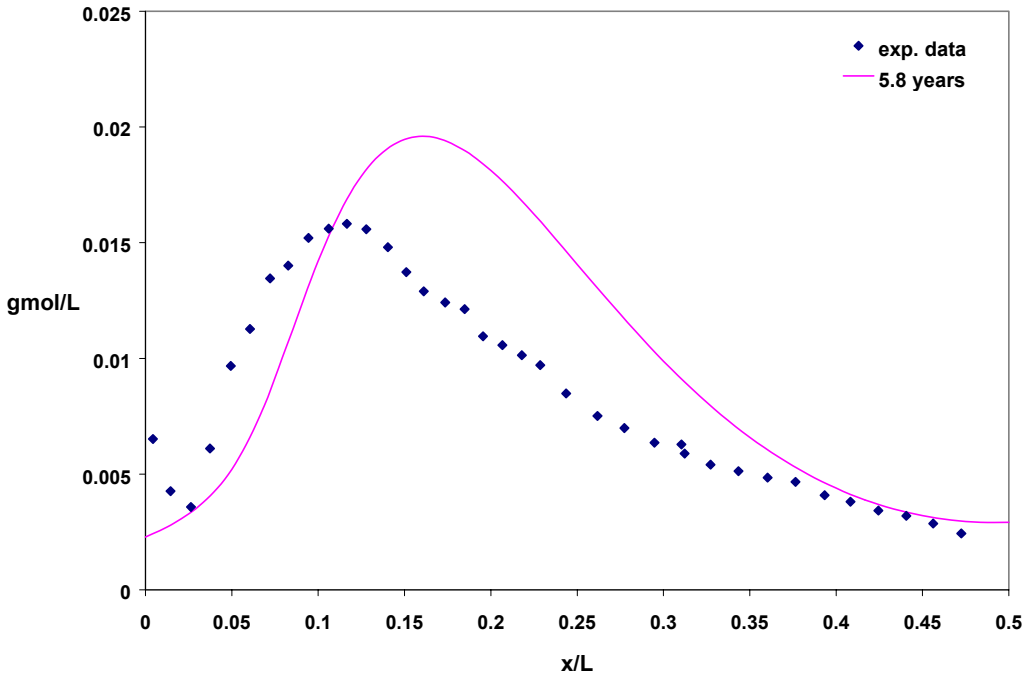

Figure 4.4.8: Ketone concentration plot for 5.8 years of shelf aging. Experimental data obtained from Daly and Yin.

The model achieved the essence of the experimental data. This can again be explained by the failure of the model to predict accelerated growth of the ketone concentration with shelf age. Since the model was fitted for 10.9 years of shelf age, the corresponding profile for 5.8 years was higher than the experimental values.

4.4.2 Accelerated aging

For accelerated aging, we again increased all the parameters by an order of magnitude. The diffusivity coefficient by calculations came to be approximately 10 times those obtained for shelf aging except for hydroperoxide decomposition reaction whose reaction rate constant (k_5) was increased by an order of magnitude of 7. The revised parameters are given in Table 4.8.

Table 4.8: The parameters for accelerated aging for model IV.

Parameters	Values	Units
K_1	5.00×10^{-1}	L/mol. s
K_2	3.60×10^{-3}	L/mol. s
K_3	5.50×10^{-2}	L/mol. s
K_4	3.90×10^{-3}	L/mol. s
K_5	5.00×10^{-7}	1/s
K_6	3.00×10^{-7}	L^2/mol^2. s
R* (initial alkyl radical conc.)	4.25×10^{-3}	gmol/L
D_{O2} (diffusivity of oxygen in PE)	6.40×10^{-9}	dm^2 / sec

The model was applied for accelerated aging period of 1, 3, 5, 7, 9, and 13 weeks. Since the rate constant were chosen arbitrarily, it is quite possible that the actual time of aging to be considered could be lower than the ones given above. Hence, it was felt

necessary to predict the behavior of hydroperoxide at lower accelerated aging time. Further, for shelf aging, the hydroperoxide decomposition was determined by the optimization not to occur which was in sync with our assumption to obtain linear profile for hydroperoxide. But, at elevated temperatures, there are studies that clearly show hydroperoxide decompose [43,54]. The rate of decomposition of hydroperoxides was increased by an order of magnitude of 7. The increase in the rate constant was in order to obtain the trend for hydroperoxides as observed by Coote et al. [14] for accelerated aging. The ketone concentration profiles are given in Figure 4.4.9 and those for corresponding hydroperoxides are given in Figure 4.4.10.

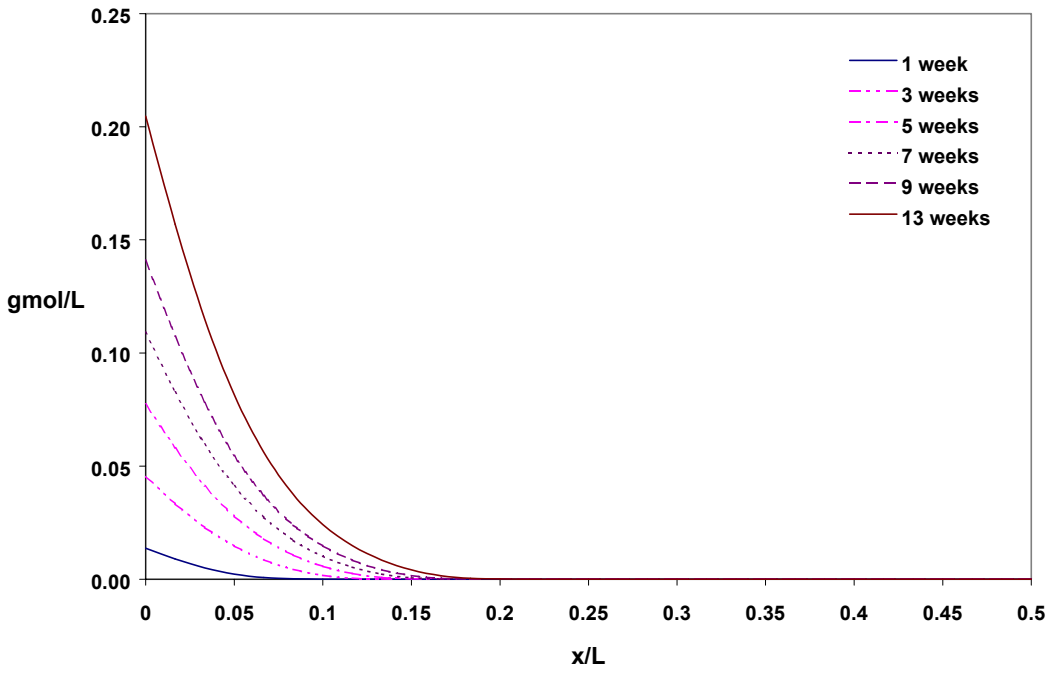

Figure 4.4.9: Ketone concentration plot for different accelerated aging period.

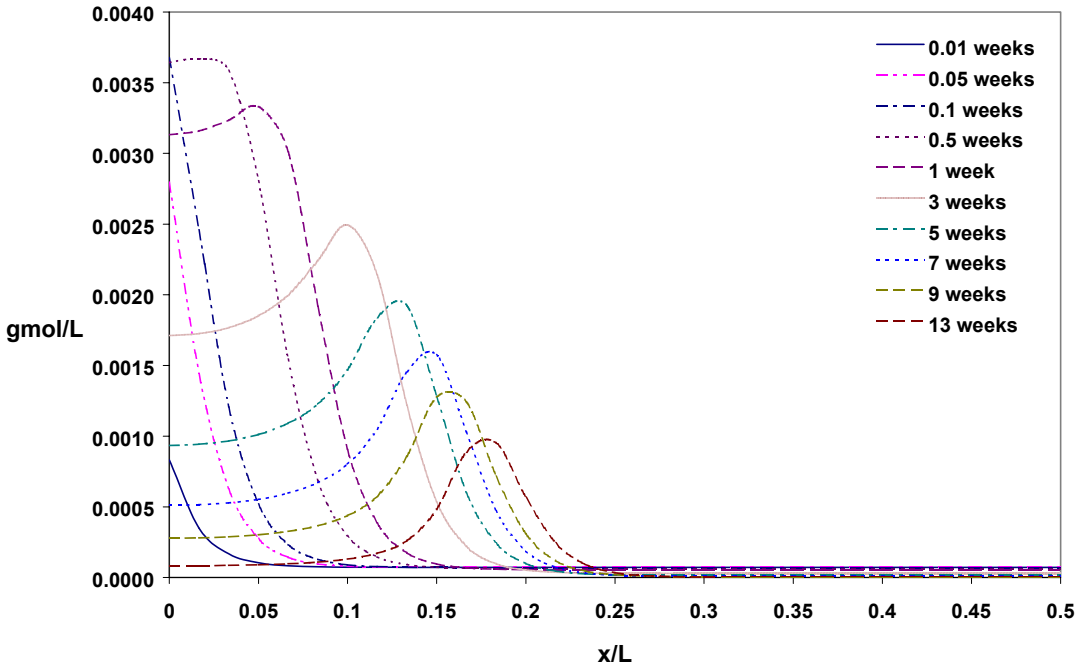

Figure 4.4.10: Hydroperoxide concentration plot for different accelerated aging period.

The ketone curve as expected kept increasing with time. The hydroperoxide curve shifted to the right with aging time. In this model, the hydroperoxide profile did increase up to 0.5 weeks of shelf aging and then decrease. Coote et al. [14] observed this increase of hydroperoxide roughly up to 5 weeks and then decrease beyond it. But, as mentioned earlier, the rate constants are not obtained by fitting any accelerated aging data but chosen arbitrarily for representation purpose. Hence, the time of shelf aging are also not fixed. The success of this model lies in its ability to predict the behavior of ketone and hydroperoxide observed for accelerated aging. Further, due to the non-availability of more reactions involving hydroperoxides, the model has achieved significant leap towards understanding the acceleration process. The ketone concentration for accelerated aging was again 5 times as compared to shelf aging profile.

4.4.3 Shelf aging at reduced oxygen concentration

The model was applied to varying O_2 atmosphere. The concentrations of O_2 explored were 20% (atmospheric content), 10%, 8%, 6%, 3%, 2% (in-vivo oxidation atmosphere) and 0% (or inert atmosphere). The results are plotted in Figure 4.4.11.

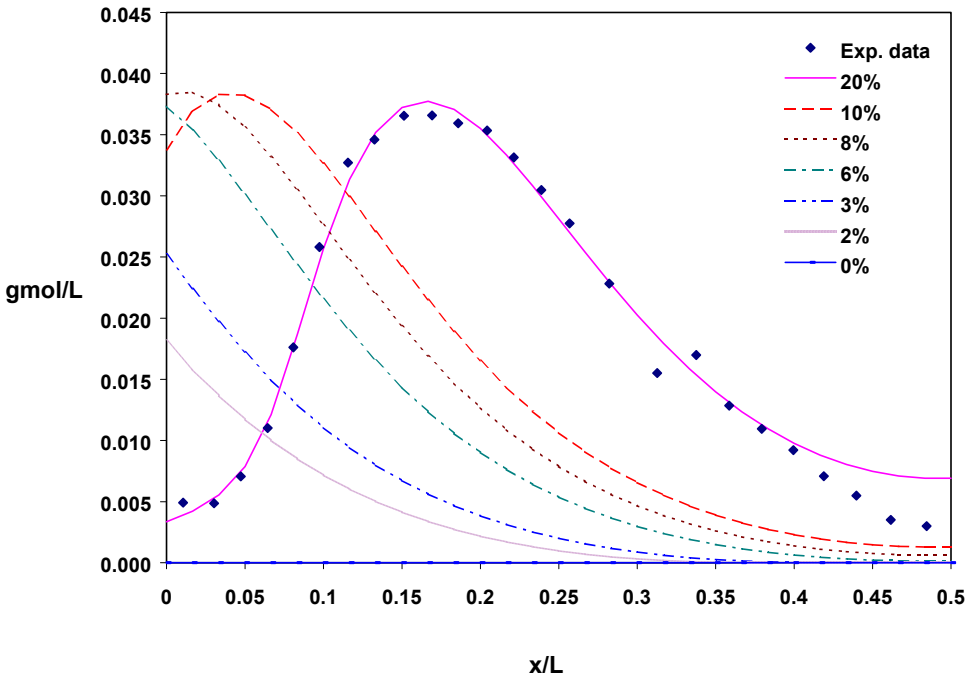

Figure 4.4.11: Variation of ketone concentration with oxygen concentration for shelf age period of 10.9 years.

The model gave results similar to model II, which included the irreversible formation of ROOH. The model predicted that an oxygen-free atmosphere was helpful in preventing formation of ketones to a large extent. The ketone curve shifted to the left with the maximum O_2 concentration at the surface at around 8% value. For in-vivo oxygen levels (ca. 2%), the oxidation was less severe as compared to same period of shelf

aging. The maximum ketone formation for in-vivo oxidation was at the surface and the ketone concentration decreased with the depth.

4.4.4 Shelf aging at different initial alkyl radical concentration

The increase in the irradiation dose would also have an effect on the ketone concentration. We applied the model to the following concentration of the alkyl radicals: $1.0R_i$, $1.2R_i$, $1.5R_i$, $2.0R_i$, 3.0Ri, and $3.5R_i$ where again R_i was the concentration of alkyl radicals we employed for determining best fit for Daly's [12] 10.9 years of shelf aging data. The results for higher irradiation dose are given in Figure 4.4.12. The results obtained are for 10.9 years of shelf aging. The experimental data are taken from Daly and Yin [12].

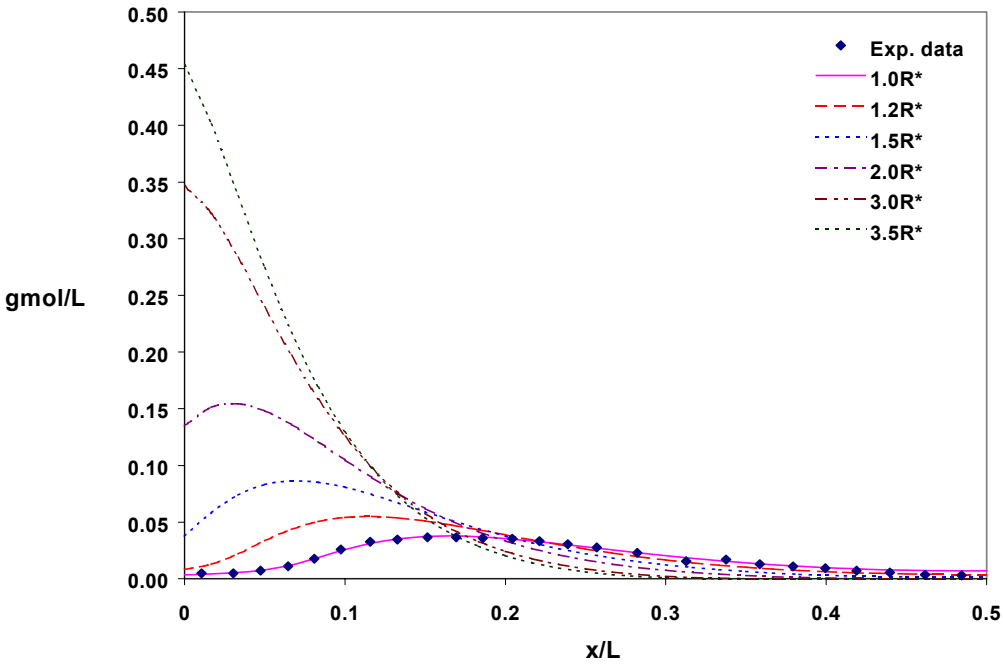

Figure 4.4.12: Variation of ketone concentration with higher initial alkyl radical concentration (higher irradiation dose). Plots made for 10.9 years of shelf aging.

The model predicted that the increase in the irradiation dose would lead to increase in the concentration of ketone with the shift of the maximum concentration towards the surface. Thus, oxidative degradation of the polymer could be expected to be higher at higher irradiation doses with shelf aging in atmospheric oxygen.

The model was also applied to the case where the irradiation dose was lower than normal and correspondingly the concentration of initial alkyl radicals were reduced. The cases considered were $0.9R_i$, $0.8R_i$, $0.6R_i$, $0.3R_i$, and 0.1Ri. The shelf age period was 10.9 years and the experimental data were taken from Daly and Yin et al. [12]. The results are given in Figure 4.4.13.

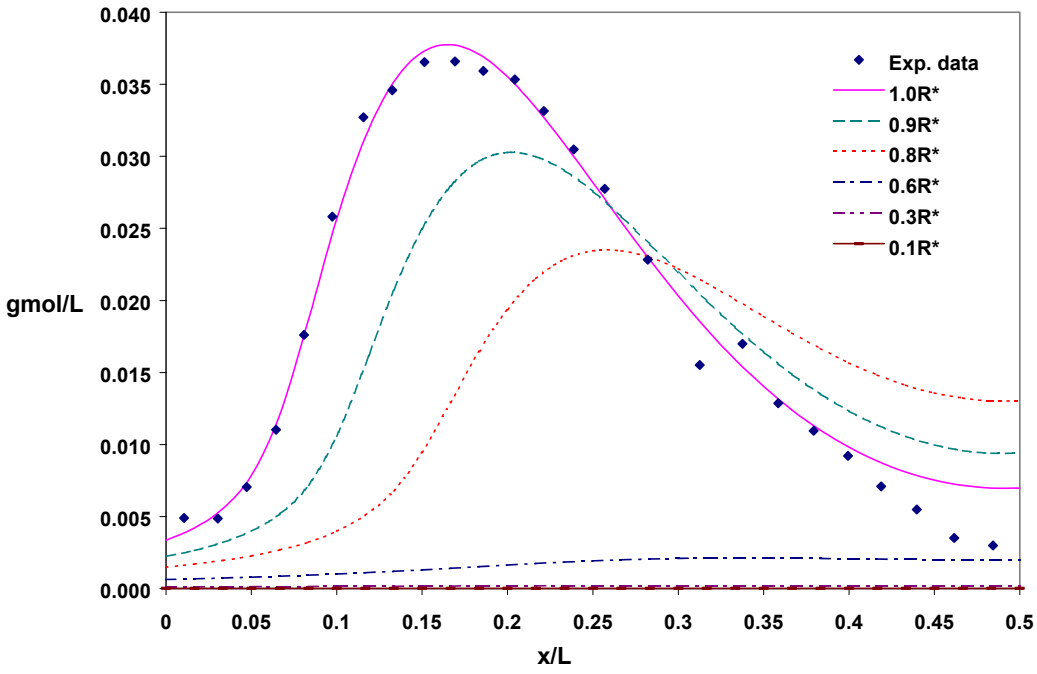

Figure 4.4.13: Variation of ketone concentration with reduced initial alkyl radical concentration. The plots are made for shelf age of 10.9 years.

The lower concentration of initial alkyl radical reduced the formation of ketone and thus prevented extensive degradation. The model revealed this fact and predicted that for lower concentrations of initial alkyl radicals, the degradation would be lesser. It was clearly observed that the concentration of ketone decreased rapidly with the fall in the initial alkyl radical concentrations. The decrease in the concentration of ketone was not linear. This can be explained again by the reactions that involved the formation of ketone. When initial alkyl radical concentrations were reduced, it correspondingly reduced the peroxy radical concentration. The combined effect of this reduction led to a non-linear decrease in the concentration of ketone. To illustrate this, we plotted the individual plots for R'* (Figure 4.4.14) and R'O_2* (Figure 4.4.15) with depth of the polymer for 10.9 years of shelf aging but at reduced initial alkyl radical concentration of 0.9 R_i, 0.8 R_i, 0.6 R_i, 0.3 R_i, and 0.1 R_i.

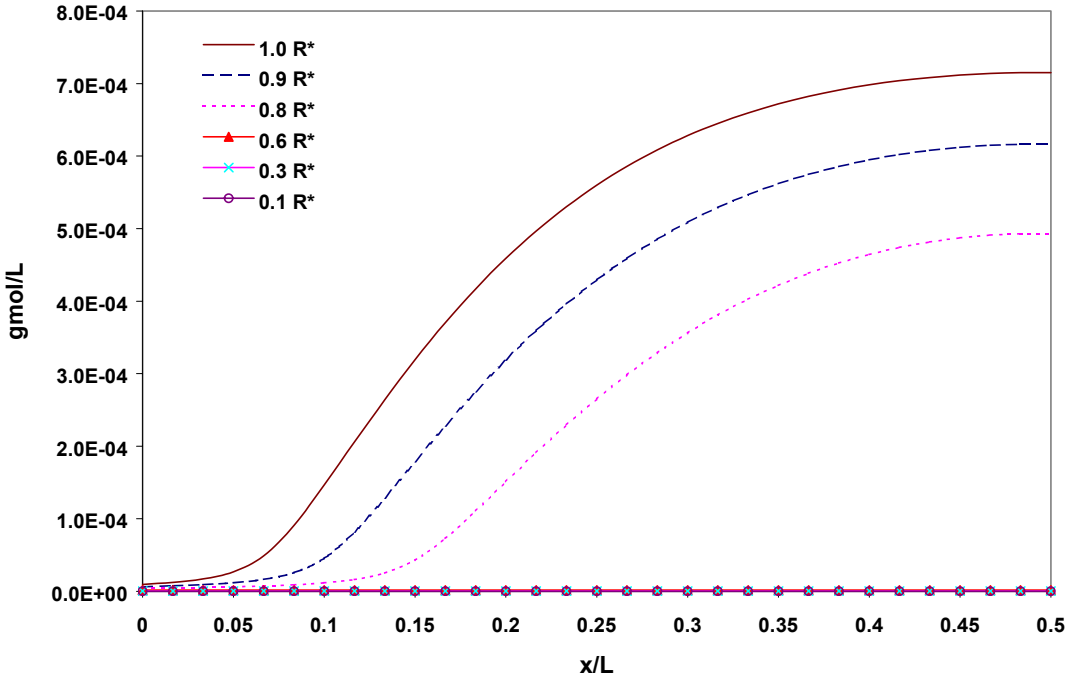

Figure 4.4.14: Variation of R'* with reduced initial alkyl radical concentration. All plots for 10.9 years of shelf aging.

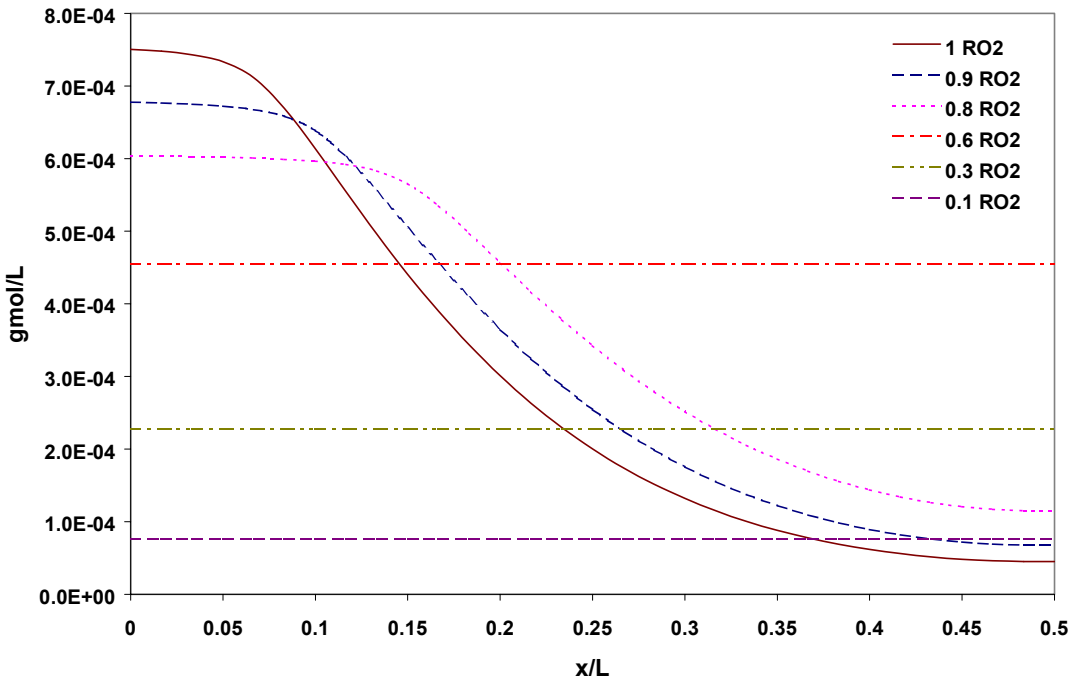

Figure 4.4.15: Variation of R'O_2* with reduced initial alkyl radical concentration. Plots are made for 10.9 years of shelf aging.

From Figure 4.4.14, the alkyl radical concentration for 10.9 years of shelf aging decreases rapidly from 0.8 Ri to 0.6 Ri. This is because of rapid consumption of alkyl radicals by its reaction with oxygen. The rapid consumption of alkyl radicals leads to the formation of peroxy concentration profile with the depth of the polymer. One observes from Figure 4.4.15, that the peroxy radicals decreased with initial alkyl radical concentration near the surface. The combined effect of alkyl and peroxy radicals leads to the rapid decline in the concentration of final ketone concentration.

4.4.5 Fitting to O'Neill's experimental data

O'Neill et al. [30] using Electron Spin Resonance (ESR) spectroscopy, observed that alkyl radicals generated by irradiation of the polymer decayed after about 70 days and led to the formation of more stable peroxy radicals. They provided data for the decay of alkyl radicals with time for up to 50 days. Since model IV has been quite successful with experimental data by Daly and Yin [12] and Coote et al. [14], the model was also applied to O'Neill's experimental data for alkyl radicals decay [30]. The polymer was irradiated up to 11.25 Mrad of irradiation, which was 4 times higher than normal. The initial radical concentration calculated by equation reported by Daly and Yin [12] was 2.62×10^{-2} gmol/L. There was no distinction made by the authors between crystalline and amorphous regions and also the ESR technique will determine the total concentration of alkyl radicals throughout the polymer film including both crystalline and amorphous regions. Further, the polymer sample used by O'Neill et al. [30] was 50 μm in size. A normal PE component has crystalline region of the size of 10 – 50 μm [15]. So it was

unlikely that the polymer had properly demarked crystalline and amorphous region. Further, if there were any slight demarcation, due to the small size of the polymer component, the diffusion of alkyl radicals within the crystalline region to the interface will be rapid. Hence, we assumed that all radicals in crystalline and amorphous regions could participate in the decay process. Similarly the oxygen diffusion within the polymer will also be rapid due to small size and we assumed that the concentration of oxygen throughout the polymer was uniform, equal to the solubility of oxygen in PE component at normal conditions. The fit to the experimental data by O'Neill [30] is given in Figure 4.4.16.

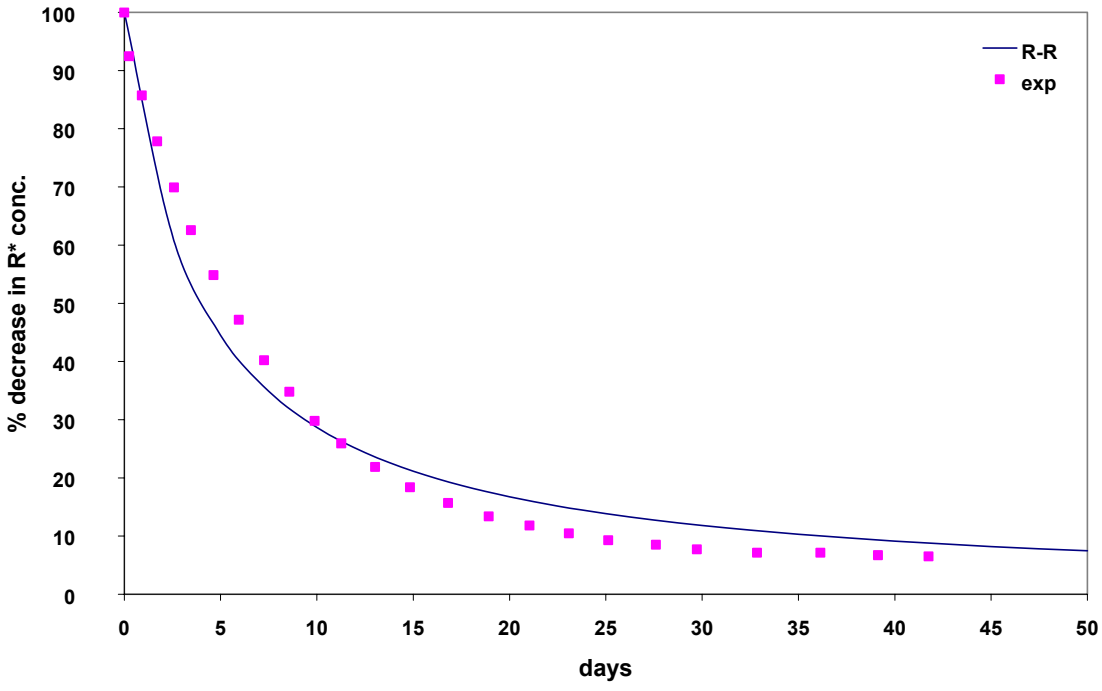

Figure 4.4.16: Alkyl radical decay predicted by model IV fitted to O'Neill et al., [30].

Since the polymer was of a different kind and also because of higher irradiation dose, the parameters obtained for the fit were quite different from those for shelf aging. Also the initial alkyl radicals were considered in their entirety, hence, the cross-linking reaction was employed in the model. The alkyl radicals included both the alkyl radicals formed, R* and R'*. From Figure 4.4.16, the model was observed to predict the experimental data very well. This served to add to the merit of this model. The parameters that best fitted the experimental data are given in Table 4.9.

Table 4.9: Parameters that fit O'Neill et al's [30] experimental data for alkyl radical decay, employing model IV. The time for shelf age was 50 days.

Parameters	Values	Units
K_1	5.00×10^{-2}	L/mol. s
K_2	5.60×10^{-4}	L/mol. s
K_3	1.70×10^{-4}	L/mol. s
K_4	2.00×10^{-3}	L/mol. s
K_5	5.00×10^{-14}	1/s
K_6	5.00×10^{-8}	L^2/mol^2. s
K_7	1.10×10^{-4}	L/mol. s
R* (initial alkyl radical conc.)	4.25×10^{-3}	gmol/L
C_{O2} (Concentration of oxygen in PE)	7.23×10^{-5}	mol / L

In the above table, reaction rate constant K_7 corresponds to cross-linking reaction between two alkyl radicals.

$$R^* + R^* \rightarrow R\text{-}R \qquad (k_7)$$

The alkyl radicals involved both types of radicals, R* and R'*.

Chapter 5

Conclusions

In all the four models discussed above, the reaction between alkyl and peroxy radicals to form ketone has been found to play a prominent role in the formation of the subsurface ketone peak.

$$R^* + RO_2^* \rightarrow 2RCO + 2R^*$$

Daly and Yin [12] employed the reaction to obtain the subsurface ketone peak [12], albeit derived incorrectly. The correct form of this reaction was given by William [41], which we have employed in all our models. There are other theoretical explanations available for the formation of subsurface peak such as one provided by Sun et. al. [55]. They found that because of the irradiation method employed that results in back-scattering of the gamma radiations, the alkyl radicals continuously increases with the depth of the polymer component. The oxygen by simultaneous diffusion and reaction assumes a continuously decreasing profile with the depth of the polymer. The interaction of the alkyl radicals and oxygen could result in the formation of ketone subsurface peak. The initial alkyl radical concentration that participates in the reaction was an order of magnitude higher than the initial oxygen concentration. Coote et al. [14] showed that the profile of the alkyl radicals formed at the beginning was constant with the depth of the polymer component. Some of the alkyl radicals in the latter case would react immediately with oxygen to form peroxy radicals and thus the oxygen would manifest itself in form of

peroxy radicals. The peroxy radicals would assume a decreasing profile with depth of the polymer. The alkyl radical concentration at the surface will be less due to its reaction with oxygen. The concentration will increase with the depth of the polymer as the oxygen concentration decreases. Thus we have decreasing profile of peroxy radicals and on the other hand an increasing profile of the alkyl radicals. The reaction between alkyl and peroxy radicals leads to the formation of ketone with a subsurface peak. In all the models considered, this has been assumed and has given us good representation of the ketone subsurface peak. The importance of reaction between alkyl and peroxy radicals cannot be overemphasized. The constant alkyl radical concentration with the depth of the polymer seems to be a more likely occurrence as observed by Coote et al. [14].

In all the four models discussed there were results that are common to all of them. The first was the basis of selection of reaction routes, viz. the concentration of ketone for shelf aging. All of the models fitted the experimental ketone concentration very well for 10.9 years of shelf aging experimental data by Daly and Yin [12]. The models however, could not predict the accelerated production of ketone after 4 years [14]. This resulted in not so good fit for the 5.8 years of experimental data by Daly and Yin [12]. All the models considered predicted higher ketone concentration than the experimental data for 5.8 years of shelf aging.

The aim of this study was also to seek a model that would give a good representation of hydroperoxide concentration. Model I gave a very poor simulation of hydroperoxide concentration profile with depth of the polymer. The concentration of

hydroperoxide continuously decreased with the depth of the polymer and did not remain constant with shelf age. A Model II was successful in terms of the ketone fit. For the hydroperoxide concentration, the profile decreased with depth of the polymer. It leveled out near the center of the polymer component. Further, the concentration remained constant with shelf age as had been observed by Coote et al. [14]. This has been a good depiction of the shelf aging process though not accurate. This was because the drop in hydroperoxide concentration was more than an order of magnitude while the results obtained by Coote et al. [14] showed that the drop from the surface concentration to the bulk was around 50%. A Model III included the reaction contended by Petruj and Marchal [24]. This reaction was added to improve the hydroperoxide profile in terms of making it more constant with depth of the polymer, but was unsuccessful in doing so. Finally, Model IV contained a different set of chemical reactions considered for the hydroperoxide profile. This model was based on the work and arguments of Matsuo and Dole [23]. The model considered the formation of second-generation alkyl radicals from initial alkyl radicals, which were generated by irradiation. The second-generation alkyl radicals were formed simultaneously with the formation of hydroperoxides. These alkyl radicals did not have sufficient energy to form more hydroperoxides and the formation of hydroperoxide stopped. The second-generation alkyl radicals only participated in the formation of ketones and other oxidative degradation products. If the initial alkyl radicals formed by irradiation were assumed to have a constant concentration with depth of the polymer, the corresponding concentration of hydroperoxide would also have a constant concentration with depth of the polymer. Due to participation of all types of alkyl radicals (R* and R'*) and peroxy radicals (RO_2* and $R'O_2$*) in oxidative degradation reaction,

the hydroperoxides slopes slightly with the depth of the polymer which was exactly what Coote et al. observed for shelf aging [14]. The model, however, did not provide a sharp drop in the hydroperoxide concentration from the surface to the depth of 0.025 mm. The time required for the complete formation of hydroperoxide to assume a constant value profile was more than two years for the kind of reaction parameters obtained by optimization.

All the models predicted the accelerated aging very well for ketones. The ketone concentration assumed a decreasing profile with the depth of the polymer as observed by Coote et al. [14]. The ketone concentration increased with time for accelerated aging. None of the first three models were able to predict the nature of the profiles for hydroperoxide similar to what Coote observed, viz. the concentration of hydroperoxide first increased up to 5 weeks of accelerated aging and then decreased with time. The fourth model was very successful in predicting the trend of the hydroperoxide concentrations for accelerated aging. The trend was observed for lesser time of aging but the rate constants chosen for this representation were arbitrary which make the aging period arbitrary. If the involvement of hydroperoxide can be determined to a considerable accuracy leading to the formation of species such as acids, esters, etc., one can hope to get a reasonable representation of the hydroperoxide concentration with the depth of the polymer, both for shelf aging and accelerated aging. Further, the profiles of various species has to be determined with the depth of the polymer as against finding bulk values that are reported in the literature [9,40,56]. It is also quite possible that one of the dormant reactions involving hydroperoxides during shelf aging may become active

during the accelerated aging since they were carried out at elevated temperatures [54]. There are many dimensions to the nature of this problem and has to be evaluated considering one case at a time.

All four models provide similar results for oxidation under reduced oxygen concentration and different initial alkyl radical concentration. The reduced oxygen concentration is of considerable importance for UHMWPE orthopedic component manufacturing industry since it has been proved to help reduce oxidative degradation of the polymer. Shelf aging in the absence of oxygen showed negligible formation of ketone and suggested it to be the best way of storing the polymer before implant, for example, the vacuum foil pack utilized by Johnson and Johnson [14]. The models also gave an idea about the nature of the profile in-vivo. The concentration of oxygen in-vivo is around $1/8^{th}$ of the atmospheric concentration [15] and amounts to ~ 2% of oxygen in the atmosphere. The ketone levels in in-vivo predicted by the models was considerably less as compared to shelf aging at ambient conditions. The models predicted higher ketone concentration at the surface of the polymer in in-vivo conditions and did not predict a subsurface peak. The severe degradation observed in certain retrieved components reported [11] at the subsurface may be because of polymer being continuously subjected to mechanical stress due to body joint motions and/or prior shelf aging before implantation of the polymer component in to the body which were anywhere between 0 and greater than 8 years. A good test of this result would be subjecting a PE component which is irradiated fresh to undergo mechanical wear test and determine the position of

maximum failure. The models predict that it would be surface rather than subsurface that would show maximum failure.

The models predicted higher oxidative degradation for higher initial alkyl radical concentration corresponding to higher gamma irradiation dose. Similarly the ketone concentration decreased with lower initial alkyl radical concentration. The decrease in the ketone concentration was observed to be non-linear with the decrease in the initial alkyl radical concentration. Hence extinguishing of the alkyl radicals by heat treatment or adding scavengers in the polymer may lead to lesser degradation in the polymer and would significantly add to the service life of the polymer. The results are advantageous in the sense that the irradiation dose has to be reduced to only 60% of the current irradiation dose to substantially reduce the formation of ketones and subsequent oxidative degradation.

Model IV was also successful in predicting the alkyl radical decay with the model fitting the experimental data by O'Neill et al [30]. In all the four models considered, model IV has been the most successful in representing the existing experimental data for the following reasons:

1) The model was able to fit the experimental ketone concentration very well along with a very good representation of the hydroperoxide concentration for shelf aging.

2) The model quite accurately predicted the ketone and hydroperoxide concentration profile for accelerated aging. The model accurately captured the hydroperoxide concentration trend.
3) The model predicts well the ketone concentration at reduced oxygen concentration. The model gives good insight in to the effect of reduced initial alkyl radical concentration and with the success it has achieved in explaining shelf and accelerated aging, it forms an invaluable guide for further experiments.
4) The model was also successful in fitting the experimental data of O'Neill et al. [30], which provides information about the decay of alkyl radicals. Since these data were taken from different set of experiments, the fitting parameters were different than ones used for shelf aging.

For model IV, few reactions played major role in the prediction of trends and fitting of experimental data values. The model was based on the formation of second-generation alkyl radicals along with simultaneous production of hydroperoxides. In the latter part of oxidation, these second-generation alkyl radicals played active role in the formation of oxidative degradation process. For obtaining the ketone subsurface peak, the reaction between alkyl and peroxy radicals is the most important (given by reaction 4, model IV). This reaction provided the trends obtained for low and high initial alkyl radical concentration and for low oxygen concentration at the surface. For the ketone concentration for accelerated aging, it is the elevated concentration of initial alkyl radicals that provides the decreasing nature of the profiles obtained. This is clear when

we compare accelerated aging with irradiation of the polymer at higher irradiation dose (corresponding to the higher initial alkyl radical concentration).

For the hydroperoxide profiles for the shelf aging and the accelerated aging conditions, the formation of hydroperoxides from first-generation alkyl radicals is of great consequence. This provides the constant profile of hydroperoxides for the shelf aging. The increase and then decrease in the concentration of hydroperoxides for accelerated aging primarily follows reaction of the type $A \rightarrow B \rightarrow C$. The hydroperoxides are not formed once the initial set of first-generation alkyl radicals are consumed and hence we can observe the depletion of hydroperoxides with time.

The reaction contended by Petruj and Marchal [24] does not affect the 10.9 years of shelf-aged ketone fit to a large extent except refining the fit. The removal of the reaction would not much affect the profiles obtained for all the aging conditions considered, although its addition does seem to benefit to some extent to the fitting of the shelf-aged experimental data.

Chapter 6

Recommendation for future work

The model IV obtained has been successful in fitting two different sets of experimental data, one for shelf aged, ketone concentration from Daly and Yin [8] and other for decay of alkyl radicals from O'Neill et al [30]. The model also has successfully predicted the trend of ketone and hydroperoxide profiles for accelerated aging given by Coote et al. [14]. This model provides a good tool to investigate more in to the nature of oxidative degradation of the polymer.

The above modeling was particularly done for irradiation and storage of the polymer in air. The irradiation of the polymer in air is not much practiced nowadays and irradiation in reduced oxygen atmosphere or inert atmosphere is the norm of the day [15]. Further, new techniques for sterilization, such as gas plasma irradiation are being developed which boast of high rate of success [26]. This has been found to reduce the oxidative degradation of the polymer substantially. The current research in the topic of UHMWPE is now focused on the degradation of the polymer in-vivo. New materials with superior properties over UHMWPE for orthopedic implants are currently being investigated. For irradiated polymer, degradation in-vivo is caused because of the oxygen dissolved in the polymer and diffusion of synovial fluid components in to the polymer such as oxygen, fatty acids, esters, proteins, etc. Costa et al. [6] has presented work on oxidation in retrieved components. Ester has been the main product determined with acids and ketones being formed to almost equal extent. Model IV developed in Chapter 4

has been able to predict the degradation in the polymer when it is subjected to reduced oxygen concentration usually found in-vivo. The model predicted the ketone concentration, which forms the major product of oxidative degradation, to be highest at the surface and decreases in to the bulk of the polymer. Though the effect of oxygen on the polymer in-vivo was well modeled, the effects of other species present in-vivo such as fatty acids, esters etc. has not been considered fully. It would be interesting to apply these models to the in-vivo oxidation process in more detail. It would be necessary to study the effect of the various species on the in-vivo oxidation of the polymer with the depth of the polymer and also in time. Once the species concentration variation is determined, it would be possible to incorporate reactions from literature in various models discussed in these studies to predict the oxidative degradation. Since esters and acids have been found to a considerable extent in the retrieved components their distribution within the polymer with time can be investigated. This should be done with simultaneous investigation of the ketones and hydroperoxides. Further, the investigation of these species will add to the understanding of the oxidative degradation process.

In oxidative degradation of irradiated polymer, the major reason for oxidation is not oxygen but the presence of alkyl radicals. Studies have proved that sterilization applying non-irradiated techniques such as EtO sterilization and gas plasma sterilization do not cause much physical, chemical, and mechanical change in the PE component [26,27]. EtO has its issues and gas plasma sterilization is not yet widely used and gamma sterilization still remains the technique for sterilization. And the problems associated with this technique will be studied well in to the 21st century. Application of Model IV to fit

O'Neill's et al. [30] data can help to understand the time for which these alkyl radicals are active. Annealing of the polymer results in the cross-linking of the polymer thereby improving its mechanical properties. The technique of annealing increases the rate constant for cross-linking and can also be modeled. To help analyze the situation more correctly, it might be necessary to study the profile of alkyl radicals with the depth of the polymer with shelf age and accelerated aging of the polymer. This will help ascertain the profile obtained in Figure 4.4.6 for alkyl radicals and would also throw some light on the accelerated production of ketones during shelf aging. Further, this would help understand the cross-linking process within the polymer, which helps improve the mechanical properties of the polymer.

Chapter 7

References:

1. Agrawal, C. M., "Reconstructing the Human Body using Biomaterials", JOM,1, (1998), 31.

2. Flynn, M., M. S. Thesis, Worcester Polytechnic Institute, May 1996.

3. Perry, R. H., Green, G. W., "Perry's Chemical Engineer's Handbook", McGraw Hill, New York, sixth edition, 1984.

4. Sun, D. C., Schmidig, G., Yau, S. S., Jeanty, M., Wang, A., Stark, C., Dumbleton, J. H., "Correlation between oxidation, cross linking, and wear performance of UHMWPE", In 43rd Annual Meeting, Orthopaedic Research Society, pg 783, 1997.

5. Lee, K., Lee, K. H., "Wear of shelf – aged UHMWPE acetabular liners", Wear, 225 – 229, (1999), 728 – 733.

6. Costa, L., Luda, M. P., Trossarelli, L., Brach del Prever, E. M., Crova, M., Gallinaro, P., "In-vivo UHMWPE biodegradation of retrieved prosthesis", Biomaterials, 19, (1998), 1371 – 1385.

7. Premnath, V., Harris, W. H., Jasty, M., Merrill, E. W., "Gamma sterilization of UHMWPE articular implants: an analysis of the oxidation problem", Biomaterials, 17, (1996), 1741 – 1753.

8. Keller A., "Radiation effects and crystallinity in polyethylene and paraffin". In: Bassett D. C., ed., "Developments in Crystalline Polymers". London: Applied science, 1982: vol. 1, 37.

9. Goldman, M., Gronsky, R., Long, G. G., Pruitt, L., "The effects of hydrogen peroxide and sterilization on the structure of ultra high molecular weight polyethylene", Polymer Degradation and Stability, Vol. 62, (1998), 97 – 104.

10. Edidin, A. A., Jewett, C. W., Kalinowski, A., Kwarteng, K., Kurtz, S. M., "Degradation of mechanical behaviour in UHMWPE after natural and accelerated aging", Biomaterials, Vol. 21, (2000), 1451 – 1460.

11. Kennedy, F. E., Currier, J. H., Plumet, S., Duda, J. L., Gestwick, D. P., Collier, J. P., Currier, B. H., Dubourg, M-C, "Contact fatigue failure of Ultra – High Molecular Weight Polyethylene bearing components of knee Prostheses", Paper

No. 99 – Trib – 28, STLE/ASME Tribology Conference, Orlando, Fl., Oct. 10 – 13, 1999.

12. Daly, B. M., Yin, J., "Subsurface oxidation of polyethylene", J. Biomed. Mat. Res., 42, (1998), 523 – 529.

13. Willie, B. M., Gingell, D. T., Bloebaum, R. D., Hofmann, A. A., "Possible explanation for the white band artifact seen in clinically retrieved polyethylene tibial components", Journal of Biomedical Materials Research, Vol. 52, Issue 3, (2000), 558-566.

14. Coote, C. F., Hamilton, J. V., McGimpsey, W. G., Thompson, R. W., "Oxidation of Gamma – Irradiated Ultrahigh Molecular Weight Polyethylene", J. App. Polym. Sci., Vol. 77, (2000), 2525 – 2542.

15. Kurtz, S. M., Muratoglu, O. K., Evans, M., Edidin, A. A., "Advances in the processing, sterilization, and cross-linking of ultra-high molecular weight polyethylene for total joint arthroplasty", Biomaterials, 20, (1999), 1659 – 1688.

16. Goldring, S. R., Schiller, A., Roelke, M., Rourke, C. M., O'Neill, D. A., and Harris, W. H., "The synovial-like membrane at the bone-cement interface in loose total hip replacements and its proposed role in bone lysis", J. Bone Joint Surg., 65 – A, (1983), 575 – 584.

17. Jasty, M., Bragdon, C. R., Lee, K. R., Hanson, A. E., Goetz, D. D., "Clinical variables affecting wear of the polyethylene acetabular component in Total Hip Anthroplasty: An Analysis of 160 components retrieved from autopsy and revision surgery", 39th Ann. Meeting, Orthopaedic Res. Soc., San Francisco, CA, February 15 – 18, 1993, The Orthopaedic Research Society, Chicago, IL, 1993, p 291.

18. Wroblewski, B. M., "Direction and rate of socket wear in Charnley low-friction arthroplasty", J. Bone Joint Surg., 67B, (1985), 757-761.

19. Rimnac, C. M., Wilson, P. D., Jr., Fuchs, M. D., Wright, T. M., "Acetabular cup wear in total hip arthroplasty", Orthop. Clin. North Am. 19, (1988), 631.

20. Clark, I. C., Campbell, P., Kossousky, N., "Debris-Mediated Osteolysis – A Cascade Phenomenon involving motion wear. Particulates, Macrophage Induction, and Bone Lysis," Particulate Debris from Medical Implants: Mechanisms of Formation and Biological Consequences. ASTM STP 1144 K. R. St. John Ed. American Society for Testing and Materials. Philadelphia, (1992), 7-26.

21. Wang, A., Sun, D. C., Stark, C., Dumbleton, J. H., "Wear mechanisms of UHMWPE in total joint replacements", Wear, 181 – 183, (1995), 241 – 249.

22. Wang, A., Sun, D. C., Yau, S. S., Edwards, B., Sokol, M., Essner, A., Polineni, V. K., Stark, C., Dumbleton, J. H., "Orientation softening in the deformation and wear of ultra – high molecular weight polyethylene", Wear, 203 – 204, (1997), 230 – 241.

23. Matsuo, H., Dole, M., "Irradiation of Polyethylene. IV. Oxidation Effects", J. Chem. Phys., 63, (1959), 837 – 843.

24. Petruj, J., Marchal, J., "Mechanism of ketone formation in the thermooxidation and radiolytic oxidation of low-density polyethylene", Radiat. Phys. Chem., Vol. 16, (1979), 27 – 36.

25. Bellare, A., Schnablegger, H., Cohen, R. E., "A small-angle X-ray scattering study of high-density polyethylene and ultra-high molecular weight polyethylene", Macromolecules, 17, (1995), 2325 – 33.

26. Goldman, M., Lee, M., Gronsky, R., Pruitt, L., "Oxidation of ultra-high molecular weight polyethylene characterized by Fourier Transform Infrared Spectrosopy", J. Biomed. Mater. Res., 37, (1997), 43 – 50.

27. Collier, J. P., Sutula, L. C., Currier, B. H., Currier, J. H., Wooding, R. E., Williams, I. R., Farber, K. B., Mayor, M. B., "Overview of polyethylene as a bearing material: comparison of sterilization methods", Clin. Orthop, 333, (1996), 76 – 86.

28. White, S. E., Paxson, R. D., Tanner, M. G., Whiteside, L. A., "Effects of sterilization on wear in total knee arthroplasty", Clin. Orthop., 331, (1996), 164 – 71.

29. Goldman, M., Pruitt, L., "A comparison of the effects of gamma radiation and plasma sterilization on the molecular structure, fatigue resistance, and wear behaviour of UHMWPE", J. Biomed. Mater. Res., 40, (1998), 378 – 84.

30. O'Neill, P., Birkinshaw, C., Leahy, J. J., Barklie, R., "The role of long lived free radicals in the ageing of irradiated ultra high molecular weight polyethylene", Polymer degradation and Stability, 63, (1999), 31 – 39.

31. Jahan, M. S., McKinny, K. S., "Radiation-sterilization and subsequent oxidation of medical grade polyethylene: an ESR study", Nuclear Instruments and Methods in Physics Research B, 151, (1999), 207 – 212.

32. Zagorski, Z. P., Rafalski, A., "Free radicals in irradiated unstabilized polypropylene, as seen by diffuse reflection absorption spectrophotometry", Radiat. Phys. Chem., 52, (1998), 257 – 260.

33. Seguchi, T., Tamura, N., "Mechanism of decay of alkyl radicals in Irradiated Polyethylene on exposure to air as studied by Electron Spin Resonance", J. Phys. Chem., 77, (1973), 40.

34. Michaels, A. S., Bixler, H. J., "The measurement of diffusion constants of gases in polymers by sorption techniques", J. Polym. Sci., 50, (1961), 413.

35. Costa, L., Luda, M. P., Trossarelli, L., Brach del Prever, E. M., Crova, M., Gallinaro, P., "Oxidation in orthopaedic UHMWPE sterilized by gamma – radiation and ethylene oxide", Biomaterials, 19, (1998), 659 – 668.

36. Sun, D. C., Schmidig, G., Stark, C., Dumbleton, J. H., "A simple accelerated aging method for simulations of long-term oxidative effects in UHMWPE implants", In 42nd Annual Meeting, Orthopaedic Research Society, paper no. 493, February 1996, Atlanta, Georgia.

37. Sun, D. C., Stark, C., Dumbleton, J. H., "Development of an accelerated aging method for evaluation of long-term irradiation effects on UHMWPE implants", Polym. Reprints, 1994, 35, 969 – 70.

38. McKellop, H., Yeom, B., Sun, D. C., Sanford, W. M., "Accelerated aging of irradiated UHMW polyethylene for wear evaluations", Trans. 42nd Orthop. Res. Soc., 21, (1996), 483.

39. Hikmet, R., Keller, A., "Crystallinity Dependent Free radical formation and decay in irradiated polyethylene in the presence of oxygen", Radiat. Phys. Chem., Vol. 29, No. 1, (1987), 15 – 19.

40. Tidjani, A., "Comparison of formation of oxidation products during photo – oxidation of linear low density polyethylene under different natural and accelerated weathering conditions", Polymer degradation and Stability, 68, (2000), 465 – 469.

41. William, J. L., "Stability of Polypropylene to Gamma Irradiation", Radiation Effects on Polymers, Ed. Roger L. Clough and Shalaby W. Shalaby, Chapter 35, 554 – 568.

42. Costa, L., Luda, M. P., Trossarelli, L., "Ultra-high molecular weight polyethylene: I. Mechano-oxidative degradation", Polymer Degradation and Stability, 55, (1997), 329 – 338.

43. Costa, L., Luda, M. P., Trossarelli, L., "Ultra-high molecular weight polyethylene: II. Thermal and photo-oxidation", Polymer Degradation and Stability, 58, (1997), 41 – 54.

44. Tabb, D. L., Sevcik, J. J., Koenig, J. L., "Fourier Transform Infrared Study of the effects of Irradiation on Polyethylene", Journal of Polymer Science, 13, (1975), 815 – 824.

45. Goldman, M., Gronsky, R., Ranganathan, R., Pruitt, L., "The effects of gamma radiation sterilization and ageing on the structure and morphology of medical grade ultra high molecular weight polyethylene", Polymer, Vol. 37, No. 14, (1996), 2909 – 2913.

46. Nakamura, K., Ogata, S., Ikada, Y., "Assessment of heat and storage conditions on ϒ - ray and electron beam irradiated UHMWPE by electron spin resonance", Biomaterials, 19, (1998), 2341 – 2346.

47. Edgar, T. F., Himmelblau, D. M., "Optimization of Chemical Process", McGraw-Hill Inc., 1988.

48. Snir, M., Otto, S. W., Huss-Lederman, S., Walker, D. W., Dongarra, J., "MPI: The complete reference", MIT Press, 1996.

49. Pauly, S., in Permeability and Diffusion Data, Polymer Handbook, Vol. 1, 4th ed.; Wiley: New York, 1999; pg 543.

50. Torikai, A., Goetha, R., Nagaya, S., Fueki, K., "Radiation – induced Degradation of Polyethylene: Role of amorphous region in the formation of oxygenated products and the mechanical propertied", Polymer Degradation and Stability, Vol. 16, (1986), 199 – 212.

51. Streicher, R. M., "Sterilization and long term aging of medical – grade UHMWPE", Radiat. Phys. Chem., 46, (1995), 893 – 896.

52. Cunliffe, A. V., Davis, A., "Photo-Oxidation of Thick Polymer samples – Part II: The influence of oxygen diffusion on natural and artificial weathering of polyolefin", Polymer Degradation and Stability, Vol. 4, (1982), 17 –37.

53. N. Bach, incomplete reference in reference 23.

54. Gugumus, F., "Physico-chemical aspects of polyethylene processing in an open mixer: 6. Discussion of hydroperoxide formation and decomposition", Polymer Degradation and Stability, 68, (2000), 337 – 352.

55. Sun, D. C., Schmidig, G., Stark, C., Dumbleton, J. H., "On the origins of a subsurface oxidation maximum and its relationship to the performance of UHMWPE implant", Transactions: Twenty – first annual meeting of the Society for Biomaterials in conjunction with the 27th International Biomaterials Symposium, March 18 – 22, 1995, Vol. XVIII, San Francisco, California.

56. Ohnishi, S., Sugimoto, S., Nitta, S., “Electron spin resonance study of radiation oxidation of polymers. III A. Results for Polyethylene and some general remarks”, Journal of Polymer Science: Part A, Vol. 1, (1963), 605 – 623.

Appendix A.1

Forward difference explicit method to solve PDE for model IV

```
c     Program Explicit
c     ***************

c     This Program calculates the spatial and temporal variation in the
c     concentration of four reactants.

c     This program uses the irreversible formation of ROOH. Does not
c     include the decomposition of RCO. Includes the formation of RCO
c     from ROOH (by pet. reaction) and also the decomposition of ROOH
c     to other products. The cage reaction for this case is assumed not
c     to occur according to the contention given by Petruj et. al.

c     REACTION SCHEME

c     R + O2 -> RO2                (k1)
c     RO2 + RH -> ROOH + Rp        (k2)
c     R + R -> R2                  (k3)
c     Rp + O2 -> RpO2              (k4)
c     RpO2 + Rp -> 2RCO+2Rp        (k5)
c     RpO2+ROOH+RH -> RCO+R*+H2O   (k6)
c     ROOH -> products             (k7)

c     ****************************************************************
c     |Declaration

      double precision L,D,R,k1,k2,k3,k4,k5,k6,k7
      double precision RI,OS,RHI
      double precision age, pito

c     ****************************************************************

      open(unit=1,File='cn.inp',status='old')
      open(unit=2,file='cn.out',status='old')

c     print*, 'SEC = ', ISEC

      rewind(unit=1)

      read(1,*)L
      read(1,*)D
```

```
      read(1,*)OS
      read(1,*)RI
      read(1,*)RHI
      read(1,*)age

      age = age*365*24*3600
c     age = age*7*24*3600

      read(1,*)k1
      read(1,*)k2
      read(1,*)k3
      read(1,*)k4
      read(1,*)k5
      read(1,*)k6
      read(1,*)k7

      call CNC(L,D,OS,RI,RHI,age,k1,k2,k3,k4,k5,k6,k7)

      close(1)
      close(2)

      stop
      end

c     ****************************************************************
c     Calling Subroutine CNC
c     ****************************************************************


      subroutine CNC(L,D,OS,RI,RHI,age,k1,k2,k3,k4,k5,k6,k7)

      parameter p = 40
      double precision L,D,OS,RI,RHI,age,k1,k2,k3,k4,k5,k6,k7
      double precision O2(p), R(p), RO2(p), Rp(p), RpO2(p)
      double precision ket(p), ROOH(p), RH(p)
      double precision A(8), pt
      double precision dx, tau, dtau, delx
      double precision m1,m10,m2,m3,m4,m40,m5,m6,m7
      integer m,n,tp


c     ## Non dimensionalizing the time interval ##
c     ------------------------------------------

      read(1,*)n
```

```
      tp = 1000
      pt = 1/(float(tp))
      tau = (age*D)/(L**2)
      dtau = (tau*pt)/n

c     ## Non dimensionalizing the length ##
c     ------------------------------------

      read(1,*)m
      dx = L/m
      delx = dx/L

      call ini(O2,R,RO2,Rp,RpO2,ket,ROOH,RH,RHI,RI,m)

      m1  = (k1*RI*dtau*L**2)/D
      m10 = (k1*OS*dtau*L**2)/D
      m2  = (k2*RI*dtau*L**2)/D
      m3  = (k3*RI*dtau*L**2)/D
      m4  = (k4*RI*dtau*L**2)/D
      m40 = (k4*OS*dtau*L**2)/D
      m5  = (k5*RI*dtau*L**2)/D
      m6  = (k6*(RI**2)*dtau*L**2)/D
      m7  = (k7*dtau*L**2)/D

      print*,'m2 = ',m2

      do k = 1,tp
      do j = 1,n
       do i = 1,m+1

        if(i.eq.1)then

          A(1)  = 1.0

          A(2)  = R(i) - m10*O2(i)*R(i) - m3*R(i)**2
     v          - m3*R(i)*Rp(i)
     v          - m5*R(i)*RpO2(i)
     v          - m5*R(i)*RO2(i)

          A(3)  = RO2(i) + m10*O2(i)*R(i) - m2*RH(i)*RO2(i)
     v          - m5*Rp(i)*RO2(i)
     v          - m5*Rp(i)*RO2(i)
     v          - m5*R(i)*RO2(i)
     v          - m6*RO2(i)*ROOH(i)*RH(i)

          A(4)  = ROOH(i) + m2*RO2(i)*RH(i) - m7*ROOH(i)
```

```
      A(5)  = Rp(i) + m2*RO2(i)*RH(i) - m40*Rp(i)*O2(i)
     v          + m5*Rp(i)*RpO2(i) + m6*RpO2(i)*ROOH(i)*RH(i)
     v          - m3*Rp(i)**2 - m3*R(i)*Rp(i)
     v          + m5*Rp(i)*RO2(i) + 2*m5*RpO2(i)*R(i)
     v          + m6*RO2(i)*ROOH(i)*RH(i)

      A(6)  = RpO2(i) + m40*Rp(i)*O2(i) - m5*Rp(i)*RpO2(i)
     v          - m6*RpO2(i)*ROOH(i)*RH(i)
     v          - m5*R(i)*RpO2(i)

      A(7)  = ket(i) + 2.0*m5*RpO2(i)*Rp(i)
     v               + 2.0*m5*R(i)*RpO2(i)
     v               + 2.0*m5*Rp(i)*RO2(i)
     v               + 2.0*m5*R(i)*RO2(i)
     v              + m6*RpO2(i)*ROOH(i)*RH(i)
     v               + m6*RO2(i)*ROOH(i)*RH(i)

      A(8)  = RH(i) - m2*RO2(i)*RH(i) - m6*RpO2(i)*ROOH(i)*RH(i)
     v          - m6*RO2(i)*ROOH(i)*RH(i)

    elseif(i.eq.m+1)then

      A(1) = O2(i-1)

      A(2)  = R(i) - m10*O2(i)*R(i) - m3*R(i)**2
     v          - m3*R(i)*Rp(i)
     v          - m5*R(i)*RpO2(i)

      A(3)  = RO2(i) + m10*O2(i)*R(i) - m2*RH(i)*RO2(i)
     v          - m5*Rp(i)*RO2(i)
     v          - m5*Rp(i)*RO2(i)
     v          - m5*R(i)*RO2(i)
     v          - m6*RO2(i)*ROOH(i)*RH(i)

      A(4)  = ROOH(i) + m2*RO2(i)*RH(i) - m7*ROOH(i)

      A(5)  = Rp(i) + m2*RO2(i)*RH(i) - m40*Rp(i)*O2(i)
     v          + m5*Rp(i)*RpO2(i) + m6*RpO2(i)*ROOH(i)*RH(i)
     v          - m3*Rp(i)**2 - m3*R(i)*Rp(i)
     v          + m5*Rp(i)*RO2(i) + 2*m5*RpO2(i)*R(i)
     v          + m6*RO2(i)*ROOH(i)*RH(i)

      A(6)  = RpO2(i) + m40*Rp(i)*O2(i) - m5*Rp(i)*RpO2(i)
     v          - m6*RpO2(i)*ROOH(i)*RH(i)
     v          - m5*R(i)*RpO2(i)
```

```
      A(7)  = ket(i) + 2.0*m5*RpO2(i)*Rp(i)
     v              + 2.0*m5*R(i)*RpO2(i)
     v              + 2.0*m5*Rp(i)*RO2(i)
     v              + 2.0*m5*R(i)*RO2(i)
     v              + m6*RpO2(i)*ROOH(i)*RH(i)
     v              + m6*RO2(i)*ROOH(i)*RH(i)

      A(8)  = RH(i) - m2*RO2(i)*RH(i) - m6*RpO2(i)*ROOH(i)*RH(i)
     v        - m6*RO2(i)*ROOH(i)*RH(i)

    else

      A(1)  = O2(i) - m1*O2(i)*R(i) - m4*O2(i)*Rp(i)
     v       +dtau*((O2(i+1)-2*O2(i)+O2(i-1))/(delx**2))

      A(2)  = R(i) - m10*O2(i)*R(i) - m3*R(i)**2
     v        - m3*R(i)*Rp(i)
     v        - m5*R(i)*RpO2(i)
     v        - m5*R(i)*RO2(i)

      A(3)  = RO2(i) + m10*O2(i)*R(i) - m2*RH(i)*RO2(i)
     v        - m5*Rp(i)*RO2(i)
     v        - m5*R(i)*RO2(i)
     v        - m6*RO2(i)*ROOH(i)*RH(i)

      A(4)  = ROOH(i) + m2*RO2(i)*RH(i) - m7*ROOH(i)

      A(5)  = Rp(i) + m2*RO2(i)*RH(i) - m40*Rp(i)*O2(i)
     v        + m5*Rp(i)*RpO2(i) + m6*RpO2(i)*ROOH(i)*RH(i)
     v        - m3*Rp(i)**2 - m3*R(i)*Rp(i)
     v        + m5*Rp(i)*RO2(i) + 2*m5*RpO2(i)*R(i)
     v        + m6*RO2(i)*ROOH(i)*RH(i)

      A(6)  = RpO2(i) + m40*Rp(i)*O2(i) - m5*Rp(i)*RpO2(i)
     v        - m6*RpO2(i)*ROOH(i)*RH(i)
     v        - m5*R(i)*RpO2(i)

      A(7)  = ket(i) + 2.0*m5*RpO2(i)*Rp(i)
     v              + m6*RpO2(i)*ROOH(i)*RH(i)
     v              + 2.0*m5*R(i)*RpO2(i)
     v              + 2.0*m5*Rp(i)*RO2(i)
     v              + 2.0*m5*R(i)*RO2(i)
     v              + m6*RpO2(i)*ROOH(i)*RH(i)
     v              + m6*RO2(i)*ROOH(i)*RH(i)
```

```
          A(8)  = RH(i) - m2*RO2(i)*RH(i) - m6*RpO2(i)*ROOH(i)*RH(i)
     v             - m6*RO2(i)*ROOH(i)*RH(i)

          endif

          O2(i)   = A(1)
          R(i)    = A(2)
          RO2(i)  = A(3)
          ROOH(i) = A(4)
          Rp(i)   = A(5)
          RpO2(i) = A(6)
          ket(i)  = A(7)
          RH(i)   = A(8)

         enddo
        enddo
        enddo

        h = -delx

        do i = 1,m+1
         h = h + delx
         ket(i) = ket(i)*RI
         O2(i) = O2(i)*OS
         R(i) = R(i)*RI
         RO2(i) = RO2(i)*RI
         ROOH(i) = ROOH(i)*RI
         Rp(i) = Rp(i)*RI
         RpO2(i) = RpO2(i)*RI
         RH(i) = RH(i)*RI
       write(*,30)ket(i)
      v  ,O2(i),R(i),RO2(i),Rp(i),RpO2(i),ROOH(i)
       write(2,30)ket(i)
      v  ,O2(i),R(i),RO2(i),Rp(i),RpO2(i),ROOH(i)
 30     format(7(g10.4,1x))
        enddo

        print*,'Exiting the Program'

        return
        end


c       ***************************************************************
c       Subroutine INI
c       ***************************************************************
```

```
      subroutine ini(O2,R,RO2,Rp,RpO2,ket,ROOH,RH,RHI,RI,m)

      parameter p = 40
      double precision O2(p),R(p),RO2(p),Rp(p),RpO2(p),ket(p),ROOH(p)
      double precision RH(p), RHI, RI
      integer m,n


       do i = 1, m+1
         O2(i) = 1.0
         R(i) = 1.0
         RO2(i) = 0.0
         Rp(i) = 0.0
         RpO2(i) = 0.0
         ket(i) = 0.0
         ROOH(i) = 0.0
         RH(i) = RHI/RI
       Enddo

      return
      end

c     ****************************************************************
```

INPUT DATA

File cn.inp

Parameters that best fit the curve (for shelf aging):

0.0575	---L (dm)
6.40e-10	---Do2 (dm2/s)
7.23e-05	---O2 at surface (mol/L)
7.60e-04	---R* (RI mol/L)
66.4	---RH (mol/L)
10.9	---age (years)
5.00e-02	---k1 (L/mol sec).. R + O2 -> RO2
3.60e-04	---k2 (L/mol sec).. RO2+RH -> ROOH + Rp
0.00e-00	---k3 (L/mol sec).. R + R -> R2
5.70e-03	---k4 (L/mol sec).. Rp + O2 -> RpO2
3.90e-04	---k5 (L/mol sec).. Rp + RpO2 -> 2 ket+2Rp
3.00e-08	---k6 (L/mol RpO2+ROOH+RH->ROOH+RCO+Rp+H2O
1.00e-14	---k7 (/sec) ROOH -> products
6000	---# of temporal intervals

30 ---# of spacial intervals

Parameters for accelerated aging:

0.0575 ---L (dm)
6.40e-09 ---Do2 (dm2/s)
7.23e-05 ---O2 at surface (mol/L)
4.25e-03 ---R* (RI mol/L)
66.4 ---RH (mol/L)
1.0 ---age (years)
5.00e-01 ---k1 (L/mol sec).. R + O2 -> RO2
3.60e-03 ---k2 (L/mol sec).. RO2+RH -> ROOH + Rp
0.00e-00 ---k3 (L/mol sec).. R + R -> R2
5.70e-02 ---k4 (L/mol sec).. Rp + O2 -> RpO2
3.90e-03 ---k5 (L/mol sec).. Rp + RpO2 -> 2 ket+2Rp
3.00e-07 ---k6 (L/mol RpO2+ROOH+RH->ROOH+RCO+Rp+H2O
5.00e-07 ---k7 (/sec) ROOH -> products
6000 ---# of temporal intervals
30 ---# of spacial intervals

Appendix A.2

Optimization program for determining parameters for model II

```
c     Program to solve a nonlinear least squares problem by solving
c     partial differential equation and obtaining the values of the rate constant parameters.
c     It uses Lenningard Maquardt technique to solve the problem.

c     **The reaction scheme involves the irreversible formation of ROOH
c     with ROOH decomposing to give ketone.**

c     The IMSL library is used for optimization subroutine.

c     Program begins:

c     MAIN PROGRAM
c     **************************Declaration**************************

      IMPLICIT NONE

      integer MM, NN, LDFJAC, p
      parameter (MM=31, NN=6, LDFJAC=31, p=40)
      double precision  XGUESS(NN), XLB(NN), XUB(NN), XSCALE(NN)
      double precision  RPARAM(7), frco(31)
      double precision  X(NN), FSCALE(MM)
      double precision  FVEC(MM), FJAC(LDFJAC,NN)
      double precision  O2(p), R(p), RO2(p), ket(p), ROOH(p)
      double precision  L,D,OS,RI,RH,age,dtau,delx,tau,dx

      integer IBTYPE,i, IPARAM(6)
      integer Ntemp, Nspac

      EXTERNAL DBCLSF
      EXTERNAL FCN
      EXTERNAL INI
      EXTERNAL DU4LSF

      COMMON /FCNC/ frco
      COMMON /INIC1/ Ntemp, Nspac
      COMMON /INIC2/ L,D,OS,RH,RI,dtau,delx

c     ************************************************************

c     opt.inp inputs the values of the initial guesses for the programme,
```

```
c       the upper and the lower bounds, the values of the constants
c       for the polymer.

c       ** Opening input files **

        open(unit=1,file='opt.inp',status='old')
        open(unit=2,file='RCO.dat',status='old')

c       ** Opening output file **

        open(unit=3,file='chk.out',status='old')
        open(unit=4,file='opt.out',status='old')

        rewind(unit=1)
        rewind(unit=2)

        read(1,*)L
        read(1,*)D
        read(1,*)OS
        read(1,*)RI
        read(1,*)RH
        read(1,*)age

        age = age*365*24*3600

        read(1,*)Ntemp
        read(1,*)Nspac

        RH = RH/RI

        do i = 1,NN
          read(1,*) XGUESS(i), XLB(i), XUB(i)
        enddo

c       ** Reading the experimental data values **

        do i = 1,MM
         read(2,*) frco(i)
        enddo


c       ** Ntemp are the number of temporal intervals **
c       ** Nspac are the number of spacial intervals **

C       ## Non dimensionalizing the time interval ##
C       ------------------------------------------
```

```
      tau = (age*D)/(L**2)
      dtau = tau/Ntemp


C     /* Ntemp (30000) is the no. of temporal divisions and is
C     different from NN (2-5) which is the no. of variables (the
C     rate constants) to be optimised */


C     ## Non dimensionalizing the length ##
C     -----------------------------------
      dx = L/Nspac
      delx = dx/L

C     Nspac (30) is the no. of spacial intervals and is different
C     from MM (31) which is the no. of data points (same as M+1)


c     ** Setting the IMSL parameters **
c     ^^^^^^^^^^^^^^^^^^^^^^^^^^^^^^^^

      do i = 1,MM
        FSCALE(i) = 1.0
      enddo

      do i = 1,NN
       XSCALE(i) = 1.0
      enddo

c     ** Changing the default value of the number of iterations **

      CALL DU4LSF(IPARAM,RPARAM)
      IPARAM(3) = 1000
      IPARAM(4) = 4000
      IPARAM(5) = 1000
c     IPARAM(6) = 1

c     IPARAM(1) = 0
      IBTYPE = 0


c     >> Calling the IMSL subroutine
c     ------------------------------

      call DBCLSF(FCN,MM,NN,XGUESS,IBTYPE,XLB,XUB,XSCALE,
```

```
     v         FSCALE,IPARAM,RPARAM,X,FVEC,FJAC,LDFJAC)

      do i = 1,NN
        write(4,10)i,X(i)
        write(*,10)i,X(i)
 10      format(3x,'k(',i2,') = ',g11.4)
      enddo

      write(4,102)IPARAM(3), IPARAM(4)
 102    format(/,3x,'The number of iterations = ',i11,/,3x,'The
     v      number of function evaluations is = ',i11,/)

c      ** Calling the subroutine for evaluating the function **

      call INI(ket,O2,R,RO2,ROOH,X,NN)


      do i = 1,Nspac+1
      write(4,30)ket(i),O2(i),R(i),RO2(i),ROOH(i)
 30    format(5(g14.4,2x))
      enddo

      close(1)
      close(2)
      close(3)
      close(4)

      stop
      end

c     ***********************************************************************
c      Calling subroutine FCN to calculate the difference function
c     ***********************************************************************

      subroutine FCN(MM,NN,X,F)

      parameter p = 40
      integer MM, NN
      double precision  frco(31)
      double precision  X(NN), F(MM)
      double precision  O2(p), R(p), RO2(p), ket(p), ROOH(p)

      COMMON /FCNC/ frco

      write(3,79)
      write(*,79)
```

```
 79    Format("Entering FCN")

c      ** Calling the subroutine for evaluating the function **

       call INI(ket,O2,R,RO2,ROOH,X,NN)

       do i = 1,NN
         write(3,110)i,X(i)
         write(*,110)i,X(i)
 110     format(3x,'k(',i2,') = ',g11.4)
       enddo

       write(3,76)
 76    format(/)

       do i = 1,MM
        F(i) = abs(frco(i)-ket(i))
       enddo
       return
       end

c      ***************************************************************
c      Subroutine INI
c      ***************************************************************

       subroutine INI(ket,O2,R,RO2,ROOH,X,NN)

       parameter (p = 40)
       integer Nspac, Ntemp, NN
       double precision O2(p),R(p),RO2(p),ket(p)
       double precision dtau,delx,age,tau,dx
       double precision ROOH(p), A(5), X(NN), m(NN+1)
       double precision L,D,OS,RI,RH

       COMMON /INIC1/ Ntemp, Nspac
       COMMON /INIC2/ L,D,OS,RH,RI,dtau,delx

       write(*,69)
 69    format(/,'Entering INI',/)

c      ** Calculating the non dimensionalized rate constants **

       m(1)  = (X(1)*RI*dtau*L**2)/D
       m(2)  = (X(1)*OS*dtau*L**2)/D
       m(3)  = (X(2)*RI*dtau*L**2)/D
       m(4)  = (X(3)*RI*dtau*L**2)/D
```

```
      m(5)  = (x(4)*dtau*L**2)/D
      m(6)  = (x(5)*dtau*L**2)/D

      m(7)  = (x(6)*RI*L**2*dtau)/OS

c     ** Initializing the matrix **

      do i = 1, Nspac+1
        O2(i) = 1.0
        R(i) = 1.0
        RO2(i) = 0.0
        ket(i) = 0.0
        ROOH(i) = 0.0
      enddo

c     ** Initializing the dummy variable **

      do i = 1,5
       A(i) = 0.0
      enddo

      do j = 1,Ntemp+1
       do i = 1,Nspac+1

        if(i.eq.1)then

          A(1) = 1.0

          A(2) = R(i) - m(2)*O2(i)*R(i) + m(3)*RO2(i)*RH
     v              + m(4)*R(i)*RO2(i) - m(6)*R(i)**2

          A(3) = RO2(i) + m(2)*O2(i)*R(i) - m(3)*RO2(i)*RH
     v               - m(4)*R(i)*RO2(i)

          A(4) = ket(i) + 2*m(4)*R(i)*RO2(i) + m(5)*ROOH(i)

          A(5) = ROOH(i) + m(3)*RO2(i)*RH - m(5)*ROOH(i)
     v               - m(6)*ROOH(i)

        elseif(i.eq.Nspac+1)then

          A(1) = O2(i-1)

          A(2) = R(i) - m(2)*O2(i)*R(i) + m(3)*RO2(i)*RH
     v              + m(4)*R(i)*RO2(i) - m(6)*R(i)**2
```

```
      A(3) = RO2(i) + m(2)*O2(i)*R(i) - m(3)*RO2(i)*RH
     v                - m(4)*R(i)*RO2(i)

      A(4) = ket(i) + 2*m(4)*R(i)*RO2(i) + m(5)*ROOH(i)

      A(5) = ROOH(i) + m(3)*RO2(i)*RH - m(5)*ROOH(i)
     v                - m(6)*ROOH(i)

     else

      A(1) = O2(i) - m(1)*O2(i)*R(i)
     v          +dtau*((O2(i+1)-2*O2(i)+O2(i-1))/(delx**2))

      A(2) = R(i) - m(2)*O2(i)*R(i) + m(3)*RO2(i)*RH
     v             + m(4)*R(i)*RO2(i) - m(6)*R(i)**2

      A(3) = RO2(i) + m(2)*O2(i)*R(i) - m(3)*RO2(i)*RH
     v                - m(4)*R(i)*RO2(i)

      A(4) = ket(i) + 2*m(4)*R(i)*RO2(i) + m(5)*ROOH(i)

      A(5) = ROOH(i) + m(3)*RO2(i)*RH - m(5)*ROOH(i)
     v                - m(6)*ROOH(i)

     endif

     O2(i)   = A(1)
     R(i)    = A(2)
     RO2(i)  = A(3)
     ket(i)  = A(4)
     ROOH(i) = A(5)
    enddo
   enddo

   do i = 1,Nspac+1
    ket(i)  = ket(i)*RI
    O2(i)   = O2(i)*OS
    R(i)    = R(i)*RI
    RO2(i)  = RO2(i)*RI
    ROOH(i) = ROOH(i)*RI
   enddo

   return
   end

c     ****************************************************************
```

INPUT DATA

File opt.inp

```
0.0575                          ---L (dm)
1.14e-10                         ---D (dm2/s)
7.23e-05                         ---O2 at surface (mol/L)
3.49e-03                         ---R* (RI mol/L)
66.4                            ---RH (mol/L)
10.9                            ---age (years)
300000                           ---# of temporal intervals (N)
30                              ---# of spacial intervals  (M)
1.950e-02   0.0   0.1               --- k1
0.100e-02   0.0   0.1               --- k2
1.390e-03   0.0   0.1               --- k3
0.100e-02   0.0   0.1               --- k4
0.100e-02   0.0   0.1               --- k5
0.100e-02   0.0   0.1               --- k6
```

File RCO.dat

Experimental Ketone Concentration

```
  0.4877e-02
  0.6179e-02
  0.8050e-02
  0.1088e-01
  0.1512e-01
  0.2069e-01
  0.2654e-01
  0.3146e-01
  0.3484e-01
  0.3660e-01
  0.3694e-01
  0.3614e-01
  0.3452e-01
  0.3234e-01
  0.2983e-01
  0.2718e-01
  0.2452e-01
  0.2195e-01
  0.1955e-01
  0.1734e-01
  0.1535e-01
  0.1359e-01
```

0.1206e-01
0.1075e-01
0.9653e-02
0.8759e-02
0.8058e-02
0.7541e-02
0.7201e-02
0.7032e-02
0.7032e-02

Appendix A.3

Parallel program for optimizing parameters for Daly and Yin's [8] model

```
c     Program to solve a nonlinear least squares problem by solving
c     partial differential equation
c     and obtaining the values of the rate constant parameters.
c     It uses DIRECT SEARCH technique to solve the problem.
c     Parallel computation is employed to calculate the function at
c     each search step.

c     Program begins:

c     MAIN PROGRAM
c     **************************Declaration************************

      include 'mpif.h'

      parameter (MM=31, NN=2, LDFJAC=31)
      double precision  KLB(NN), KUB(NN)
      double precision  k(NN), u(NN), p(NN)
      double precision  F, upsilon, delk(NN), min
      double precision  frco(31),L,D,OS,RI,RH,age
      double precision  diff, A, AF(0:4)
      double precision  Qreal(7), Fprev, pp(2), change

      double precision in(2,1), out(2,1), aout

      double precision starttime, endtime, telapse

      integer ind

      integer N,M, Qint(2), bu(0:4)
      character*1 pause

c     ************************************************************

      call MPI_INIT(ierr)
      call MPI_COMM_RANK(MPI_COMM_WORLD, myid, ierr)
      call MPI_COMM_SIZE(MPI_COMM_WORLD, numprocs, ierr)

      open(unit=1,file='dsm.inp',status='old')
      open(unit=3,file='exp.dat',status='old')
```

```
      open(unit=2,file='dsm.out',status='old')

      rewind(unit=1)
      rewind(unit=3)


c     // Supplying with the bounds on the parameters //

      starttime =  MPI_WTIME()

     if(myid.eq.0)then

      do i = 1,NN

       KLB(i) = 0.00
       KUB(i) = 1.00

      enddo

      do i = 1,7
         read(1,*)Qreal(i)
      enddo

c      write(*,*)'Qreal(1) = ',Qreal(1)

      do i = 1,2
         read(1,*)Qint(i)
      enddo

      do i = 1,NN
       read(1,*) k(i)
       u(i) = k(i)
      enddo

      do i = 1,MM
       read(3,*) frco(i)
      enddo

      call FCN(MM,NN,k,F,frco,L,D,OS,RI,RH,age,N,M,myid)
      min = F

      endif

      call MPI_BCAST(Qint,2,MPI_INTEGER,0,
     v      MPI_COMM_WORLD,ierr)
```

```
      call MPI_BCAST(Qreal,11,MPI_DOUBLE_PRECISION,0,
     v      MPI_COMM_WORLD,ierr)

      call MPI_BCAST(k,2,MPI_DOUBLE_PRECISION,0,
     v      MPI_COMM_WORLD,ierr)

      call MPI_BCAST(frco,31,MPI_DOUBLE_PRECISION,0,
     v      MPI_COMM_WORLD,ierr)


      call MPI_BCAST(min,1,MPI_DOUBLE_PRECISION,0,
     v      MPI_COMM_WORLD,ierr)

      call MPI_BARRIER(MPI_COMM_WORLD,ierr)


  113   format(/,'Press any key to begin:')
  114   format(A1)
  114   format(A1)

      L  = Qreal(1)
      D  = Qreal(2)
      OS = Qreal(3)
      RI = Qreal(4)

      RH = Qreal(5)/RI

      age= Qreal(6)*365*24*3600

      Fprev = Qreal(7)

      N = Qint(1)
      M = Qint(2)

      ii = 0.0

  120    diff = abs(Fprev - min)

     Fprev = min

      do i = 1,NN
        if(diff.ge.1e-01)then
         delk(i) = k(i)/2
        elseif(diff.lt.1e-01.and.diff.gt.1e-02)then
         delk(i) = k(i)/4
```

```
      elseif(diff.le.1e-02.and.diff.gt.1e-04)then
       delk(i) = k(i)/6
      elseif(diff.le.1e-04.and.diff.gt.1e-06)then
       delk(i) = k(i)/8
      else
       delk(i) = k(i)/10
      endif
    enddo

    if(myid.eq.0)then

      call FCN(MM,NN,k,F,frco,L,D,OS,RI,RH,age,N,M,myid)

    elseif(myid.eq.1)then

      u(1) = k(1) + delk(1)
      u(2) = k(2)
      call FCN(MM,NN,u,F,frco,L,D,OS,RI,RH,age,N,M,myid)

    elseif(myid.eq.2)then

      u(1) = k(1) - delk(1)
      u(2) = k(2)
      call FCN(MM,NN,u,F,frco,L,D,OS,RI,RH,age,N,M,myid)

    elseif(myid.eq.3)then

      u(1) = k(1)
      u(2) = k(2) + delk(2)
      call FCN(MM,NN,u,F,frco,L,D,OS,RI,RH,age,N,M,myid)

    elseif(myid.eq.4)then

      u(1) = u(1)
      u(2) = k(2) - delk(2)
      call FCN(MM,NN,u,F,frco,L,D,OS,RI,RH,age,N,M,myid)

    endif


    call MPI_GATHER(F,1,MPI_DOUBLE_PRECISION,AF,1,
   v         MPI_DOUBLE_PRECISION,0,MPI_WORLD_COMM,ierr)

    in(1,1) = F
    in(2,1) = myid
```

```
      call MPI_REDUCE(in,out,1,MPI_2DOUBLE_PRECISION,MPI_MINLOC,0,
     v           MPI_COMM_WORLD,ierr)

      call MPI_BARRIER(MPI_COMM_WORLD,ierr)


      if(myid.eq.0)then

        aout = out(1,1)
        ind = out(2,1)

        if(ind.eq.1)then
         k(1) = k(1) + delk(1)
          min = AF(0)
        elseif(ind.eq.2)then
          k(1) = k(1) - delk(1)
          min = AF(0)
        elseif(ind.eq.3)then
          k(2) = k(2) + delk(2)
          min = AF(0)
        elseif(ind.eq.4)then
          k(2) = k(2) - delk(2)
          min = AF(0)
        else
          min = AF(0)
        endif

        if(min.lt.1e-02)then
           goto 110
        else
           ii = ii + 1
           pp(ii) = min
        endif

       if(ii.eq.2)then

        change = abs(pp(1)-pp(2))
        write(*,141)change
141       format(/,3x,'change = ',g11.4,/)

        if(change.lt.1e-16)then
         write(*,141)change
          do i = 1,NN
           k(i) = k(i) + k(i)*0.01
          enddo
        endif
```

```
        ii = 0

       endif


       write(*,103)min
103      format(/,3x,'F = ',g11.4,/)

       endif

      call MPI_BCAST(min,1,MPI_DOUBLE_PRECISION,0,
     v          MPI_COMM_WORLD,ierr)

      call MPI_BCAST(k,2,MPI_DOUBLE_PRECISION,0,
     v          MPI_COMM_WORLD,ierr)

      call MPI_BARRIER(MPI_COMM_WORLD,ierr)


      do i = 1,NN
        u(i) = k(i)
      enddo

       if(min.gt.1e-02)then
          goto 120
       endif

110    if(myid.eq.0)then
      write(2,10)
      write(*,10)
10     format(3x,'The best rate constants evaluated are as follows:',/)

       do i = 1,NN
        write(2,41)i,k(i)
        write(*,41)i,k(i)
41       format(//,3x,'k(',i2,') = ',g11.4,/)
       enddo

       write(2,42)F
       write(*,42)F
42       format(/,3x,'F = ',g11.4,/)

      endif

      endtime = MPI_WTIME()
```

```
      telapse = endtime – starttime
      print*,'Time elapsed',telapse

      call MPI_FINALIZE(ierr);

      close(1)
      close(2)
      close(3)

      stop
      end

c     ************************ Main Program ends******************
c     ***************************************************************
c     Calling subroutine FCN to calculate the difference function
c     ***************************************************************

      subroutine FCN(MM,NN,X,F,frco,L,D,OS,RI,RH,age,N,M,myid)

      integer p
      parameter (p = 40)
      integer M,N, MM, NN, myid
      double precision  X(NN), F
      double precision  A(5)
      double precision  S(MM)
      double precision  O2(p), R(p), RO2(p), ket(p)
      double precision  dx, tau, dtau, delx, m1,m10,m2
      double precision frco(31),L,D,OS,RI,RH,age

c     ## Non dimensionalizing the time interval ##
c     ------------------------------------------

      tau = (age*D)/(L**2)
      dtau = tau/N

c     /* N (30000) is the no. of temporal divisions and is different
c        from NN (2-5) which is the no. of variables (the rate
c        constants) to be optimised */

c     ## Non dimensionalizing the length ##
c     -----------------------------------

      dx = L/M
      delx = dx/L
```

```
c      /* M (30) is the no. of spacial intervals and is different
c         from MM (31) which is the no. of data points (same as M+1)*/

       call ini(O2,R,RO2,ket,ROOH,M)

       m1  = (X(1)*RI*dtau*L**2)/D
       m10 = (X(1)*OS*dtau*L**2)/D
       m2  = (X(2)*RI*dtau*L**2)/D

       do i = 1,5
        A(i) = 0.0
       enddo

       do j = 1,N
        do i = 1,M+1

         if(i.eq.1)then

           A(1) = 1.0

           A(2) = R(i) - m10*O2(i)*R(i) + m2*R(i)*RO2(i)

           A(3) = RO2(i) + m10*O2(i)*R(i) - m2*R(i)*RO2(i)

           A(4) = ket(i) + m2*R(i)*RO2(i)

        elseif(i.eq.M+1)then

           A(1) = O2(i-1)
           A(2) = R(i-1)
           A(3) = RO2(i-1)
           A(4) = ket(i-1)
c          A(5) = ROOH(i-1)

       else

           A(1) = O2(i) - m1*O2(i)*R(i)
     v           + dtau*((O2(i+1) - 2*O2(i) + O2(i-1))/(delx**2))

           A(2) = R(i) - m10*O2(i)*R(i) + m2*R(i)*RO2(i)

           A(3) = RO2(i) + m10*O2(i)*R(i) - m2*R(i)*RO2(i)

           A(4) = ket(i) + m2*R(i)*RO2(i)
        endif
```

```
      O2(i)   = A(1)
      R(i)    = A(2)
      RO2(i)  = A(3)
      ket(i)  = A(4)
c     ROOH(i) = A(5)

       enddo
      enddo

      do i = 1,M+1
       ket(i) = ket(i)*RI
       O2(i) = O2(i)*OS
       R(i) = R(i)*RI
       RO2(i) = RO2(i)*RI
      enddo


      F = 0.0

      do i = 1,MM
       S(i) = ABS(frco(i)-ket(i))
       F = F + S(i)**2
      enddo

      F = F**0.5

      do i = 1,NN
        write(2,101)i,X(i)
        write(*,101)i,X(i)
 101          format(3x,'k(',i2,') = ',g11.4,/)
      enddo

      return

      end


c     ***************************************************************
c     Subroutine INI
c     ***************************************************************

      subroutine ini(O2,R,RO2,ket,ROOH,M)

      integer p
      parameter (p = 40)
```

```
      double precision O2(p),R(p),RO2(p),ket(p)
c     double precision ROOH(p)
      integer M

      do i = 1, M+1
        O2(i)   = 1.0
        R(i)    = 1.0
        RO2(i)  = 0.0
        ket(i)  = 0.0
c       ROOH(i) = 0.0
      enddo

      return
      end

c     ****************************************************************
```

INPUT DATA

File dsm.inp

0.0575	---L (dm)
1.14e-9	---Do2 (dm2/s)
7.23e-5	---O2 at surface (mol/L)
6.98e-3	---RI (mol/L)
66.4	---RH (mol/L)
10.9	---age (years)
300000	---# of temporal intervals (N)
30	---# of spacial intervals (M)
1.08e+8	--- Fini
1.263e-03	--- k1
2.615e-07	--- k2
1.162e-05	--- k3
4.177e-07	--- k4
6.529e-10	--- k5

File exp.dat

Experimental ketone concentration considered for optimization

0.4877e-02
0.6179e-02
0.8050e-02
0.1088e-01
0.1512e-01
0.2069e-01
0.2654e-01
0.3146e-01
0.3484e-01
0.3660e-01
0.3694e-01
0.3614e-01
0.3452e-01
0.3234e-01
0.2983e-01
0.2718e-01
0.2452e-01
0.2195e-01
0.1955e-01
0.1734e-01
0.1535e-01
0.1359e-01
0.1206e-01
0.1075e-01
0.9653e-02
0.8759e-02
0.8058e-02
0.7541e-02
0.7201e-02
0.7032e-02
0.7032e-02

Appendix A.4

Sequential Program for Direct Search Method

```
c     Program to solve a nonlinear least squares problem by solving
c     partial differential equation
c     and obtaining the values of the rate constant parameters.
c     It uses DIRECT SEARCH technique to solve the problem.

c     Program begins:

c     MAIN PROGRAM
c     **************************Declaration***************************

      parameter (MM=31, NN=2, LDFJAC=31)
      double precision  KLB(NN), KUB(NN)
      double precision  k(NN), u(NN), p(NN)
      double precision  F, Fini, upsilon, delk, min
      double precision  frco(31),L,D,OS,RI,RH,age
      double precision  diff
      double precision  starttime, endtime, telapse
      integer N,M

c     ************************************************************

      call MPI_INIT(ierr)
      call MPI_COMM_RANK(MPI_COMM_WORLD,myid,ierr)
      call MPI_COMM_SIZE(MPI_COMM_WORLD,numprocs,ierr)

      open(unit=1,file='dsm.inp',status='old')
      open(unit=3,file='exp.dat',status='old')
      open(unit=2,file='dsm.out',status='old')

      rewind(unit=1)
      rewind(unit=3)

c     // Supplying with the bounds on the parameters //

      starttime = MPI_WTIME()

      do i = 1,NN

       KLB(i) = 0.00
       KUB(i) = 1.00
```

```
      enddo

      read(1,*)L
      read(1,*)D
      read(1,*)OS
      read(1,*)RI
      read(1,*)RH
      read(1,*)age
      read(1,*)N
      read(1,*)M
      read(1,*)Fini

      do i = 1,NN
       read(1,*) k(i)
       u(i) = k(i)
      enddo

      age = age*365*24*3600

      RH = RH/RI

      do i = 1,MM
       read(3,*) frco(i)
      enddo


      ii = 0
120    do 121 i = 1,NN

      call FCN(MM,NN,k,F,frco,L,D,OS,RI,RH,age,N,M)
      A = F

      diff = Fini - A

        if(diff.ge.1e-01)then
         delk = k(i)*1.0
        elseif(diff.lt.1e-01.and.diff.gt.1e-02)then
         delk = k(i)/2
        elseif(diff.le.1e-02.and.diff.gt.1e-04)then
         delk = k(i)/4
        elseif(diff.le.1e-04.and.diff.gt.1e-06)then
         delk = k(i)/8
        else
         delk = k(i)/10
        endif
```

```
      u(i) = k(i) + delk
      up = u(i)
      call FCN(MM,NN,u,F,frco,L,D,OS,RI,RH,age,N,M)
      AP = F

     u(i) = k(i) - delk
      if(u(i).gt.0e0)then
       un = u(i)
       call FCN(MM,NN,u,F,frco,L,D,OS,RI,RH,age,N,M)
       AN = F
      else
       AN = A
       un = k(i)
      endif

      if(AN.lt.A.and.AN.lt.AP)then
       min = AN
       k(i) = UN
      elseif(A.lt.AN.and.A.lt.AP)then
       min = A
      elseif(AP.lt.A.and.AP.lt.AN)then
       min = AP
       k(i) = UP
      else
       min = A
      endif

      do j = 1,NN
       u(j) = k(j)
      enddo


      if(min.lt.1e-02)then
       goto 110
      else
       Fini = min
      endif

     ii = ii + 1
     p(ii) = min

     if(ii.eq.2)then
     diff = abs(p(1)-p(2))
        write(*,141)diff
141       format(/,3x,'diff = ',g11.4,/)
       if(diff.lt.1e-20)then
```

```
          write(*,141)diff
c         do i = 1,NN
          k(i) = k(i) + k(i)*0.125
c         enddo
         endif
          ii = 0
        endif

         write(*,103)min
 103      format(/,3x,'F = ',g11.4,/)

 121    continue

        if(F.gt.1e-02)then
         goto 120
        endif

c       write(2,43)F
c       write(*,43)F
c  43   format(/,3x,'F = ',g11.4,/)

 110   write(2,10)
      write(*,10)
 10    format(3x,'The best rate constants evaluated are as follows:',/)

        do i = 1,NN
         write(2,41)i,k(i)
         write(*,41)i,k(i)
 41       format(//,3x,'k(',i2,') = ',g11.4,/)
        enddo

       write(2,42)F
       write(*,42)F
 42     format(/,3x,'F = ',g11.4,/)

       endtime = MPI_WTIME()

       telapse = endtime – starttime
       print*,'Time for sequential simulation: ',telapse

       call MPI_FINALIZE(ierr)

       close(1)
       close(2)
       close(3)
```

```
      stop
      end



c     ****************************************************************
c     Calling subroutine FCN to calculate the difference function
c     ****************************************************************

      subroutine FCN(MM,NN,X,F,frco,L,D,OS,RI,RH,age,N,M)

      integer p
      parameter (p = 40)
      integer M,N, MM, NN
      double precision  X(NN), F
      double precision  A(5)
      double precision  S(MM)
      double precision  O2(p), R(p), RO2(p), ket(p)
c     double precision  ROOH(p)
      double precision  dx, tau, dtau, delx, m1,m10,m2
c     double precision  m3,m4,m5
      double precision frco(31),L,D,OS,RI,RH,age

      write(2,79)
 79    Format(/,"Entering FCN",//,60('*'),//)

c     ## Non dimensionalizing the time interval ##
c     ------------------------------------------

      tau = (age*D)/(L**2)
      dtau = tau/N

c     /* N (30000) is the no. of temporal divisions and is different
c        from NN (2-5) which is the no. of variables (the rate
c        constants) to be optimised */

c     ## Non dimensionalizing the length ##
c     -----------------------------------

      dx = L/M
      delx = dx/L


c     /* M (30) is the no. of spacial intervals and is different
c        from MM (31) which is the no. of data points (same as M+1) */
      call ini(O2,R,RO2,ket,ROOH,M)
```

```
      m1  = (X(1)*RI*dtau*L**2)/D
      m10 = (X(1)*OS*dtau*L**2)/D
      m2  = (X(2)*RI*dtau*L**2)/D
c     m3  = (X(3)*RI*dtau*L**2)/D
c     m4  = (X(4)*RI*dtau*L**2)/D
c     m5  = (X(5)*dtau*L**2)/D

      do i = 1,5
       A(i) = 0.0
      enddo

      do j = 1,N
       do i = 1,M+1

        if(i.eq.1)then

          A(1) = 1.0

          A(2) = R(i) - m10*O2(i)*R(i) + m2*R(i)*RO2(i)

          A(3) = RO2(i) + m10*O2(i)*R(i) - m2*R(i)*RO2(i)

          A(4) = ket(i) + m2*R(i)*RO2(i)

c         A(5) = ROOH(i) + m2*RO2(i)*RH - m3*ROOH(i)*R(i)
c    v                   - m5*ROOH(i)

       elseif(i.eq.M+1)then

          A(1) = O2(i-1)
          A(2) = R(i-1)
          A(3) = RO2(i-1)
          A(4) = ket(i-1)
c         A(5) = ROOH(i-1)

       else

          A(1) = O2(i) - m1*O2(i)*R(i)
     v           + dtau*((O2(i+1) - 2*O2(i) + O2(i-1))/(delx**2))

          A(2) = R(i) - m10*O2(i)*R(i) + m2*R(i)*RO2(i)

          A(3) = RO2(i) + m10*O2(i)*R(i) - m2*R(i)*RO2(i)

          A(4) = ket(i) + m2*R(i)*RO2(i)
```

```
c          A(5) = ROOH(i) + m2*RO2(i)*RH - m3*ROOH(i)*R(i)
c     v                   - m5*ROOH(i)



         endif

        O2(i)   = A(1)
        R(i)    = A(2)
        RO2(i)  = A(3)
        ket(i)  = A(4)
c       ROOH(i) = A(5)

        enddo
       enddo

       do i = 1,M+1
         ket(i) = ket(i)*RI
         O2(i) = O2(i)*OS
         R(i) = R(i)*RI
         RO2(i) = RO2(i)*RI
c        ROOH(i) = ROOH(i)*RI
c       write(2,30)ket(i),O2(i),R(i),RO2(i),ROOH(i)
c       write(*,30)ket(i),O2(i),R(i),RO2(i),ROOH(i)
c 30     format(5(2x,g14.4))
       enddo

       write(2,61)
       write(*,61)
 61         format(//,3x,60('*'),/)

       F = 0.0

       do i = 1,MM
        F = F + S(i)**2
       enddo

       F = F**0.5

       do i = 1,NN
         write(2,101)i,X(i)
         write(*,101)i,X(i)
 101           format(3x,'k(',i2,') = ',g11.4,/)
       enddo
```

```
      return

      end


c     ****************************************************************
c     Subroutine INI
c     ****************************************************************

      subroutine ini(O2,R,RO2,ket,ROOH,M)

      integer p
      parameter (p = 40)
      double precision O2(p),R(p),RO2(p),ket(p)
c     double precision ROOH(p)
      integer M

       do i = 1, M+1
          O2(i)   = 1.0
          R(i)    = 1.0
          RO2(i)  = 0.0
          ket(i)  = 0.0
c         ROOH(i) = 0.0
       enddo

      return
      end

c     ****************************************************************
```

INPUT DATA:

File dsm.inp

```
0.0575          ---L (dm)
1.14e-9         ---Do2 (dm2/s)
7.23e-5         ---O2 at surface (mol/L)
6.98e-3         ---RI (mol/L)
66.4            ---RH (mol/L)
10.9            ---age (years)
300000          ---# of temporal intervals (N)
30              ---# of spacial intervals  (M)
1.08e+8         --- Fini
1.263e-03       --- k1
2.615e-07       --- k2
1.162e-05       --- k3
```

4.177e-07 --- k4
6.529e-10 --- k5

File exp.dat

Experimental ketone concentration considered for optimization

0.4877e-02
0.6179e-02
0.8050e-02
0.1088e-01
0.1512e-01
0.2069e-01
0.2654e-01
0.3146e-01
0.3484e-01
0.3660e-01
0.3694e-01
0.3614e-01
0.3452e-01
0.3234e-01
0.2983e-01
0.2718e-01
0.2452e-01
0.2195e-01
0.1955e-01
0.1734e-01
0.1535e-01
0.1359e-01
0.1206e-01
0.1075e-01
0.9653e-02
0.8759e-02
0.8058e-02
0.7541e-02
0.7201e-02
0.7032e-02
0.7032e-02

Appendix A.5

Program to fit O'Neill et al. [30] data with model IV

```
c     Program Explicit
c     ***************

c     This Program calculates the spatial and temporal variation in the
c     concentration of four reactants.

c     This program uses the irreversible formation of ROOH. Does not
c     include the decomposition of RCO. Includes the formation of RCO
c     from ROOH (by pet. reaction) and also the decomposition of ROOH
c     to other products. The cage reaction for this case is assumed not
c     to occur according to the contention given by Petruj et. al.

c     REACTION SCHEME

c     R + O2 -> RO2                (k1)
c     RO2 + RH -> ROOH + Rp        (k2)
c     R + R -> R2                  (k3)
c     Rp + O2 -> RpO2              (k4)
c     RpO2 + Rp -> 2RCO+2Rp        (k5)
c     RpO2+ROOH+RH -> RCO+R*+H2O   (k6)
c     ROOH -> products             (k7)

c     ****************************************************************
c     |Declaration

      double precision L,D,R,k1,k2,k3,k4,k5,k6,k7
      double precision RI,OS,RHI
      double precision age, pito

c     ****************************************************************

      open(unit=1,File='cn.inp',status='old')
      open(unit=2,file='cn.out',status='old')

      rewind(unit=1)

      read(1,*)L
      read(1,*)D
      read(1,*)OS
      read(1,*)RI
      read(1,*)RHI
```

```
      read(1,*)age

      age = age*24*3600

      read(1,*)k1
      read(1,*)k2
      read(1,*)k3
      read(1,*)k4
      read(1,*)k5
      read(1,*)k6
      read(1,*)k7

      call CNC(L,D,OS,RI,RHI,age,k1,k2,k3,k4,k5,k6,k7)

      close(1)
      close(2)

      stop
      end

c     ****************************************************************
c     Calling Subroutine CNC
c     ****************************************************************

      subroutine CNC(L,D,OS,RI,RHI,age,k1,k2,k3,k4,k5,k6,k7)

      parameter p = 40, df = 20
      double precision L,D,OS,RI,RHI,age,k1,k2,k3,k4,k5,k6,k7
      double precision O2(p), R(p), RO2(p), Rp(p), RpO2(p)
      double precision ket(p), ROOH(p), RH(p)
      double precision A(8), pt, store(21)
      double precision dx, tau, dtau, delx, g, gb
      double precision m1,m10,m2,m3,m4,m40,m5,m6,m7
      integer m,n,tp,tr

c     ## Non dimensionalizing the time interval ##
c     ------------------------------------------

      read(1,*)n

      tp = 1000
      pt = 1/(float(tp))
      g = tp*n

c     %% g is the total number of temporal divisions,
c     df is division factor %%
```

```
      gb = g/df
      print*,'g  = ',g
      print*,'gb = ',gb

c     %% gb is the number of temporal intervals after which data is to
c     be sought %%

      tau = (age*D)/(L**2)
      dtau = (tau*pt)/n

c     ## Non dimensionalizing the length ##
c     ------------------------------------

      read(1,*)m
      dx = L/m
      delx = dx/L

c     RH = RHI/RI

      call ini(O2,R,RO2,Rp,RpO2,ket,ROOH,RH,RHI,RI,m)

      m1  = (k1*RI*dtau*L**2)/D
      m10 = (k1*OS*dtau*L**2)/D
      m2  = (k2*RI*dtau*L**2)/D
      m3  = (k3*RI*dtau*L**2)/D
      m4  = (k4*RI*dtau*L**2)/D
      m40 = (k4*OS*dtau*L**2)/D
      m5  = (k5*RI*dtau*L**2)/D
      m6  = (k6*(RI**2)*dtau*L**2)/D
      m7  = (k7*dtau*L**2)/D

      print*,'m2 = ',m2

      do i = 0,df
       store(i) = 0.0
      enddo

      ij = 1
      tr = 0

      do k = 1,tp
      do j = 1,n
       do i = 1,m+1

        if(i.eq.m+1)then
```

```
      A(1) = O2(i-1)
      A(2)  = R(i) - m10*O2(i)*R(i) - m3*R(i)**2
     v           - m3*R(i)*Rp(i)
     v           - m5*R(i)*RpO2(i)
      A(3)  = RO2(i) + m10*O2(i)*R(i) - m2*RH(i)*RO2(i)
     v           - m5*Rp(i)*RO2(i)
      A(4)  = ROOH(i) + m2*RO2(i)*RH(i) - m7*ROOH(i)
      A(5)  = Rp(i) + m2*RO2(i)*RH(i) - m40*Rp(i)*O2(i)
     v           + m5*Rp(i)*RpO2(i) + m6*RpO2(i)*ROOH(i)*RH(i)
     v           - m3*Rp(i)**2 - m3*R(i)*Rp(i)
     v           + m5*Rp(i)*RO2(i) + 2*m5*RpO2(i)*R(i)
      A(6)  = RpO2(i) + m40*Rp(i)*O2(i) - m5*Rp(i)*RpO2(i)
     v           - m6*RpO2(i)*ROOH(i)*RH(i)
     v           - m5*R(i)*RpO2(i)
      A(7)  = ket(i) + 2.0*m5*RpO2(i)*Rp(i)
     v                + m6*RpO2(i)*ROOH(i)*RH(i)
      A(8)  = RH(i) - m2*RO2(i)*RH(i) - m6*RpO2(i)*ROOH(i)*RH(i)

    else

      A(1)  = 1.0
      A(2)  = R(i) - m10*O2(i)*R(i) - m3*R(i)**2
     v           - m3*R(i)*Rp(i)
     v           - m5*R(i)*RpO2(i)
      A(3)  = RO2(i) + m10*O2(i)*R(i) - m2*RH(i)*RO2(i)
     v           - m5*Rp(i)*RO2(i)
      A(4)  = ROOH(i) + m2*RO2(i)*RH(i) - m7*ROOH(i)
      A(5)  = Rp(i) + m2*RO2(i)*RH(i) - m40*Rp(i)*O2(i)
     v           + m5*Rp(i)*RpO2(i) + m6*RpO2(i)*ROOH(i)*RH(i)
     v           - m3*Rp(i)**2 - m3*R(i)*Rp(i)
     v           + m5*Rp(i)*RO2(i) + 2*m5*RpO2(i)*R(i)
      A(6)  = RpO2(i) + m40*Rp(i)*O2(i) - m5*Rp(i)*RpO2(i)
     v           - m6*RpO2(i)*ROOH(i)*RH(i)
     v           - m5*R(i)*RpO2(i)
      A(7)  = ket(i) + 2.0*m5*RpO2(i)*Rp(i)
     v                + m6*RpO2(i)*ROOH(i)*RH(i)
      A(8)  = RH(i) - m2*RO2(i)*RH(i) - m6*RpO2(i)*ROOH(i)*RH(i)

    endif

    O2(i)   = A(1)
    R(i)    = A(2)
    RO2(i)  = A(3)
    ROOH(i) = A(4)
    Rp(i)   = A(5)
```

```
        RpO2(i) = A(6)
        ket(i)  = A(7)
        RH(i)   = A(8)

        enddo

        tr = tr + 1

        if(tr.eq.gb)then
         store(ij) = A(2) + A(5)
         ij = ij+1
         tr = 0
        endif

       enddo
      enddo

      do j = 0,df

       if(j.eq.0)then
        store(0) = RI
        write(*,32)store(j)
        write(2,32)store(j)
       else
        store(j) = store(j)*RI
        write(*,32)store(j)
        write(2,32)store(j)
 32      format(3x,g12.4,2x)
       endif

      enddo

      print*,'Exiting the Program'

      return
      end


c     ****************************************************************
c     Subroutine INI
c     ****************************************************************

      subroutine ini(O2,R,RO2,Rp,RpO2,ket,ROOH,RH,RHI,RI,m)

      parameter p = 40
      double precision O2(p),R(p),RO2(p),Rp(p),RpO2(p),ket(p),ROOH(p)
```

```
      double precision RH(p), RHI, RI
      integer m,n

       do i = 1, m+1
         O2(i) = 1.0
         R(i) = 1.0
         RO2(i) = 0.0
         Rp(i) = 0.0
         RpO2(i) = 0.0
         ket(i) = 0.0
         ROOH(i) = 0.0
         RH(i) = RHI/RI
       enddo

      return
      end

c     ****************************************************************
```

INPUT DATA

File cn.inp

```
0.0575          ---L (dm)
0.64e-09        ---Do2 (dm2/s)
7.23e-05        ---O2 at surface (mol/L)
2.62e-02        ---R* (RI mol/L)
66.4            ---RH (mol/L)
50.0            ---age (years)
5.00e-02        ---k1 (L/mol sec).. R + O2 -> RO2
5.60e-04        ---k2 (L/mol sec).. RO2+RH -> ROOH + Rp
1.10e-04        ---k3 (L/mol sec).. R + R  -> R2
1.70e-04        ---k4 (L/mol sec).. Rp + O2 -> RpO2
2.00e-03        ---k5 (L/mol sec).. Rp + RpO2 -> 2 ket+2Rp
5.00e-08        ---k6 (L/mol RpO2+ROOH+RH->ROOH+RCO+Rp+H2O
5.00e-14        ---k7 (/sec) ROOH -> products
6000            ---# of temporal intervals
30              ---# of spacial intervals
```